Masters Research Project:
A reconstruction of the Holocene fire and environmental history from Kinrara Lagoon, north Queensland:

By Rainy Comley

Supervisors: Prof. Michael Bird, Dr. Cassandra Rowe, Dr. Chris Wurster.

Thesis submitted by Rainy Comley in partial fulfilment of requirements for Masters of Philosophy Research Thesis (Natural and Physical Sciences) in the college of science and engineering of James Cook University.

Access Page

I, the undersigned, the author of this thesis, understand that James Cook University will make it available for use within the University Library and, by microfilm or other photographic means, allow access to users in other approved libraries. All users consulting this thesis will have to sign the following statement: "In consulting this thesis I agree not to copy or closely paraphrase it in whole or in part without the written consent of the author; and to make proper written acknowledgment for any assistance which I have obtained from it". Beyond this, I do not wish to place any restriction on access to this thesis. Users of this thesis are advised that the policy for preparation and acceptance of Masters theses does not guarantee that they are entirely free of inappropriate analyses or conclusions. Users may direct enquiries regarding particular theses to the relevant College head.

Declaration

I declare that this thesis is my own work and has not been submitted in any form for another degree or diploma at any university or other institution of tertiary education. Information derived from the published or unpublished work of others has been acknowledged in the text and a list of references is given.

Acknowledgements

I'd like to thank my three supervisors Michael Bird, Cassandra Rowe, and Chris Wurster. Without their help, guidance, and encouragement the probability of me getting a Master Degree would have been zero. I would like to thank the present, past and future Traditional owners of the Kinrara region, the Gugu Badhun Aboriginal nation upon who's land this study is based. I would like to thank the property owners Shane and Robyn O'Brien who access to the Kinrara Lagoon which is located on their estate adjacent to Kinrara National Volcanic Park. I would like to thank Julies James who worked on sampling the core with me for her Masters and my project. I would like to also thank the following people for listening to me ramble about my study or helped me in some manner, in no particular order: Jen Whan, Ting Li, Emma Rehn, Mike Kneppers, Xennephone Hadeen, Jordi Nelis, Jordahna Haig, Costijn Zwart, and Michael Brand. Lastly, I would like to thank my partner Amba-lea Nowlan who listened to the largest amount of rambling.

This research was partly funded by AINSE award ALNGRA11038, the Australian Research Council Centre of Excellence for Australian Biodiversity and Heritage (CE170100015) and an Australian Research Council Laureate Fellowship to M.I.B (FL140100044).

Abstract

Fire is an integral component of many Australian ecosystems, and tropical savannas in particular. Reconstructing past fire regimes can help us better understand the links between fire, vegetation, climate and humans over long temporal and large spatial scales. Further, a relative paucity of palaeoenvironmental records exists in the southern hemisphere compared to the northern hemisphere.

This project is based on a 7-meter (m) sediment core collected from Kinrara Lagoon, a permanent, spring-fed water body in the savanna region of northeast Queensland. The aim of the project is to determine the palaeoenvironmental history of the region over the period represented in the core with a particular emphasis on developing a record of fire incidence and intensity for the region surrounding the lagoon. Five stratigraphic units from Unit 1 at the top/ modern to Unit 5 are evident in the core, and a chronology for the core was developed from 37,000 yrs cal BP to the present based on 17 radiocarbon dates. The study pairs a geochemical measure of pyrogenic carbon (PyC) – stable polycyclic aromatic carbon (SPAC) abundance by hydrogen pyrolysis - with charcoal particle counting to help infer the fire history of the study region. Stable carbon isotope composition of SPAC is also used to determine the proportions of C_4 (grassy) and C_3 (woody) vegetation burnt and the total organic carbon to provide information on lagoon processes.

The late Pleistocene section from time 37,227 to 11,500 cal yr BP (Unit 5) is dominated throughout by lithogenic elements, including basaltic fragments in the upper section, indicating that the unit was not deposited in a lagoon environment, and there was local active volcanism. Starting at 37,000 cal yr BP C_3 vegetation was

being burnt which progressed to being C_4 dominated implying a period of significantly lower rainfall. This likely corresponds to the last Glacial Maximum, though the timing of changes in this interval are poorly constrained. This period suggests relatively low levels of fire throughout.

The early Holocene from 11,500 to 8750 cal yr BP, (Units 4) incorporates the initial damming of the lagoon by basalt lava from the Kinrara Volcano and rapid carbonate sedimentation, against a regional background of rising sea levels and the establishment of wetter and warmer Holocene environments. The lagoon underwent a rapid transition to a much larger lagoon-like water body, because of damming, and because of a regional trend to higher rainfall. Carbonate sedimentation was the result of CO_2-rich Spring water that has maintained a permanent water body since damming. Fire intensity and frequency remained relatively low during this period when compared to the entirety of the record. The $\delta^{13}C_{SPAC}$ values indicated a change from a dry grassy savanna to a wooded savanna over this period.

The middle Holocene 8750 – 3600 cal yr BP (Units 3), was the warmest and wettest period in the record and equates broadly to the Holocene optimum in Australia. The monsoon was reliable and strong, leading to the regular seasonal flushing of the lagoon and hence the cessation of carbonate precipitation. During this phase, two short periods of intense fire occurred, the first at 7778 cal yr BP and the second at 6924 cal yr BP. These two major peaks are considered to relate to local volcanism at the time. Apart from the two major peaks, the middle Holocene was uniformly and stable in terms of fire intensity and frequency, higher than in Unit 4.

The late Holocene section of the core represented in Units 2 and 1 covers 3600 cal yr BP to the present. This period encompasses the time associated with an inferred intensification of the ENSO at ~2800 cal BP, associated with increased regional climate variability including drought events, evident in the episodic resumption of carbonate precipitation and attendant changes in fire incidence. Clear indicators of indigenous fire management, expressed as increased char flux, decreased MAR_{SPAC} and increased $\delta^{13}C_{SPAC}$ are evident only from ~500 cal yr BP. European occupation and resultant cessation of indigenous fire management in the last Century saw a return to less frequent, but more intense fires.

Table of Contents

List of Figures

List of Tables

List of Abbreviations

cal yr BP	Calibrated years before present
EA-IRMS	Elemental Analysis-Isotope Ratio Mass Spectrometry
ENSO	El Niño Southern Oscillation
HyPy	Hydrogen Pyrolysis
IPWP	Indo-Pacific Warm Pool
ITCZ	Intertropical Convergence Zone
JCU	James Cook University
Ka	Kiloannum (thousands of years ago)
Km	Kilometre
LGM	Last Glacial Maximum
m	meter
NT	Northern Territory
PNG	Papua New Guinea
PyC	Pyrogenic carbon
QLD	Queensland
SOI	Southern Oscillation Index
SPAC	Stable Polycyclic Aromatic Carbon
TOC	Total organic carbon
$\delta^{13}C$	Carbon isotope composition

Chapter 1. Introduction

1.1 Fire in the savanna environment:

Globally, savannas represent a wide variety of vegetation types including woodlands, grasslands, sclerophyll woodlands, plains, steppe and heathlands (Tothill et al., 1985; Rowe et al., 2022b). They are characterised by the coexistence of discontinuous scattered tree cover (woody) – predominantly *Eucalyptus* in Australia – above a grassy understory. Usually, savannas develop in tropical and subtropical climatic regions (Figure 1) (Tothill et al., 1985; Moore et al., 2016), and tropical savannas occupy around one-third of Australia, from Broome (Western Australia, WA) in the tropical north to Cape York Peninsula in Queensland (Qld) to the east, encompassing the top end of the Northern Territory (NT) and the surrounds of the Gulf of Carpentaria (Figure 2), herein referred to as northern Australia (Ritchie & Bolitho., 2008; Edwards et al., 2013). These tropical savannas merge southward into subtropical savanna zones (Tothill et al., 1985).

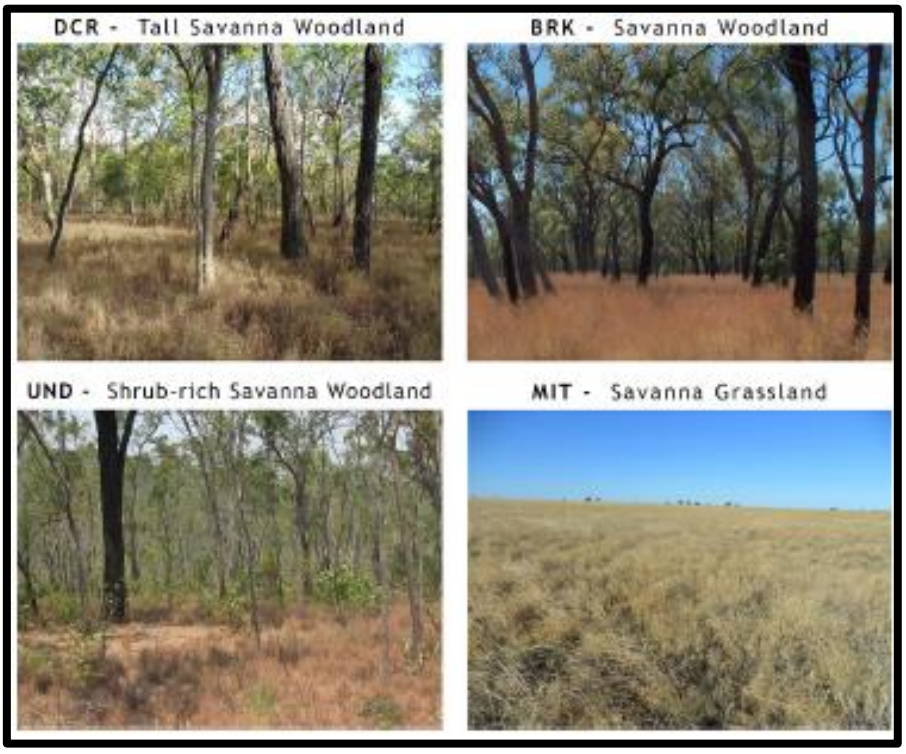

Figure 1: Savanna landscapes (Saiz et al., 2015).

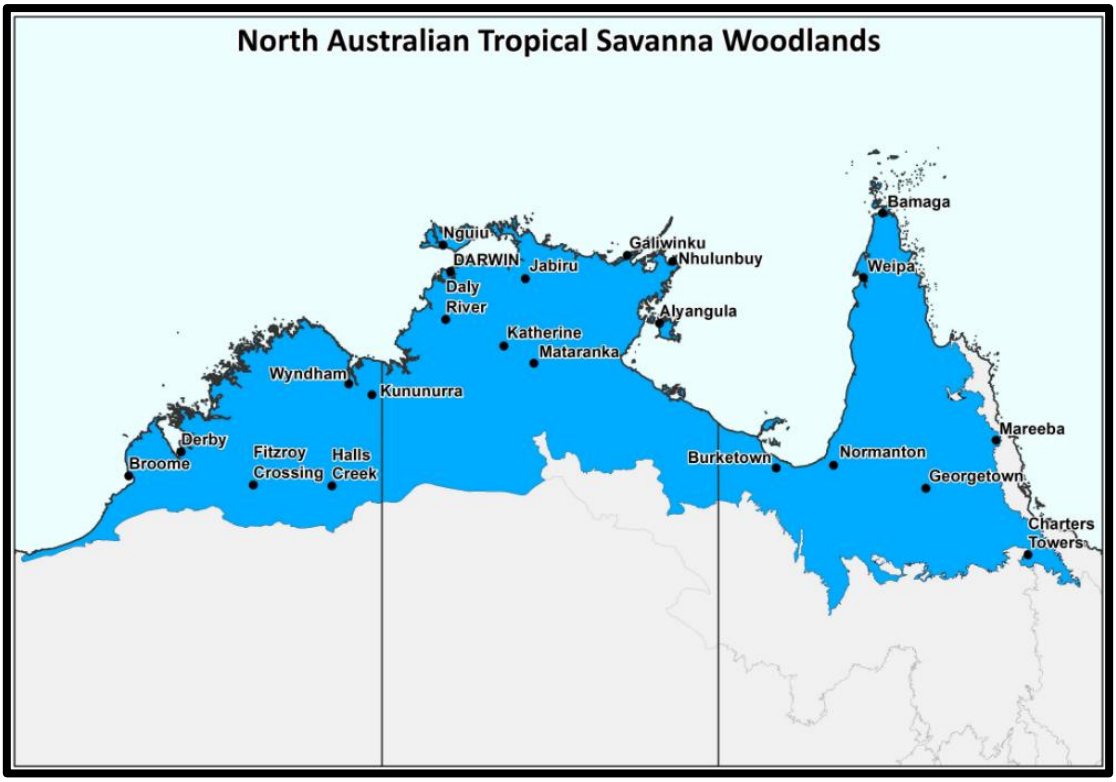

Figure 2: North Australian Tropical Savanna Woodlands (Australian Government Department of Climate Change, Energy, the Environment and Water., 2021).

In a global context, Australian savanna environments are largely intact and in good ecological health, valuable in this regard - a status attributable to low population density and minimal infrastructure (Andersen et al., 2003; Scheiter et al., 2015). Savanna dynamics are governed by the interplay of a variety of factors including climate (particularly seasonal and inter-annual changes in water availability), fire and human activity.

This thesis will first discuss what is known about the savanna regions of Australia, in the present and the past, and then provide a new long-term record of savanna landscape dynamics derived from a core collected from Kinrara Lagoon. The primary focus of this thesis is on Holocene fire incidence and vegetation change around the site.

Fire is a major factor controlling the productivity and structure of savannas (Moore et al., 2016). Australia, and particularly its northern regions, represent one of the most fire-prone landscapes in the world (Hesse et al., 2004; Yates et al., 2008; Ma et al., 2016). Australia is also the driest inhabited continent on Earth (Hesse et al., 2004; Yates et al., 2008; Ma et al., 2016). Fire can decrease landscape stability, affect biogeochemical, and hydrological processes, change radiation balance and greenhouse gas emissions (Crutzen & Goldammer,. 1993; ; Yates et al., 2008; Mooney et al., 2011; Beringer et al., 2015; Marlon et al., 2016; Voelker et al., 2016). Fire influences the diversity, abundance, and distribution of flora and faunal species across a landscape (Bond et al., 2003; Beringer et al., 2015). It also influences the interplay between the trees and grasses through the suppression of woody sapling growth, maintaining or altering the structure of these ecosystems (Bond et al., 2003; Beringer et al., 2015).

Fire is such a dominant influence on woody biomass in these savanna regions, that there is generally lower actual tree cover than potential vegetation estimates, a phenomenon also partly attributable to the seasonal nature of rainfall. High amounts of grass biomass developed in the wet season cure and then burn during the dry season (Maraseni et al., 2016; Ondei et al., 2017). These grasses are highly flammable and cover large areas. They form loosely packed fuel loads with a significant surface-to-volume ratio that enhances burning (Rowe et al., 2022b). This then produces a flame zone - “fire trap” – near the ground which suppresses tree seedling establishment (Saiz et al., 2018; Rowe et al., 2022b). Burning of the groundcover and understory keeps tree seedlings down, though typically larger trees that have escaped the fire trap are less impacted (Saiz et al., 2018). Fire is a major feature of savanna regions globally to the extent that the burning of these ecosystems contributes over

one-third of the total biomass burnt worldwide each year, with the tropical savanna regions of Australia sustaining on average 400,000 km^2 burnt each year (Russell-Smith et al., 2009; Andersen et al., 2012; Meyer et al., 2012). If a savanna is not maintained by regular and consistent fires, woody thickening can occur with eventual forest encroachment (Moore et al., 2016).

Fire is an integral aspect of many Australian ecosystems, and savanna environments in particular. Reconstructing past fire regimes can help us better understand the links between fire, vegetation, climate systems and human activity over large temporal and spatial scales (Mooney et al., 2011; Finsinger et al., 2014; Scheiter et al., 2015; Saltré et al., 2016). Australia-wide, cooler climatic periods are regarded as times of reduced fire occurrence, with warmer climatic phases characterised by more burning (Mooney et al., 2011; Barr., 2012). During cooler, drier periods, the biomass availability for burning is generally lower. Under such climates, grass proportions expanded in savannas to replace woody taxa. Re-thickening by woody plants during warmer and wetter climates helped facilitate an increase in fire. In general, therefore, fire activity during the Last Glacial Maximum (LGM) was low (Black et al., 2006; Petherick et al., 2017)

The manner and degree to which human arrival into Australia (65,000 – 45,000 cal yr BP) altered fire regimes is hotly debated (O'Connell & Allen., 2004). Some sources suggest that Aboriginal arrival had a direct effect on fire regimes through the increase of ignition via cultural burning practices (Johnson., 2016). An alternative explanation is that the arrival of people had an indirect effect on fire regimes by the hunting and consequent extinction of megafauna which caused an increase in dry fuel loads and hence an increase in burning (Johnson., 2016).

Alternatively, some sources suggest there is insufficient evidence to support either of these hypotheses, and instead the Aboriginal peoples contributed only localised changes in fire regimes, and the changes seen in palaeo records are primarily due to changes in climatic conditions (Bowman & Prior., 2004; Black et al., 2006; Mooney et al., 2011; Notaro et al., 2011).

It has been suggested that current palaeoenvironmental reconstruction techniques may not be able to pick up the influence of Aboriginal fire practices within the records and that therefore palaeoenvironmental records can only enable the identification of climatic influences (Mooney et al., 2011). It is strongly and consistently concluded that European colonisation and the associated timeline of mass landscape change and development over the last 240 years has altered fire regimes to a significant degree from the period characterized by indigenous fire management (Mooney et al., 2011).

1.2. Fire Impacts on Savanna dynamics:

Fire acts as both a destructive and regenerative force. It plays a key role in the development and the maintenance of many ecosystems around the world, but particularly tropical savannas (Mooney et al., 2011; Beringer et al., 2015). Fire influences many key ecological aspects of savanna dynamics including biodiversity; distribution of fauna and flora across the landscape; biogeochemical cycling of carbon, water and nutrients; the type and quantity of emissions released into the atmosphere; and radiation balance (Crutzen & Goldammer, 1993; Mooney et al., 2011; Fitzsimons et al., 2012; Catullo & Scott Keogh., 2014; Beringer et al., 2015; Scott et al., 2016). The most important characteristics that determine fire regime in savannas are the timing of seasonal burning, fire intensity, and fire frequency. These

are driven by fuel load and fuel moisture in turn modulated by rainfall, rainfall seasonality, temperature, windspeed and anthropogenic factors (Thomas & McAlpine., 2010; Beringer et al., 2015).

The Queensland dry season typically starts in May. However, the top grass layer continues to contain too much moisture immediately following the wet season, which results in burning being patchy in nature during this period (with an estimated intensity <1000 kWm^{-1} ; Edwards et al., 2013; Beringer et al., 2015). By the end of the dry season when the litter and grass biomass has accumulated on the soil surface and has become fully cured, larger and more intense fires occur (Andersen et al., 2003; Beringer et al., 2015).

Fire frequency and intensity is related to vegetation diversity in the savanna regions and many woody species that are present in these environments have become fire tolerant. Eucalypts, for example, have developed mechanisms to only release seeds/ buds after heating by fire. Some trees have developed tall canopies in order to protect their leaves and minimise fire damage (Mooney et al., 2011; Fitzsimons et al., 2012; Catullo & Keogh., 2014; Beringer et al., 2015; Voelker et al., 2016). In Australia, 'natural' fires are lighting-triggered, with anthropogenic fires lit by either Aboriginal cultural burning practices or as part of European fire management programs increasingly aimed at mimicking traditional burning practices (Beringer et al., 2015).

Fire is one of fundamental drivers of productivity in savanna regions (Moore et al., 2016). Juvenile tree seedling mortality rates, tree growth and plant demographics are all affected by fire regime (Moore et al., 2016). A bottleneck on tree

recruitment is imposed by fire which determines the demographics of tree recruitment and the survivability of fire-sensitive species such as *Callitris Intratropica* (Trauernicht et al., 2016). When fire regime changes – for example if fire return interval or intensity is reduced, the region may undergo thickening of woody vegetation and forest encroachment can occur (Moore et al., 2016). Conversely an increase in fire intensity is linked to the degradation fire sensitive woody vegetation and potentially a decrease in tree cover (Trauernicht et al., 2016)

1.3 Sediment coring as a source of information:

Permanent water bodies are a source of long, continuous sedimentary sequences capable of providing environmental records ('archives') that span hundreds to many thousands of years. Sediments contain various proxy indicators of local environments, including pollen, charcoal, carbonates, phytoliths and geochemical markers (Birks et al., 2001). These proxies offer a glimpse into the landscape, including the fire history, of the area surrounding the water body (Birks et al., 2001). By linking changes in these sedimentary proxies to an environmental variable (e.g. an aspect of climate), proxy data can then be used to infer multiple aspects of the local surrounding area over time. Such information can include changes in vegetation type(s), water levels, fire frequencies and their intensity (Bird et al., 2020). From the site level, once multiple records are compiled over a larger land area, wider regional inferences can be drawn in relation to the nature and timing of past environmental change. Unfortunately, savanna landscapes across Australia have yielded relatively few sedimentary records extending through the Holocene into the Pleistocene, largely because of the paucity of permanent water bodies in the seasonal tropics. This has resulted in limited regional long-term

palaeoecological knowledge, especially in the context of fire which is such an important influencer of savanna landscapes (Wurster et al., 2021a).

Poor record recovery is due to multiple factors including but not limited to, logistics in remote and sparsely populated areas, and the degradation of potential proxy indicators through the seasonal drying of most water bodies (Bird et al., 2020). A few notable Australian palaeoenvironmental records from within modern-day savanna regions include Girraween (NT) (Rowe et al., 2021; Wurster et al., 2021a), Sanamere (Qld) (Rehn et al., 2021a; Rehn et al., 2021b), Marura (NT) (Rowe et al., 2022a). with more sites discussed in section 2.1.

1.4 This project:

This project used a 7-meter (m) sediment core collected from Kinrara Lagoon, in the savanna region of northeast Qld, to infer the palaeoenvironmental history of the region with a particular focus on developing a record of fire spanning late Pleistocene and Holocene. The study pairs a geochemical measure of pyrogenic carbon (PyC) – stable polycyclic aromatic carbon (SPAC) abundance by hydrogen pyrolysis - with charcoal particle counting to help infer the fire history of the study region (Bird & Ascough., 2012; Bird et al., 2015; Saiz et al., 2015; Wurster et al., 2015; Wurster et al., 2021a). The stable carbon isotope composition of SPAC will be used to determine the past proportions of C_4 (grassy) and C_3 (woody) vegetation burnt in the Kinrara record. The study also involves development of a robust chronology for the Kinrara record utilising radiocarbon dating of SPAC, as well as macro-organic material. The proxy records produced in this study provide novel new information on fire frequency and intensity since the late Pleistocene, in an understudied savanna region. The project contributes to elucidating and understanding the broader fire history of the wider northeast Qld environment.

Furthermore, this study, in using sites such as Kinrara, can assist conservation-management practices by revealing how these poorly documented savanna systems respond to, and recover from, varying fire activity over time (Willis et al., 2007; Froyd & Willis., 2008). In turn, past records can be used by Earth system models to help understand how savanna areas may react to future climate change (Willis et al., 2007; Froyd & Willis., 2008). Reconstructions of past fire regimes can assist in the forecast of how future anthropogenic impacts will affect burning patterns and vegetation responses (Willis et al., 2007; Froyd & Willis., 2008).

This thesis is divided into an introduction, six chapters and a conclusion. The first chapters review the Holocene palaeoenvironmental history of northeastern Australia; methods used in the reconstruction of past fire and vegetation histories; a study area description; specific project methods; results and a discussion. In turn, the discussion will be broken up into four sections corresponding to the sedimentary units identified in the Kinrara core. The project aims to: (i) compare and contrast the sedimentary units; (ii) determine environmental changes as revealed by the geochemistry and char content and sedimentology of the units (iii) determine how inferred changes may correspond to climatic drivers and/or human influences; and (iv) evaluate similarities and differences between the Kinrara record and other surrounding palaeo records reported in the literature.

Chapter 2. Holocene Palaeoenvironmental History of Northeastern Australia

This chapter will first explore the general environmental trends across Australia during the Late Pleistocene and Holocene, to broadly frame the study. It will then narrow to detail palaeoenvironmental studies based within northern and northeastern Australia, discussing the proxies used within these studies to provide the more specific regional context. Although climatic and vegetation records are discussed, focus will be on those archives that have been used to draw inferences regarding past fire regimes. Geographically, this chapter starts within the Atherton Tablelands of northeast Queensland, a relatively intensively studied late Quaternary region north of the Kinrara site and expands from there.

The full Pleistocene epoch is considered to have spanned 2.58 million years ago to 11,700 calibrated years before present (cal yr BP). The last glacial cycle beginning ~129,000 years ago, peaked in glacial extent at the Last Glacial Maximum (LGM), centred at ~20,000±2000 cal yr BP (Rowe et al., 2021). Global ice sheets were at their most extensive and sea level was at its lowest at ~ 120 m below modern levels (Petherick et al., 2017). This resulted in a dramatic increase in the land area of the northeastern Australian study region, with Cape York Peninsula connected to New Guinea via the Torres Strait. The Indo-Pacific monsoon was inactive during the LGM and for a period after, resulting in changes in the distribution and amount of precipitation (Rowe et al., 2021). Decreases in temperature and lower atmospheric carbon dioxide (CO_2) were also characteristic of glacial periods (Rowe et al., 2021). Given Australia was generally cooler and drier, this influenced vegetation. Grass proportions expanded to replace woody taxa in some areas (Stevenson et al., 2001)

and such a change in vegetation structure resulted in reduced landscape burning (Mooney et al., 2011).

The Holocene period was initiated around 11,700 cal yr BP, extending to the present day. In a local context, three sub-stages in time and environment are incorporated, termed the early (~ 11,700 to 8200 cal yr BP), middle (~ 8200-4200 cal yr BP), and late Holocene (~ 4200 to 0 cal yr BP) (Walker et al., 2012). Compared with the Late Pleistocene, Holocene temperatures and precipitation levels were elevated, accompanied by increased levels of CO_2 and higher sea level. For northern Australia, monsoonal reactivation is estimated as early as 14,000 to 12,000 cal yr BP, and/or otherwise enhanced from approximately 8000 cal yr BP (Hanebuth et al., 2000; Wyrwoll & Miller, 2001 Hesse et al., 2004; Reeves et al., 2013; Burrows et al., 2014; Rehn et al., 2021a; Wurster et al., 2021b). The late Holocene is thought to be characterised by enhanced climatic variability (weakening of monsoon precipitation, and increased seasonality incorporating a more variable and extreme El Niño-Southern Oscillation, ENSO) (Denniston et al., 2013). The Holocene incorporated the most recent time of peak woody vegetation regrowth and increases in burning. Australia wide, many palaeoenvironmental records show fluctuating rises in charcoal from the LGM into the Holocene (Mooney et al., 2011).

2.1. Palaeoenvironmental studies:

When compared to the Northern Hemisphere, there is a general lack of late Quaternary data for the Southern Hemisphere. As such, most climate models are heavily biased in utilising records from the Northern Hemisphere (Carcaillet et al., 2002). This leads to models that under-represent and/or less accurately reflect Australian environmental responses to proposed anthropogenic climate change (Ma

et al., 2016). Developing a greater number of proxy environmental records from across the Southern Hemisphere is critical to improve our confidence and the predictive power of these climate change models (Ma et al., 2016).

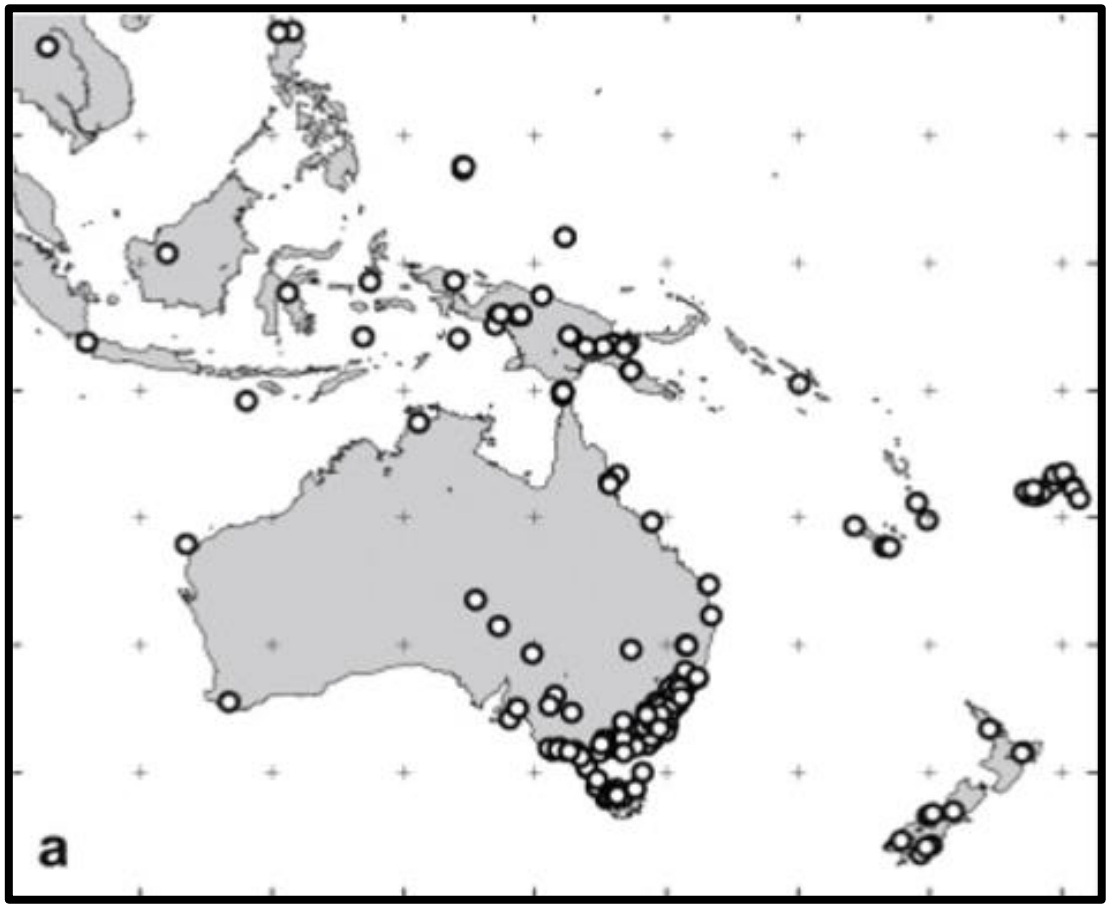

Figure 3: Distribution of Fire records (Mooney et al., 2011).

Along with the general shortage of Southern Hemisphere late Quaternary data, further paucity exists in palaeoenvironmental records representing northern Australia when compared to temperate eastern and southern Australia. This includes long-term fire records, as illustrated in Figure 3 and 4 (Kershaw, 1971; Kershaw et al., 2007; Reeves et al., 2007; Rowe, 2007; Barr, 2012; Mooney et al., 2011; Moss et al., 2013; Stevenson et al., 2015a; Stevenson et al., 2015b; Dixon et al., 2017; Field et al., 2017; Petherick et al., 2017). The scattered records representative of the northern regions of Australia are listed in Tables 1 and 2. As alluded to above, the lack of

permanent water bodies suitable for the preservation of organic sediment materials has contributed to the biased nature of the research effort represented in Figure 3. Many northern Australian waterbodies undergo site scouring by intense monsoon runoff, or most commonly are simply seasonally ephemeral in nature (Field et al., 2017). The Atherton Tablelands (see Table 1) has provided the most extensive series of long-term records underpinning an understanding of northern Australia, but its atypical wetter, rainforest regions, may not be representative of the greater region.

Figure 4: Location of Kinrara Lagoon and other palaeo records relative to the coastline of modern Australia (white line) and maximum extent of lower sea level during the Last Glacial Maximum.

It has been suggested that there was a steady increase in burning in the Australian tropics from around 73,500 to 59,000 cal yr BP, although this is based on few records (Mooney et al., 2011). Mooney et al (2011) also concluded that studies with data older than ~70,000 cal yr BP are 'too noisy' to enable any conclusive remarks to be made about even broad trends in burning (Mooney et al., 2011). Between 50,000 and 45,000 cal yr BP there was a significant change from rainforest to sclerophyll vegetation on the Atherton Tablelands, as indicated by the record from Lynch's Crater (Mooney et al., 2011; Rule et al., 2012; Lopes dos Santos et al., 2013). At this site approaching and during the LGM ~30,000 – 18,000 cal yr BP, there was a reduction in burning coinciding with lower temperatures, increased aridity, and less vegetation cover. Relatively reduced burning was also recorded at the beginning of the Holocene, followed by a steady rise over the mid to late Holocene (Mooney et al., 2011; Petherick et al., 2017).

An increase in fire occurrence during the Holocene, significant enough to partially inhibit the expansion of rainforest in the wetter parts of the Queensland region, has been suggested (Rule et al., 2012; Butler et al., 2014). The late Holocene in Northern Australia has been shown to be relatively drier, with localised aridity and increased environmental variability between different locations (Mooney et al., 2011; Reeves et al., 2013). An overall synthesis of the nature of fire regimes across Australasia was conducted by Mooney et al., (2011) who identified that, generally, across all of Australia there were charcoal peaks at 15,000 – 16,000, 11,000 – 10,000 and 4500 – 2500 cal yr BP. It has also been suggested that a millennial-scale dry event occurred at 4000 cal yr BP in Southeast Asia and northern Australia (Burrows et al., 2014).

2.1.1. Studies across the Queensland Atherton Tablelands:

Table 1: Palaeo records across the Atherton Tablelands.

Site Location	Age of record (cal yr BP)	Proxies	Distance from Kinrara (km)
Lynch's Crater, Tablelands, QLD	~230,000	Pollen, charcoal, tephra	~140
Lake Euramoo	~23,000	Pollen, charcoal	~150
Quincan Crater	~5000	Pollen, charcoal	~140
Bromfield Swamp	~4500	Pollen, charcoal	~130
Witherspoon Swamp	~8000	Pollen, charcoal	~90
Lake Barrine	~18,000	Lithological, pollen, charcoal, mineralogy, compound specific isotopes	~140
ODP-Site 820	~250 000	Coastal record, Pollen, oxygen isotopes	~240

The Atherton Tablelands is a geological region west of Cairns, up to ~120 km inland, characterised by evergreen rainforests, freshwater wetlands and eucalypt woodlands (Neldner et al., 2023). The Tablelands extend over 11,000 km^2 and are mostly more than 700 m above sea level (Neldner et al., 2023). The Atherton Tablelands experiences a summer-rain monsoon season (characterised by north-westerly winds) and a winter dry season (with southeast trade winds) (Coulter et al., 2009). The area is sensitive to ENSO cycles and is subject to cyclones. (Moss et al., 2012). The region includes a series of volcanic crater lakes, used as a unique source of late Quaternary information, both well preserved and extensive in nature (Figures 3 and 4). Six key crater lake records have been published from across the Atherton Tablelands including, Lynch's Crater, Bromfield Swamp, Lake Barrine, Witherspoon Swamp, Quincan Crater and Lake Euramoo (Table 1). A pollen and oxygen isotope study has also been done on a ~70 m marine core around 100 km off the coast from

Lynch's Crater which spans 250,000 cal yr BP (Moss & Kershaw., 2007). As a collective, numerous environmental complexities have been revealed and a nuanced vegetation history enabled. Lynch's Crater is the most highly regarded and cited, serving as the reference record for the region (Figure 3, 4 and Table 1) (Coulter et al., 2009).

Lynch's Crater has a record spanning the past 230,000 cal yr BP and has been shown to have captured proxy inputs from a wide area, including tephra originating from PNG (Kershaw., 1971; Haberle et al., 2001; Haberle & Ledru, 2001). Of relevance to this project is the lack of uppermost site sediments and therefore the lack of a complete Holocene record (Kershaw et al., 2007; Coulter et al., 2009). Overall, Lynch's Crater documents complex expansions in rainforest formations during wetter interglacial periods, alternating with expansions in sclerophyll vegetation types (e.g. savanna) during drier glacial periods (Kershaw et al., 2007). One key feature of the record from Lynch's Crater is the shift from rainforest to sclerophyll vegetation at around 45,000 cal yr BP. This has been attributed to human burning, although there is no archaeological evidence to support this claim. This proposal has been called into question based on new results from other areas suggesting that the change in fire regime was climate-related rather than relating to imposition of an anthropogenic fire regime. For example, independent records from New Caledonia can be linked to the Lynch's Crater record given both areas experienced a decline in *Araucaria* and expansion of sclerophyll forests at 45,000 cal yr BP, suggesting climate-related vegetation change (Stevenson & Hope, 2005). Furthermore, it has been suggested that vegetation change was influenced by changes in northern hemisphere insolation and ice volume, operating its effect on the

wider Queensland-western Pacific region through sea level and sea surface temperature changes (Kershaw et al., 2007).

The pollen and charcoal records from Quincan Crater and Bromfield Swamp indicate occupation of the catchments by sclerophyll vegetation from around 9700 to 7000 cal yr BP, thereafter, transitioning to a warm temperate rainforest until 2,000 cal yr BP. Across the past 2000 years sclerophyll plant communities reappeared (Kershaw, 1971; Moss et al., 2012). The record from Quincan Crater suggests a decrease in precipitation from around 2,000 cal yr BP onwards. Both Quincan Crater and Bromfield Swamp indicate a dry period with charcoal peak at around 4 060 cal yr BP, possibly associated with ENSO intensification (Burrows et al., 2014).

A pollen record spanning 23,000 cal yr BP has been collected from Lake Euramoo. This record indicates between 23,000 – 16,800 cal yr BP a sclerophyll woodland was present. This woodland transitioned over the next few thousand years to warm rainforests (16,800 to 8600 cal yr BP), and to dry degraded subtropical rainforest in the middle Holocene (Haberle, 2005; Moss et al., 2012). Charcoal accumulation into the lake increased significantly after 2700 cal yr BP (Donders et al., 2007). It has been suggested the landscape around this location is sensitive to both climate changes and human activity (Haberle, 2005). Quincan Crater and Bromfield Swamp are two good records that provide independent correlation to the Lake Euramoo record, thereby revealing a coherent broader regional trend (Donders et al., 2007).

Witherspoon Swamp is located south of Lynch's Crater and is currently dominated by sclerophyll woodlands (Moss et al., 2012). This 8000-year record is

important as it reveals long-term sclerophyll boundary trends within the Tableland wet tropics zone (Moss et al., 2012). Witherspoon Swamp's catchment was not subject to an expansion of rainforest during the Holocene (Moss et al., 2012). This site shows where the rainforest-sclerophyll boundary formed, and that it was highly stable within the region during the Holocene (Moss et al., 2012).

The last site mentioned here from the Tablelands region is Lake Barrine. Walker (2007) initially published a record from 16,000 cal yr BP the end of the Pleistocene and focused on the Holocene history of the lake environment. This study presented lithological descriptions, grain size data, charcoal data, pollen data, mineralogy, and applied 211 radiocarbon dates to the sediment sequence, yet only managed a brief treatment of vegetation and climate change. Walker (2007) focuses mostly on the water level of the lake, suggesting Lake Barrine was drier during the Pleistocene with occasional intense rainfall events during the early Holocene, including a change in precipitation and evaporation balance to wetter conditions and causing local erosion around 8000 cal yr BP (Walker, 2007). From 7300 cal yr BP rainforest started to occupy the catchment, persisting through to the present (Walker, 2007). Unfortunately, trends in the charcoal data are not explored, including what may be reasons behind an increase in charcoal between 8800 to 8200 cal yr BP (Walker, 2007). More recent studies have been undertaken at Lake Barrine, expanding our understanding of climate across the surrounding area, but without further development on local fire histories (charcoal was outside of the scope of these new papers) (Li et al., 2022; Li et al., 2023).

The Atherton Tablelands have provided several detailed long-term records that underpin understandings of northeastern Australian wet rainforested regions,

including demonstrating the savannas covered parts of the Tablelands in the past particularly during glacial phases. However, less work has been done that traces the history of rainforest-sclerophyll boundary dynamics and less still to understand the environmental history of the savanna ecosystems that abort the tablelands to the west (Kershaw, 1971; Kershaw et al., 2007).

2.1.2. Studies across the wider Savanna region:

Table 2: Palaeo records across the wider region.

Site Location	Age of record (cal yr BP)	Proxies	Distance from Kinrara
Lake of Carpentaria	~130,000	Ostracoda	~600
Complied records across New Caledonia	~24,000	Pollen, charcoal	~2000
Complied records across Papua New Guinea	~20,000	Charcoal	~1200
Complied records across Indonesia	~20,000	Charcoal	~2800
Gulf of Carpentaria, Vanderlin Island and Groote Eylandt	~10,000	Pollen, Diatoms	~600
Eastern Torres Straights	~9000	Pollen, charcoal	~950
Big Willum Swamp	~8000	SPAC, charcoal	~700
Sanamere Lagoon	~8150 - 6600	SPAC, charcoal	~850
Girraween Lagoon	~150,000	Pollen, charcoal, SPAC	~1600
Kinrara Lagoon	~37,000	Carbonates, ITRAX	0
Marura	~10,700	Pollen, charcoal,	~1200

There are a number of palaeoenvironmental records that have been developed from across the wider north Queensland to Northern Territory region, relevant to the discussion of past Australian savanna dynamics. These include Big Willum Swamp, records from the Torres Straits, Gulf of Carpentaria marine cores, Girraween Lagoon, Sanamere and Marura. Further still, expanding into areas that share climate

attributes with Australia, or were once connected to Australia, informative records can be found in Papua New Guinea New Caledonia, and Indonesia (Figure 4 and Table 2).

Big Willum Swamp is located close to Weipa, western Cape York Peninsula (Qld). This palaeo-record covers from 8000 to 0 cal yr BP. Data suggests that Big Willum was of an ephemeral nature between 5700 to 2200 cal yr BP with a low sedimentation rate. After 2200 cal yr BP, the site became a stable, permanent lake, with increased sedimentation (Proske et al., 2017b). From 600 - 400 cal yr BP the lagoon expanded further, and two significant burning periods – one at around 1000 cal yr BP and during the 19th century – were captured (Stevenson et al., 2015). A second study from Big Willum was published in 2021, spanning 3900 cal yr BP to present reveal an increase in fire around 1700 cal yr BP that peaked between 600 to 0 cal yr BP (Rehn et al., 2021a). In the same Cape York Peninsula study, Rehn et al. (2021) examined Sanamere Lagoon, with a record spanning 8000 – 6600 cal yr BP and showed relatively high fire intensity between 8000 – 7900 cal yr BP. This intensity sharply declined to the end of the record (Rehn et al., 2021b). Projects at Big Willum and Sanamere serve as examples in how to utilize multiple techniques in order to interpret the many features of a past fire regime, by combining pyrogenic carbon (as a proxy for fire intensity) and charcoal counting (as a proxy for fire frequency).

Pollen records across the Torres Strait – including Tiam Point, Zurath, Waruid, Boigu Gawat – have shown that mangrove and swamp communities dominated regional island coastal zones between 6 000 to 3 000 cal yr BP (Rowe, 2007). Inland island areas changed from rainforests and Myrtaceae-forests to open

sclerophyll woodlands (savanna) from 3 000 cal yr BP the present (Rowe, 2007). It is clear from archaeological evidence that the Torres Strait had a human presence since 9000 cal yr BP and became widely populated after 3500 – 3 000 cal yr BP (David et al., 2004; Rowe., 2006). After 4000 cal yr BP a change in vegetation resulted in a decline in tree cover coupled with an increase in charcoal abundance in swamp sediments. It was concluded that an increase in population brought about environmental changes in the island region (Rowe., 2007). Specifically, from 3800 – 3300 cal yr BP, Myrtaceae pollen percentages dropped sharply with the introduction of other open shrub species (Rowe., 2006). Reductions in forest cover were interpreted to be the result of increased fire under drier conditions, but it was considered "unlikely that naturally occurring fires could have had such a marked impact; that an anthropogenic cause is more likely" (Rowe, 2006, p. 283). Due to the close research relationship between archaeology and palaeoecology within these Torres Strait studies, they offer a clear understanding of what Holocene proxy signatures to interrogate when investigating how people directly influenced their environment.

A 130 000-year marine sediment record from the now Gulf of Carpentaria (the Gulf) has been used to provide a backdrop climatic and sea-level record for the Australian savanna region. It was found that a lake, Lake Carpentaria, was featured within of the Gulf landscape between approximately 40,000 to 12,000 cal yr BP (Reeves et al., 2007). Within this phase, Lake Carpentaria's freshest water period spanned 17,500 to 14,000 cal yr BP, suggesting higher effective regional precipitation occurred at this time. Data from islands within the Gulf add to the climate picture. The Vanderlin Island record, for example, spans the last 10,000 cal yr BP and indicates an intensification of the Australian monsoon through the early Holocene,

synchronous with sea level stabilization 7500 – 4500 cal yr BP (Prebble et al., 2005). Swamp records from Groote Eylandt confirm increased effective precipitation during the early Holocene, with similar estimated maximum delivery between 8400 to 4500 cal yr BP (Donders et al., 2007). Holocene palaeoenvironmental records from mainland NT are consistent with the climatic evidence from the Gulf reinforcing the regional nature of changes (Rehn et al., 2021b; Wurster et al., 2021b). Based on all these records, monsoonal activity and maximum precipitation in the middle Holocene was followed by a marked decline in moisture availability, after 3700 cal yr BP. This reduction in effective precipitation is possibly the result of an ENSO intensification (e.g. Prebble et al., 2005). Information from the Gulf and NT sites provide insight into what climatic trends may be influencing environments at Kinrara.

Two new study sites - at Marura and Girraween Lagoon – which are located west of the Gulf of Carpentaria in the top end of the Northern Territory have provided a breadth of palaeo knowledge from within the savanna regions (Figure 4). Pollen was explored in the Marura record which spans 10,700 cal yr BPs to present. At the 10,700 cal yr BP mark the lake was ponding with sponge growths indicating a swampy wetland and by 8800 cal yr BP the lake became an open permanent surface water with cyclic shifts from sedges to water lilies occurring (Rowe et al., 2022a). There was a further increase in water depth between 7880 to 6910 cal yr BP, at which point the sedges were drowned out, due to around a 2.5 m of water increase (Rowe et al., 2022a).

Beyond the vegetation within the water system from 10,700 to 9000 cal yr BP grasses are within the record. Between 9000 to 8500 cal yr BP grasses started to

decline with a corresponding increase in eucalypt woody growth (Rowe et al., 2022a). By 6700 cal yr BP there are more trees than grasses within the environment with a peak of trees to grass ratio between 5000 to 3000 cal yr BP (Rowe et al., 2022a). Around 2500 to 1900 cal yr BP an expansion of grasses occurs with the rest of the record up until 200 cal yr BP an increase in woody vegetation again. A decline in microcharcoal was observed from 10,080 to 6450 cal yr BP with the last 200 cal yr BP to present showing an increase in charcoal (Rowe et al., 2022a). Overall, the area experienced its highest climate variability after 3000 cal yr BP (Rowe et al., 2022a). The changes across Marura were primary driven by climate, with fire being the secondary driver of site dynamics (Rowe et al., 2022a)

The Girraween record spans ~150,000 cal yr BP and is currently the oldest terrestrial record in the northern savanna regions of Australia. Unfortunately, currently only MIS4 has been published. Broadly from the published work during the LGM Girraween saw a 40% decrease in rainfall (Rowe et al., 2021; Wurster et al., 2021a; Rowe et al., 2022a). During the middle Holocene the gradually area transformed from an open to a more wooded savanna. A SPAC record for the late Holocene has also been published which showed that ENSO intensification may have driven an increase in the extent of Indigenous fire management from around 3000 cal yr BP onwards (Wurster et al., 2021a). Girraween lagoon – alongside Sanamere and Big Willum – have all used SPAC as a proxy for fire reconstruction and advanced the method and interpretation of these proxies. Sites across NT tend to react in concert with each other to environmental change, the Holocene to a more wooded structure (Rowe et al., 2022a).

In reviewing trends further afield, sites across Papua New Guinea (PNG) contain high levels of charcoal during the last glacial-Holocene transition (17,000 – 9000 cal yr BP) (Haberle et al., 2001). A further period of charcoal increase occurred 4500 to 2000 cal yr BP, in PNG as well as Indonesia at Lake Melingtang between 5400 to 5100 cal yr BP, and around 3300 cal yr BP at Kutai Peatlands (Haberle et al., 2001; Haberle & Ledru, 2001). Several authors suggest drying across the Indo-Pacific region, incorporating ENSO intensification, as the most likely cause of increased fire activity during the late Holocene (Haberle & Ledru, 2001; Gagan et al., 2004). Although people are known to have been present in both areas at the time , it was noted by both studies that there was archaeological evidence to suggest people were solely the cause of increased burning events (Haberle et al., 2001; Haberle & Ledru, 2001; Gagan et al., 2004; Hope et al., 2005).

The island of New Caledonia is located in the southwest Pacific Ocean, ~1600 km east of the Queensland coast. Although distant from the study area, New Caledonia is also influenced by ENSO events in a similar manner to northeastern Australia. Relevant comparisons may therefore be drawn for the past 24,000 cal yr BP (Stevenson et al., 2001; Stevenson, 2004; Stevenson & Hope, 2005). The Plum Swamp site, between 14,000 – 9000 cal yr BP, was subject to climate instability. This resulted in increased burning, altering the composition of lowland rainforests with the loss of woody taxa (e.g. *Macaranga* and *Pandanus*) (Stevenson et al., 2001). Environmental instability likely reflected the glacial to interglacial climate transition. Following this time, the environment around Plum Swamp stabilised until the arrival of people, considered to have resulted in a second charcoal peak, at around 3200 cal yr BP (Stevenson et al., 2001). At swamp Lac Saint Louis, vegetation gradually began to shift from mangroves to coastal savanna, beginning 4500 cal yr BP. From 3200 cal yr BP,

vegetation changes started to occur more rapidly, also attributed to the arrival of people (Stevenson, 2004; Stevenson & Hope, 2005). Palaeoenvironmental records from New Caledonia coupled with records in northern Australia (particularly the Atherton Tablelands), support hypotheses that the main controlling factors of environmental change in the Holocene were ENSO variability and sea-level change, rather than anthropogenic impacts (Wirrmann et al., 2011). Given New Caledonia was not subject to human arrival until ~4500 cal yr BP, it is a useful location for helping to separate proxy signals for the influence of climate versus people on landscapes.

2.2. Palaeo-view model for the last 21,000 years:

PaleoView is a is a global coupled atmosphere-ocean-sea ice-land general circulation model based on the Community Climate System Model simulations (CCSM3) that allows the generation of palaeo data across any global region since the LGM (Fordham et al., 2017). These simulations can model important climate events in the past such as Heinrich Events, the Bølling–Allerød, the Antarctic Cold Reversal and the Younger Dryas (Fordham et al., 2017; Liu et al., 2009). In caution, the authors suggest that there is a critical need for more observational evidence to clarify issues with the model (Liu et al., 2009), and PaleoView should only be used as a guide until direct records can be obtained. Moreover, it was created to see how models that use palaeo data - such as this study - are extremely limited and there is a great need for more palaeo data which will increase the predictive power of these models and move towards finer resolution outputs.

Two PaleoView output maps were created by using the free access PaleoView tool which shows a change in annual mean temperature and a percentage change in

annual mean precipitation relative to modern day (Figure 5). Unfortunately, PaleoView can only produce a coarse resolution output for the Australian region. Focusing in on the current savanna regions of today, there was no notable change in temperature until around 15,000 to 11,000 cal yr BP when temperature decreased by 2˚C compared to pre-industrial. The model then suggests that between 15,000 to 21,000 cal yr BP the area was around 2 to 3.5˚s lower than pre-industrial. The model results for annual mean precipitation suggest that the rainfall in the region was largely invariant over the past 9000 years followed by 15% less rain between 21,000 to 9000 cal yr BP. The model suggests that the LGM period for the Kinrara region was cooler and drier. This model output of a cooler and drier LGM will be explored in Chapter 7.

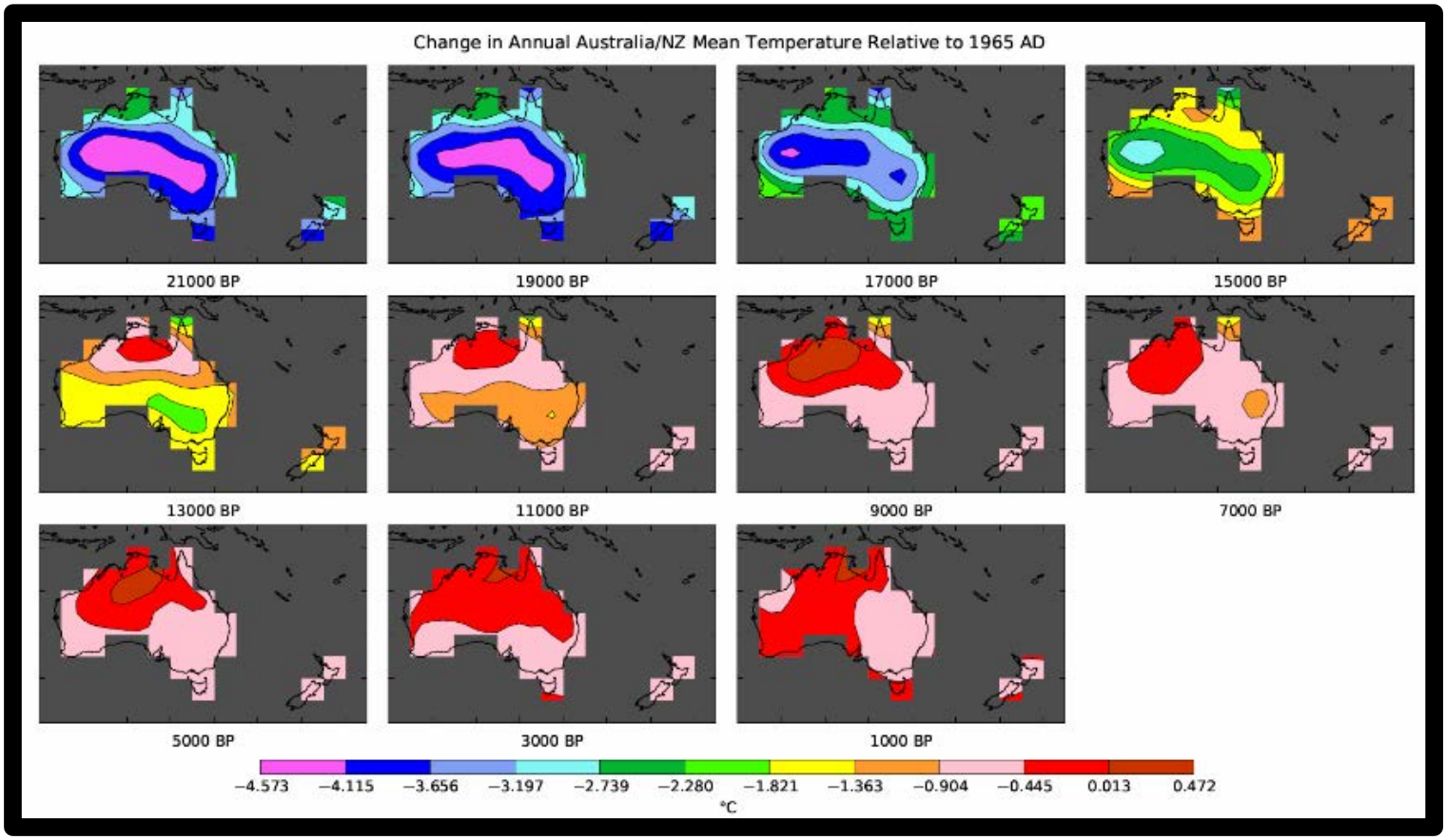

Figure 5: PaleoView Change in Annual Mean Temperature Relative to 1965.

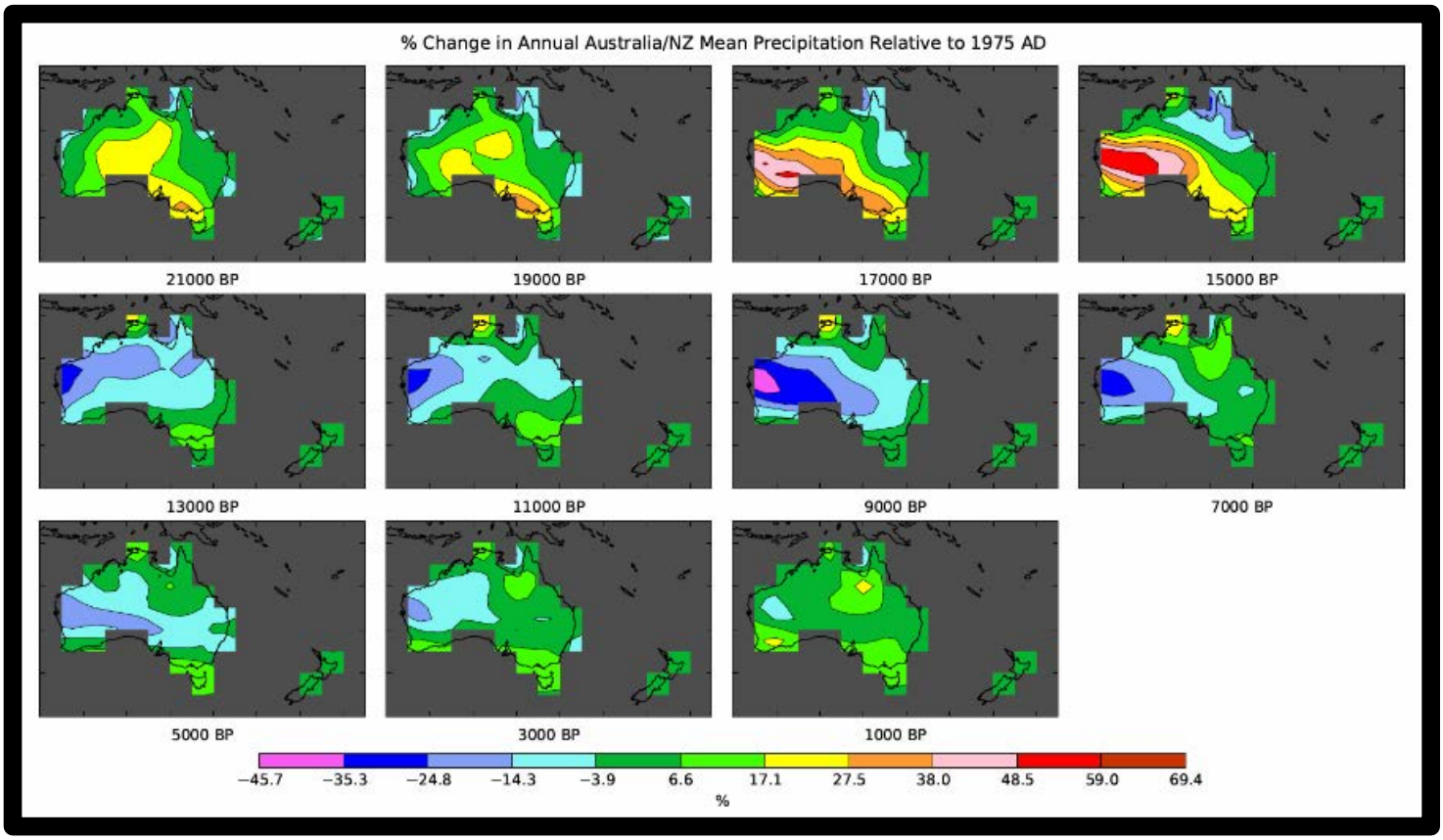

Figure 6: PaleoView % Change in Annual Mean precipitation Relative to 1975.

2.3. Chapter conclusion:

The following is a set of bullet-points of 'lessons' previously published sites and which are relevant in the aiding of the interpretation of the Kinrara record.

Late Pleistocene (~37,000 - 11,500 cal yr BP) and Last Glacial Maximum (~20,000 cal yr BP)

- LGM cooler and drier at all sites.
- Sea level was much lower than present day, ~ 120 m below modern levels (Petherick et al., 2017).
- The Tablelands saw an expansion of sclerophyll vegetation (savanna) during drier glacial periods.

Early Holocene (~11,500 - 8750 cal yr BP)

- Holocene temperatures and precipitation levels were elevated, accompanied by increased levels of CO_2 and higher sea level.
- Lake Euramoo on the Tablelands indicated a transition between sclerophyll woodlands to warm rainforests around the early Holocene – middle Holocene boundaries.
- Australia, monsoonal reactivation is estimated as early as 14,000 to 12,000 cal yr BP, and/or otherwise enhanced from approximately 8000 cal yr BP

Middle Holocene (~8750 - 3600 cal yr BP)

- The Tablelands contain warm temperate rainforest.
- To the north Marura developed to an open permanent water around 8800 cal yr BP.
- Sanamere shows high fire intensity around 8000 cal yr BP.
- The Gulf of Carpentaria, Vanderlin Island and Groote Island indicate intensification of the Australian monsoon between 7500 – 4500 cal yr BP and confirm increased effective precipitation during the early Holocene.

Late Holocene to Modern (3600 cal yr BP - present)

- The late Holocene is thought to be characterised by enhanced climatic variability (weakening of monsoon precipitation, and increased seasonality incorporating a more variable and extreme El Niño-Southern Oscillation, ENSO).
- Quincan Crater on the Tablelands indicated a change from sclerophyll vegetation into a warm temperate rainforest until 2000 cal yr BP. After 2000

cal yr BP decreased in precipitation. Bromfield swamp also saw a vegetation shift around the 2000 cal yr BP mark.

- Witherspoon swamp shows the important rainforest-sclerophyll boundary that formed, helping to understand the separation of the Tablelands and the drier lands to the south.
- To the north Girraween Lagoon shows a transformation from an open to a more wooded savanna during the middle Holocene. Further it shows that during the intensification of the ENSO around 3000 cal yr BP Indigenous fire management became dominant.
- Marura had an expansion of grasses around 2500 cal yr BP.
- Big Willum swamp, indicates significant burnings periods at 1000 and 1700 cal yr BP.
- Eastern Torres Straits, shows a shift from rainforests to open sclerophyll woodlands (savanna) from 3000 cal yr BP.
- Papua New Guinea shows an increase in charcoal between 4500 to 2000 cal yr BP.

In conducting this survey, it has become apparent that there are few archaeological sites that have been studied close to the sites where lacustrine records have been developed. Detailed archaeological evidence, particularly in relation to populations densities and use of fire, would usefully compliment the palaeoecological record, including that from Kinrara. In this regard, archaeological evidence from the wider region will be utilised within the discussion of this thesis to help identify any contribution of humans to fire regime in the past. However, a detailed, catalogue review of the evidence from archaeological sites across the region is outside the scope of this thesis.

Chapter 3. Reconstructing Past Fire and Vegetation Histories

Charcoal records are essential to assess the links between fire, vegetation, climate and humans over many temporal and spatial scales (Marlon et al., 2016). Sediment cores often contain micro and macro fragments of charcoal, the amount of which is quantified and used to reconstruct the long-term variation and trends in fire regimes, thus enabling interferences to be drawn as to how modern landscapes may change in response to changes in fire regime (Whitlock & Larsen., 2001; Birks et al., 2001; Birks et al., 2012; Marlon et al., 2016). Primary charcoal is charcoal deposited near the point of burning and secondary charcoal has accumulated during non-fire periods and subsequently been deposited into the sedimentary record through other transport mechanisms such as by wind and erosion associated with runoff (Birks et al., 2001; Whitlock & Larsen, 2001).

A range of proxies have been developed from sedimentary records that are interpreted as a measure of fire incidence in the past. These can be both physical and geochemical in nature. All techniques are potentially subject to a range of confounding issues. For example, charcoal counting is used as a proxy in sediment cores as a measure of fire incidence in the past (Whitlock & Larsen., 2001; Rowe et al., 2022b; Wurster et al., 2021b). However, post-depositional changes can occur to charcoal fragments and there is a chance that individual fire events will be missed when analysing a single sediment core. In contrast, comminution of charcoal into more abundant finer size classes as a result of sediment compaction or laboratory disaggregation can potentially yield elevated charcoal counts that are also not representative of fire incidence. These processes can result in the misinterpretation of fire frequencies in the area being studied and highlight the importance of

interpreting the results of one core / one site in the context of nearby sites to provide a more accurate picture of what is occurring in the wider region.

In addition, the combination of multiple proxies can provide further insight into fire dynamics. These proxies include pollen as a measure of changes in fire-sensitive vegetation, stable carbon isotopes to measure the relative grass-to-tree ratio and fire-altered material such as some soil minerals produced by exposure to high temperatures at the soil surface (Birks et al., 2001; Whitlock & Larsen., 2001; Birks et al., 2012). Archaeological records are also often used alongside fire proxy data to determine the likelihood of anthropogenic influence on fire regime (Rowe et al., 2022b). Using multiple proxies to reconstruct the palaeo fire histories is superior to using a single proxy, as this allows more nuanced interpretation and insight (Marlon et al., 2016). The techniques that are utilized in this study are reviewed in more detail below.

3.1. Charcoal counting:

Charcoal counting has been widely used for decades as the primary means of reconstructing past fire events from palaeo records (Mustaphi & Pisaric, 2014; Rowe et al., 2022b). Transportation, fire size, severity of area affected, and fire intensity all affect charcoal production (Whitlock & Larsen, 2001). Charcoal has the advantage that it is generally well preserved in sediment cores as easily identifiable opaque, angular black fragments (Whitlock & Larsen, 2001; Rehn et al., 2022a). Charcoal counting is typically done alongside pollen counting to link proxy-derived information on climate, fire, vegetation and in some cases human activities (Whitlock & Larsen, 2001; Rowe et al., 2022b). Charcoal is usually divided into two size fractions (Rowe et al., 2022b). Micro charcoal ranges in size between 10 to 125

µm and is counted alongside the counting of pollen (Rowe et al., 2022b). Macro charcoal is larger than 125 µm and this fraction has been shown to be of more local origin, usually sourced from within the local catchment (Rowe et al., 2022b).

Modelling of particle behaviour has confirmed that macrocharcoal is deposited initially within meters of the source while microcharcoal can travel 100 m beyond the source, with finer particles potentially travelling over much longer distances (Whitlock & Larsen, 2001). Microcharcoal is therefore considered to record a more regional signal (Whitlock & Larsen, 2001). Macrocharcoal morphology can also be used to provide information on whether the material was sourced from woody and herbaceous plants alongside other key fire variables (Mustaphi & Pisaric, 2014).

3.2. Stable Polycyclic Aromatic Carbon (SPAC):

Pyrogenic carbon (PyC) is produced by the combustion of organic matter at temperatures usually from 400-600°C in natural or anthropogenic fires, under reduced oxygen conditions (Bird et al., 1999; Bird & Ascough, 2012; Wurster et al., 2012; Bird et al., 2015; Saiz et al., 2015; Saiz et al., 2018). PyC is present in multiple forms, as a continuum from highly condensed carbon in polycyclic aromatic rings to lightly charred organic matter (Figure 7). Pyrogenic carbon is also referred to as partly charred biomass, charcoal, soot, black carbon and char (Bird & Ascough, 2012; Bird et al., 2015; Saiz et al., 2015). Although such terms are often used interchangeably, specific terms target specific parts of the PyC continuum (Figure 7). The size of the condensed polyaromatic compounds is determined by the temperature of the fires in which they were formed, with an increase in the number of condensed polyaromatic rings with increasing temperatures (Bird et al., 2015).

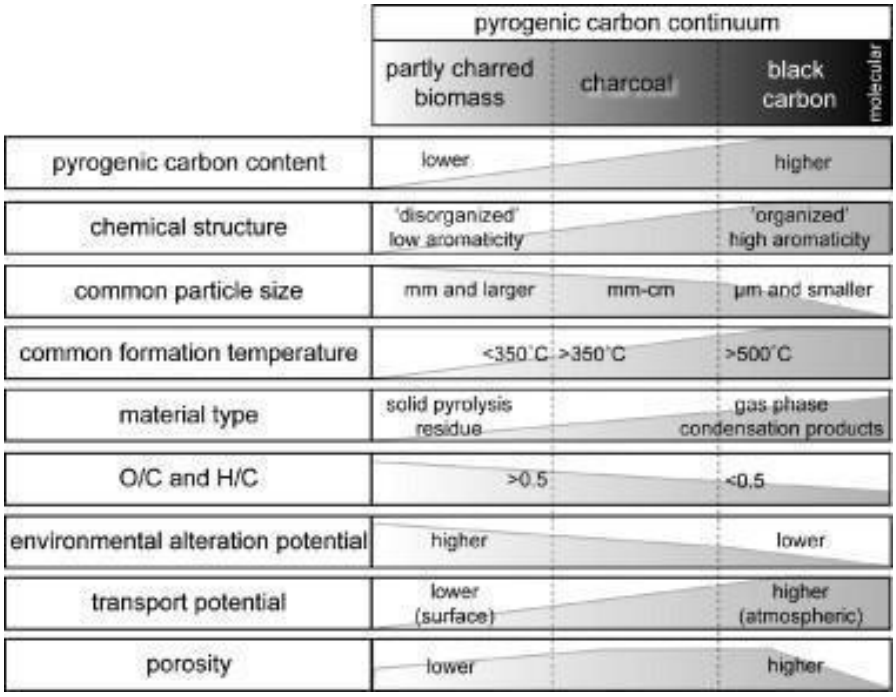

Figure 7: The Pyrogenic carbon continuum (Bird & Ascough, 2012, p. 2).

Post-depositional physical and chemical alterations of charcoal fragments have been shown to occur, however, the stable pyrogenic aromatic carbon (SPAC) fraction of the charcoal (Figure 7 – right side) has been shown to be highly resistant to post-depositional alteration (Bird & Ascough, 2012; Bird et al., 2015; Saiz et al., 2015). However, some components of the bulk PyC will be degraded into smaller PyC fragments, eventually becoming so small that counting charcoal by microscope will not be able to detect these particles. This phenomenon leads potentially to a difference in the results obtained between charcoal counting, a visual measure of particles large enough to be counted, and geochemical measures that quantify all PyC in the analytical window of the technique being used regardless of its physical form (Bird & Ascough, 2012; Bird et al., 2015; Saiz et al., 2015; Wurster et al., 2021a; Wurster et al., 2021b). The current view is that although most PyC is relatively resistant to environmental degradation, there are some alterations, both chemical

and physical, which can lead to its transformation to very fine particulates or to a dissolved form (Bird, et al., 2015).

One way to measure a component of the pyrogenic carbon continuum is via the technique of hydrogen pyrolysis. This technique isolates the PyC that is thought to be resistant to long-term degradation (Stable Polycyclic Aromatic Hydrocarbons=; SPAC - see Bird & Ascough, 2012; Wurster et al., 2012b; Saiz, et al., 2015). The technique uses high pressure, temperature, and a catalyst to hydrogenate and remove labile carbon from the samples (Wurster et al., 2012). The use of hydrogen pyrolysis has been shown to quantify SPAC abundance in a variety of sample matrices (Wurster et al., 2012; Saiz et al., 2015; Wurster et al., 2021b Rehn et al., 2021a; Rehn et al., 2022). This procedure effectively removes labile carbon from the sample leaving only SPAC in the sample, with SPAC abundance then determined by standard elemental analysis. A slight correction is applied to the abundance and stable isotope composition of the PyC in order to account for a small amount of labile carbon which is not removed during the HyPy process (Wurster et al., 2012).

3.3. Stable carbon isotopes in SPAC:

Stable carbon isotope composition – the ratio of (rare) ^{13}C to (abundant) ^{12}C can be utilised to determine the source of the SPAC and thereby aid in the interpretation of fire histories, helping to link inferences about fire to changes in land cover, land use, climate and biodiversity (Bird & Ascough, 2012; Rehn et al., 2021a; Rehn et al., 2021b; Rehn et al., 2022). This is possible in tropical regions because terrestrial plants predominantly use two photosynthetic pathways: C_3 and C_4 (White, 2013). C_3 plants are classified as such because they use the enzyme ribulose bisphosphate carboxylase oxygenase which reacts with one molecule of CO_2 to

produce two molecules of 3-phosphoglyceric acid (White, 2013). C_4 utilise the Hatch-Slack process involving an additional enzymatic step, using phosphoenolpyruvate carboxylase is used to fix the carbon and form oxaloacetate (White, 2013).

C_3 plants currently makeup 90% of all modern plant species and have a range of a $\delta^{13}C$ values of -33 to -24‰, with this range dependent on both species and environmental factors, particularly water stress (White., 2013; Rehn et al., 2022). C_3 plants include all trees, shrubs and cool climate grasses (Dominique et al., 2015). Tropical grasses and some sedges use the C_4 photosynthetic pathway, with $\delta^{13}C$ values that range from -11 to -15 ‰ (Li et al., 2023). In tropical savanna regions, carbon isotopes are particularly useful as savanna grasses and woody vegetation have distinct values and hence the relative contribution of grasses vs woody vegetation in SPAC produced by fires can be determined (Wurster et al., 2021b; Rehn et al., 2022).

3.4. Integrating measures of fire for a more nuanced understanding of changing fire regimes in the past:

It is possible to consider multiple fire proxies based on both visual counting and geochemical quantification to arrive at a more nuanced interpretation of fire regime than is possible from a single proxy alone. Globally, there are five key attributes of modern fires that determine fire regime. They are size, frequency, intensity, season, and extent of burned area (Archibaid et al., 2013). These attributes allow the delineation of 'pyromes' each characterized by a specific set of these five attributes, with control on the distribution of these pyromes exerted in part by rainfall amount and seasonality, which in turn exerts a control on vegetation type (Archibaid et al., 2013). Figure 8 shows current day modern fire pyromes occurring in the world. These pyromes include FIL (Frequent, Intense, Large), FCS (Frequent,

Cool, Small), RIL (Rare, Intense, Large), RCS (Rare, Cool, Small), and ICS (Intermediate, Cool, Small) (Archibaid et al., 2013).

Using this categorization, northern Australia is dominated by the FIL (Frequent, Intense, Large) pyrome, with regions, including parts of northeast Queensland categorized as RIL (Rare, Intense, Large). This is likely the result of the removal of indigenous land management following European colonization of Australia. From observation of Indigenous fire management in northern Australia it is likely that prior to European colonization northern Australia was part of the FCS (Frequent, Cool, Small) pyrome (Wurster et al., 2021b).

Determining changes in pyrome in the past in a sedimentary record requires the combination of several proxies. Wurster et al., (2021b) combined charcoal particle flux as a measure of fire incidence with the mass accumulation rate of SPAC (MAR_{SPAC}) as a measure of fire intensity, along the $\delta^{13}C$ values of SPAC ($\delta^{13}C_{SPAC}$) as a measure of vegetation burnt. This combination of multiple proxies enabled Wurster et al., (2021b) to infer that indigenous fire management imposed an FCS pyrome on the mesic savannas around Darwin in the Northern Territory from about 3,000 cal yr BP. This approach is not yet widely utilized but has demonstrated considerable promise for reconstructing a more complete detailed view of past changes in fire regime, as opposed to simply fire incidence.

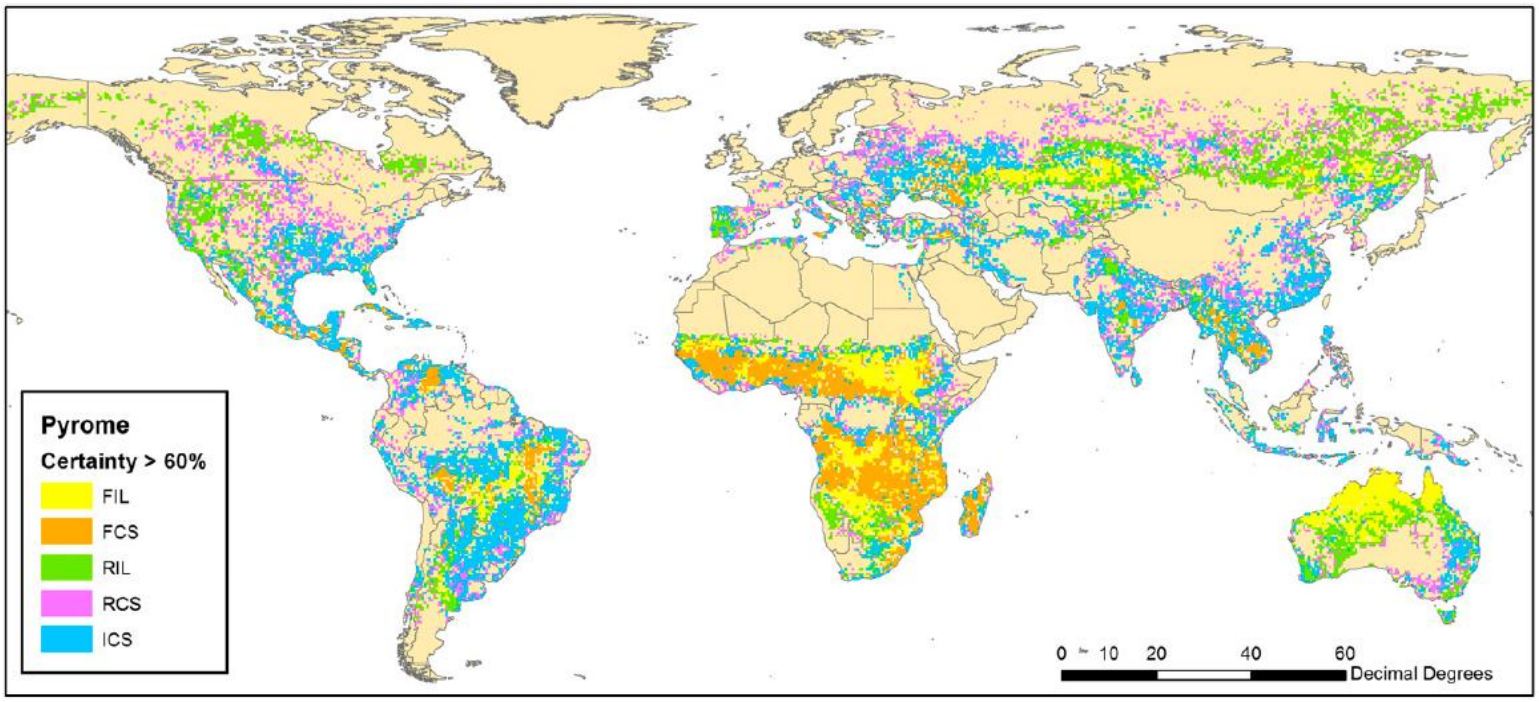

Figure 8: Pyromes categorised as FIL (Frequent, Intense, Large), FCS (Frequent, Cool, Small), RIL (Rare, Intense, Large), RCS (Rare, Cool, Small), and ICS (Intermediate, Cool, Small) (Archibaid et al., 2013, p. 6444; Archibald et al., 2017).

3.5. Chapter conclusion:

Charcoal records are essential in reconstructing past fire events. Charcoal counting can indicate fire incidence/frequency in the past but cannot alone provide a more nuanced understanding of fire regime (i.e. incidence/frequency *and* intensity). In combination with the geochemical measure of SPAC abundance, it is becoming possible to obtain this more nuanced measure of fire regime. The complementary ability to measure the $\delta^{13}C$ value of SPAC provide a further layer of information on the ratio of C3 (tree) vs C4 (grass) plants that are burning to produce the SPAC.

There are many other proxies which are used in palaeoenvironmental reconstruction. These include, trees ring widths and stable isotope compositions, compound specific isotopes of leaf waxes and other biomarkers, stable isotope studies of speleothems and lacustrine carbonates, pollen, phytoliths and more (Bird

et al., 2020). These proxy records further enable further insight through the provision of complementary information on climate and vegetation further enhancing understanding of the interactions between fire, climate, vegetation and humans. This study draws on some of these records from Kinrara Lagoon itself (James et al., 2024), and the wider region.

Chapter 4. Modern Climate Drivers

4.1. Wider modern Australia savanna region:

Rainfall seasonality and interannual variability in Northern Australia exerts significant control on both fire and vegetation in northern Australia. Hence the drivers of hydroclimate, both spatially and temporally, must be understood in order to interpret trends in both vegetation change and fire incidence (Catullo & Scott Keogh, 2014; Steinke et al., 2014).

4.2. Modern savanna types and distributions:

Savannas are characterised in Australia by the coexistence of open or scattered tree canopy – with predominantly *Eucalyptus* in the upper stratum – above a grassy understory, developing in tropical and subtropical climatic zones (Tothill et al., 1985; Moore et al., 2016). Variations in seasonal water availability is the primary factor limiting growth in these environments. Seasonal water availability affects where different plant taxa can grow and therefore the type of savanna that will result (Moore et al., 2016). Six major savanna types have been identified at the national level: 1) Monsoon Tallgrass Savanna, 2) Tropical Tallgrass Savanna 3) Subtropical Tallgrass Savanna, 4) Midgrass Savannas, 5) Midgrass on Clay Soils, and 6) Tussock Grasslands (Figure 9) (Tothill et al., 1985; Australian Government Department of Climate Change, Energy, the Environment and Water., 2015; Australian Government Department of Climate Change, Energy, the Environment and Water., 2021). The Kinrara area is located within the Tropical tallgrass savanna zone that is characterized by grass understory, dominated by *Heteropogon contortus, Bothriochloa* spp/ *and Themeda australis*. The upper stratum consists of mostly *Eucalyptus* species (Tothill et al., 1985).

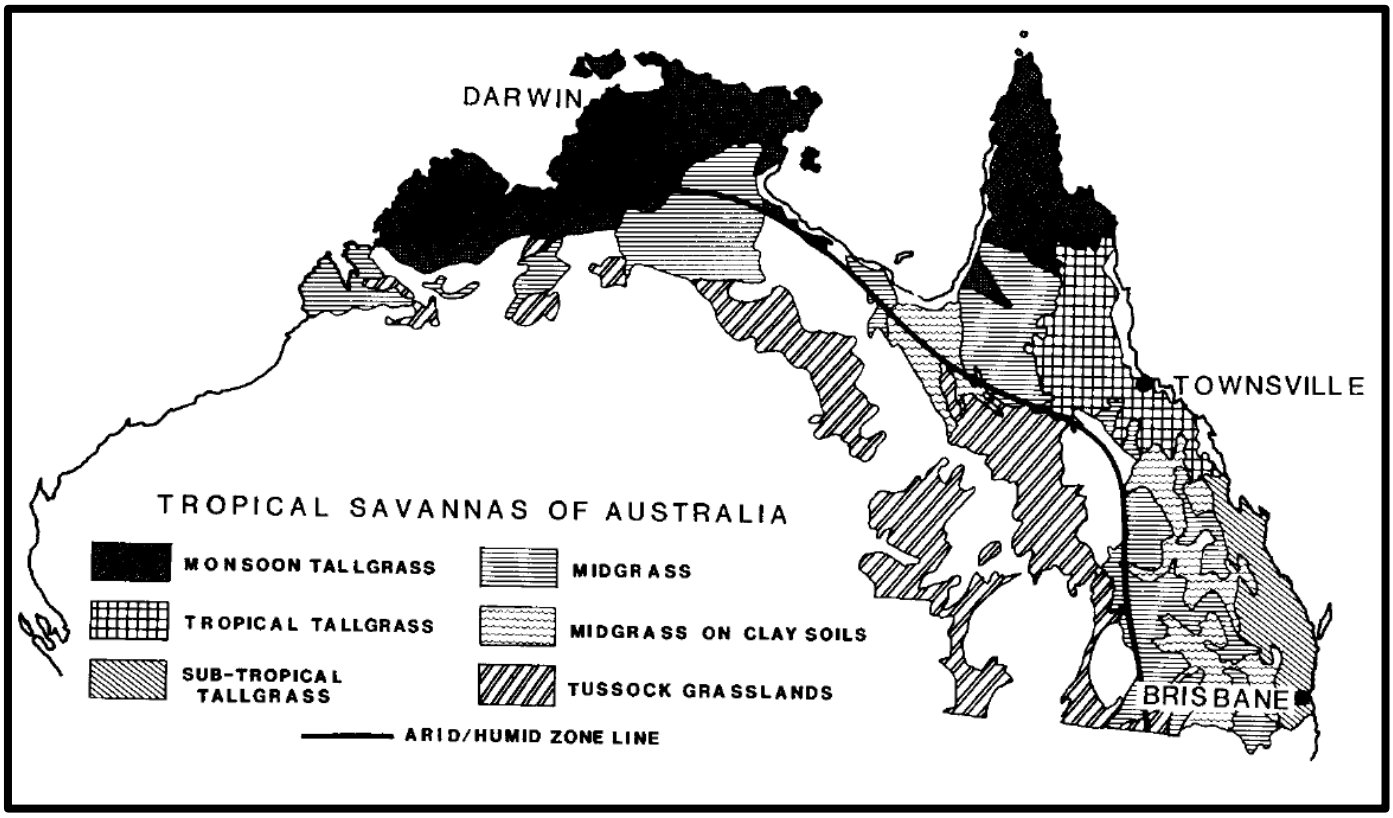

Figure 9: Tropical savannas of Australia (Tothill et al., 1985, p. 2).

4.3. Climate drivers of Australian savanna dynamics:

Savanna dynamics in northeastern Australia are currently modulated by multiple interacting climatic drivers. These include the Indonesian-Australian monsoon; El Niño-Southern Oscillation; Southeast Trade Winds; the Madden-Julian Oscillation; tropical cyclones/depressions; as well as onshore circulations and inland troughs (Risbey et al., 2009). All these climate phenomena affect rainfall on multiple temporal scales and hence drive savanna dynamics through their control on local moisture availability, seasonally and inter-annually (Figure 10).

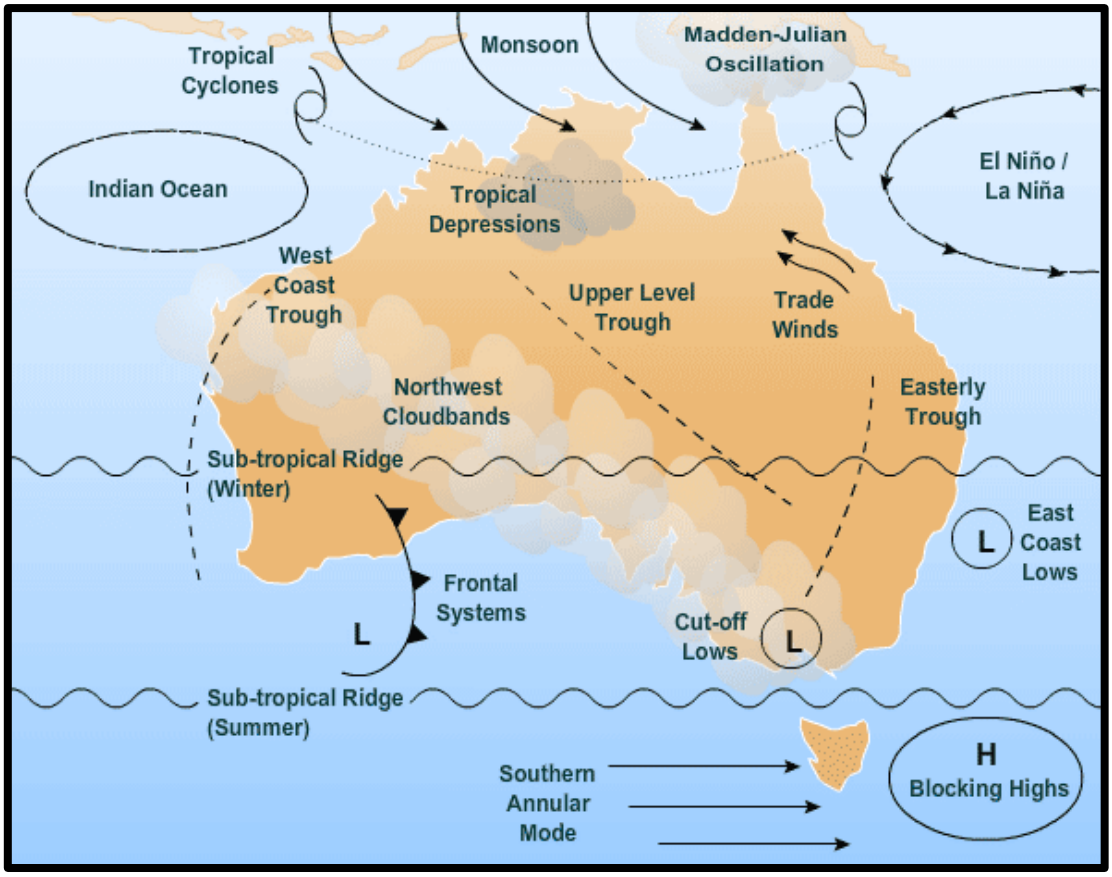

Figure 10: Modern climate drivers (Australian Government, 2010).

4.3.1. Indonesian-Australian Summer Monsoon:

The Indonesian-Australian Summer Monsoon (IASM) is a seasonal reversal in wind direction bringing moisture into northern Australia during the 'wet season' (December to April) (Hesse et al., 2004). The Inter-Tropical Convergence Zone (ITCZ) moves southward during the Austral summer bringing monsoonal rain into northern Australia (Reeves et al., 2013; Field et al., 2017). The development of the monsoon is linked to inland surface heating leading to a shift from dry south-easterly winds to moist north-westerly winds. Rainfall associated with the ITCZ results from convective uplift and cooling of warm and moist winds, forming deep convective clouds that deliver heavy rain during the monsoon season (Schneider et al., 2014; Field et al., 2017).

The monsoon also displays sub-seasonal dynamics whereby monsoon 'bursts' of rain are produced by extratropical wave packets from the Indian Ocean the origin of which have in turn have been linked to the Madden-Julian oscillation (MJO) (Berry & Reeder., 2016). The MJO is the strongest climate driver that influences the amount of rain associated with the monsoon (Risbey et al., 2009). The MJO operates on a 40-60 day cycle and affects the monsoon by altering the strength of the westerlies (Field et al., 2017). There are still major gaps in the knowledge surrounding the mechanisms underlying the dynamics of the monsoon (Steinke et al., 2014).

During the Last Glacial Maximum (LGM) the IASM was weak or inactive which suggests a drier Northern Australian climate at that time. However, the LGM potentially includes some extreme wet weather events (Reeves et al., 2013). During the deglacial period of rapid sea level rise (around 19,000 – 14,000 cal yr BP) the IASM took its approximate current form, partly explained by the flooding of the Sunda and Sahul Shelves, providing a much larger ocean surface for evaporation (Hanebuth et al., 2000; Wyrwoll & Miller., 2001; Hesse et al., 2004; Reeves et al., 2013). The middle Holocene (~7000 – 5000 cal yr BP) saw the monsoon becoming the most dominant climatic feature in the region, with a further strengthening occurring in the 16th and the 20th centuries (an observation explained by the weakening of the Pacific Walker circulation and an expansion of the ITCZ (Reeves et al., 2013; Griffith et al., 2016).

4.3.2. The El Nino- Southern Oscillation:

The El Niño-Southern Oscillation (ENSO) is a coupled ocean-atmosphere system that influences climate on an inter-annual time scale (Calvo et al., 2007;

Hesse et al., 2004). ENSO consists of two phases, the El Niño phase, which is the warm phase with negative southern oscillation index, SOI, and La Niña, the cool phase with positive SOI, (Mariani et al., 2016; Field et al., 2017). ENSO influences wind strength, temperature and significantly affects rainfall amount, hence the probability of fires (Diaz & Markgraf, 1992; Risbey et al., 2009; Barr et al., 2019). During an El Niño event there is an equatorial movement of the ITCZ and a migration of the South Pacific Convergence zone north-eastward, leading to drier conditions across northern Australia (Donders et al., 2007).

ENSO appears to have been weak in the middle Holocene but intensified around 5000 cal yr BP, becoming fully active by 3000 cal yr BP, linked to a southward movement of the ITCZ during the later Holocene (Diaz & Markgraf, 1992; Haug et al., 2001; Mooney et al., 2011; Gagan et al., 2004; Burrows et al., 2014). The exact timing of ENSO intensification remains debated, with estimates of 3000, to 6500 cal yr BP suggested by multiple authors (Mooney et al., 2011; Burrows et al., 2014; Proske et al., 2017). The intensification of the ENSO has been linked to an increase in burning across the Pacific Basin (Grove & Chappell, 2000). The implied regional variability in ENSO impacts should be considered when interpreting any proxy time series of fire.

In the tropical monsoonal savanna areas of northern Australia, fire is dependent on seasonal drying, and it has been shown that higher levels of burning are associated with the intensification of El Niño-Southern Oscillation (ENSO) after 4000 cal yr BP (Mooney et al., 2011). It is important to understand the effects of ENSO on past fire regimes, as documenting ENSO dynamics will help us follow how anthropogenic climate change will affect ENSO, which in turn can shed light on the

drivers of changes in moisture availability and hence fire activity (Moss et al., 2013). It can also be assumed that if there is a further intensification of ENSO, it will potentially equate to changes in fire frequency and intensity across northern Australia.

4.3.3. The Interdecadal Pacific Oscillation (IPO):

The IPO is an ocean-atmosphere climate phenomenon that operates in the Pacific basin. The system has two phases which oscillate every 15-30 years. A positive "warm" phase causes the West Pacific to become cooler and the Eastern Pacific to become warmer, and a negative, 'cool' phase, for which the inverse is the case (Salinger et al., 2001; Calvo et al., 2007). The IPO is a longer-term driver of sea surface temperature and wind circulation patterns in the Pacific, and unlike other ocean-atmosphere climate drivers such as the El Niño which have reasonably well understood mechanisms, the IPO is driven by the sum of multi-dynamic climatic mechanisms which are hard to define and poorly understood (Salinger et al., 2001; Calvo et al., 2007).

The IPO is important because it also modulates the frequency, strength and magnitude of EL Nino and La Nina events. The IPO therefore strengthens or weakens the teleconnections between ENSO and northern Australian precipitation, generally decreases interannual precipitation variability in northeast Australia during its positive phase and increasing interannual precipitation variability during negative phase – as has been the case since 1999 (Salinger et al., 2001; Calvo et al., 2007).

4.3.4. Southeasterly trade winds:

Lastly, northeastern areas of Australia, including the study area receive rain not only from the monsoon, but also from humid southeasterlies which are sourced from the equatorial Pacific and the Coral Sea (Reeves et al., 2013). The penetration of southeasterly-derived rainfall is inhibited by the Great Dividing Range, leading to orographic rainfall on its coastward slopes, which are forested, and creating a rain shadow west of the range occupied by the inland tropical savanna (Reeves et al., 2013). In the context of this study, changes in the penetration of rainfall from this source inland could result in differences between rainfall experienced at the Kinrara site compared to other records on the wetter Atherton Tablelands and more coastal regions to the east of the site.

Chapter 5. Site Description and Methodology

This chapter details the present-day characteristics of the study site, including climate, geology, fire regime and vegetation. Along with the site description the methods used to reconstruct the record is outlined in this chapter.

Figure 11: Kinrara Lagoon.

5.1. Local Kinrara region:

Kinrara Lagoon (18°30' 4.43"S, 145° 2' 27.74"E) is located in Northern Queensland approximately 120 km inland from the township of Ingham. The site is a permanently wet, spring-fed water body, spanning 1.25 x 0.5 km with a total area of 1.65 km^2, and a maximum water depth of 1.8 m (at the time of coring, August 2018) (Figure 11). The lagoon is relied upon for fresh water by livestock and people. The area has been utilised for cattle grazing since Kinrara Station was established between 1863 and 1880 (Queensland Government, 2022). The Water Observations from Space data (WOFS) in Figure 12 shows that from 1989 to 2020 the lagoon was wet year-round. As a permanently wet feature of the region, this has facilitated the preservation and accumulation of proxy data, otherwise susceptible to degradation

during dry conditions. The lagoon has been shown to be permanently wet and spring fed feature since at least 11 500 cal yr BP (James et al., 2024). From the lagoon outflow in the southeast, the waters flow southeast into drainage channels towards the Burdekin River (James et al., 2024).

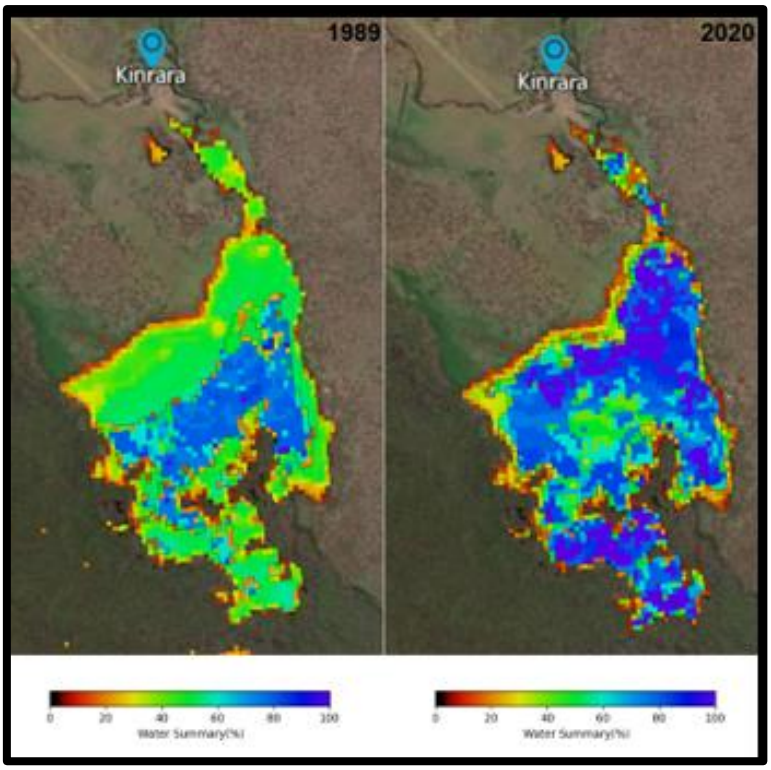

Figure 12: Map showing the Kinrara Lagoon water % in the years of 1989 and 2020 (Australian Government Geoscience Australia, 2024).

The Kinrara area is classified as a subtropical savanna with a summer-rainfall-dominated climate incorporating hot, wet summers and cooler, dry winters (Figure 13) (Australian Bureau of Meteorology, 2001; 2016). The area experiences an average annual rainfall of 758mm based on data collected between 1968-2019 from Craigs Pocket Station, 18.4km west of Kinrara Lagoon (Australian Bureau of Meteorology., 2019a; 2019b; 2019c), with coastal tropical depressions providing 90% of this rainfall in the wet season from December to April (Queensland Government Department of Environment, Science and Innovation., 2012). The area has a mean annual maximum temperature of 31.0 degrees and mean annual minimum of 16

degrees based on data collected from Mount Surprise Township, 1913 to 1978, 68.1km northwest of Kinrara lagoon (Australian Bureau of Meteorology., 2019c).

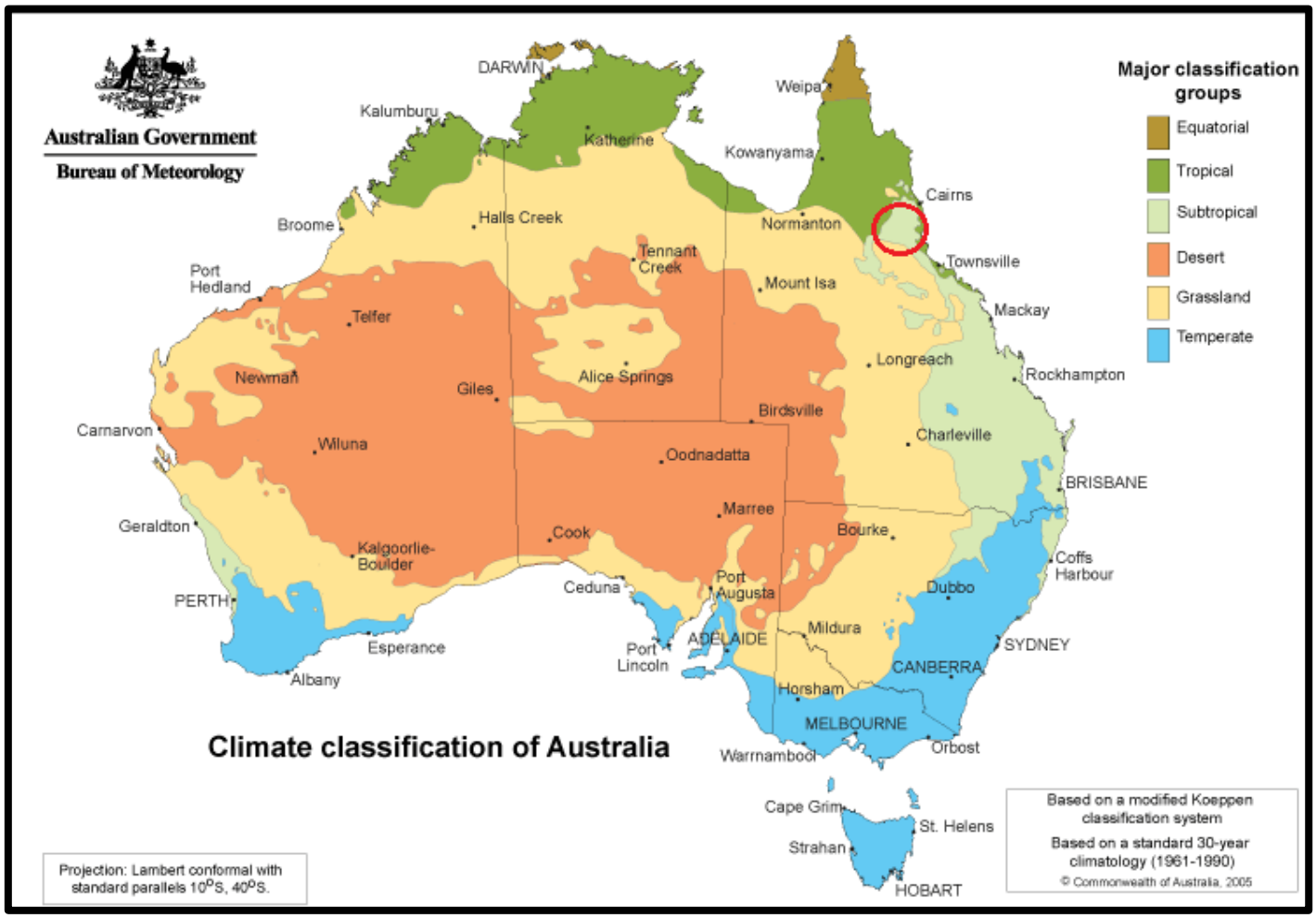

Figure 13: Map of Australia with BOM climate classification of Australia. Red circle indicating the location of Kinrara (Australian Government Bureau of Meteorology, 2016).

5.1.1. Geology:

Kinrara is located on the weathered Cenozoic basalts of the c.5500 km^2, MacBride Volcanic province (Whitehead, 2010). The lagoon in its present form resulted from the damming of Glenlofty Creek by a Holocene flow emanating from the Kinrara volcanic centre, ~20 km NW of the site (Figure 14, 15, and 16). These ropy pahoehoe basalt flows are well persevered - with minimal weathering - and extend across the local landscape and down former drainage lines for over 55 km to the Burdekin River (Figure 14, 15 and 16) (Stephenson et al., 1998; Cohen et al.,

2017; Google Earth., 2019). These are the youngest basalt flows in Queensland (Mishra et al., 2019), and yet reliable dating of these flows has proven difficult. Initial studies placed the age around 20,000 ka utilising K/Ar dating (Stephenson et al., 1998; Cohen et al., 2017). More recent attempts based on $^{40}Ar/^{39}Ar$ dating suggests at least some Kinrara flows are Holocene in age, at around 7000±2000 cal yr BP (Cohen et al., 2017).

Figure 14: Kinrara Lagoon 2022, lagoon dammed by basalt rocks.

Figure 15: Kinrara vesicular basalt rocks.

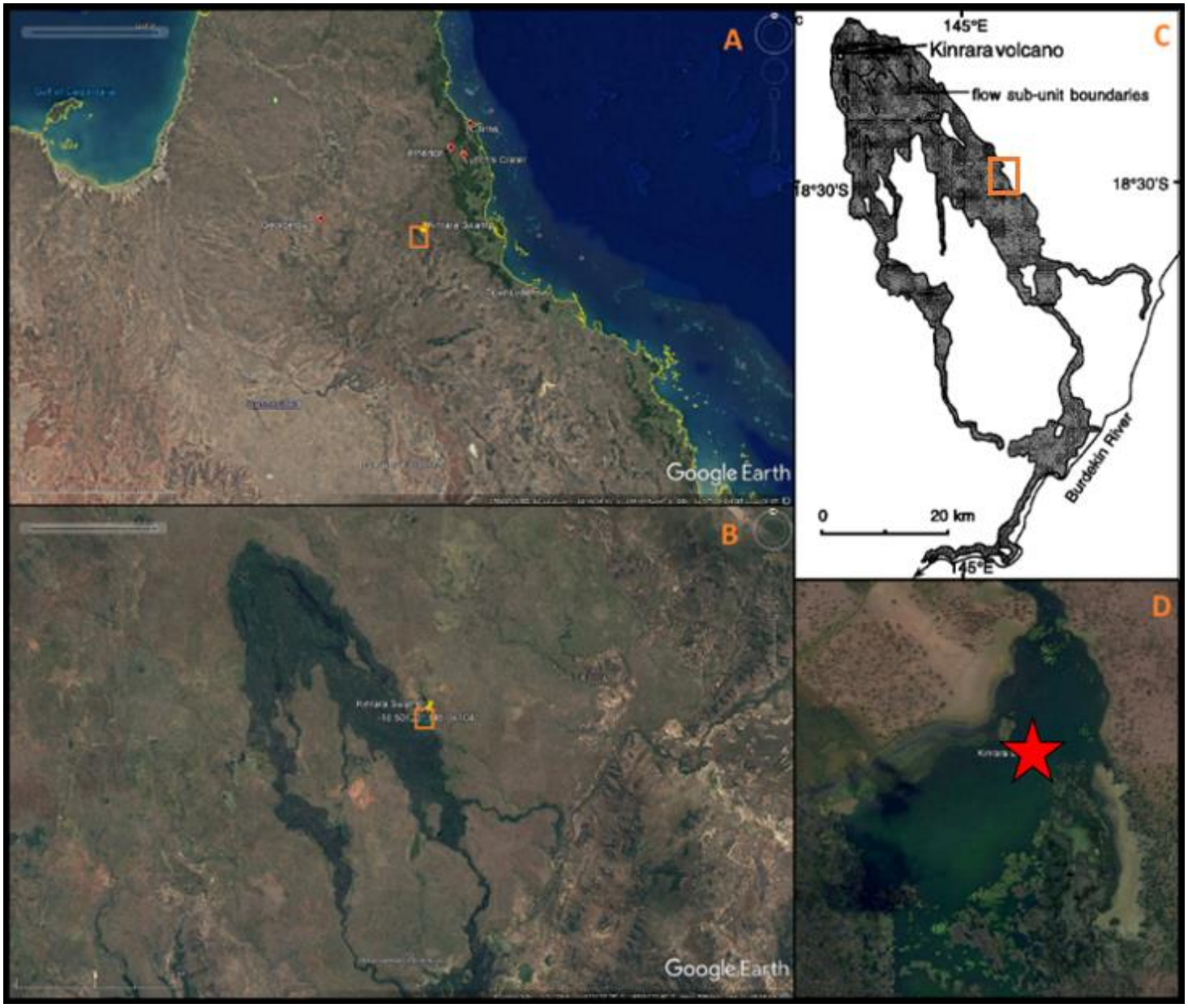

Figure 16: Kinrara Lagoon, A – Queensland context, B – Regional context, C – Kinrara lava flow (Stephenson et al., 1998) and D – Kinrara Lagoon with a red start indicating the location of where the core was collected. Orange square indicating the location of the lagoon.

It should be noted that the specific basalt flow damming the lagoon has not been directly dated, but its timing is inferred from the dating of basalt flows emanating from the volcanic centre northwest of the site. While there is a large range in dates currently, the lack of weathering of the lava flows adjacent to the lagoon and the range of ages suggested for this eruption indicate that the event certainly

occurred when people were occupying this north Queensland region (Stephenson et al., 1998; Cohen et al., 2017). Today vine thicket has established on top of the flows that emanated from Kinrara volcanic centre.

Although the basalt flows are a key visible feature of the surface landscape it should be noted that the basement underlying the flows at shallow depth is granitic, providing a local source of both quartz and orthoclase (K) feldspar (Figure 17) (Queensland Government Department of Natural Resources and Mines., 1994). The Herbert River Granite – a porphyritic biotite granite additionally demonstrates deeply weathered outcrops ~20 km north east of the lagoon (Queensland Government Department of Natural Resources and Mines., 1994) . These basement formations likely also contribute clastic input into the lagoon.

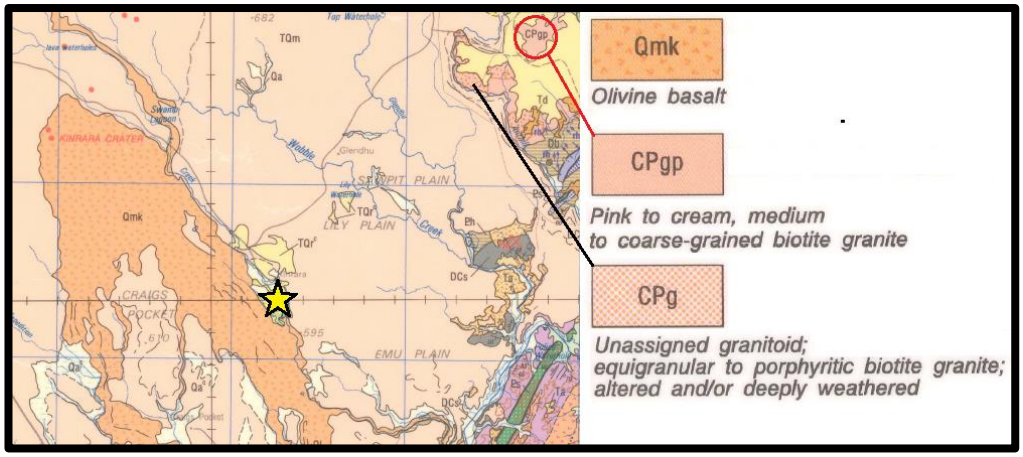

Figure 17: Geology of the Einasleigh 1:250,000 region which incorporates the Kinrara Lagoon and surrounding areas. Star highlights the Kinrara Lagoon, red circle indicating the pink biotite granites and black line indicating biotite granites that have been deeply weathered (Queensland Government Department of Natural Resources and Mines., 1994).

5.1.2. Vegetation:

The Kinrara region can be divided into two vegetation zones, the (1) "basalt flow zone" spanning over 50 kms and, (2) the areas surrounding these flows,

including the Kinrara cattle station (Figure 18, 19, 20 and 21). These two zones can be seen when looking at Figure 19: “Rainforest” being associated with the large 50 km lava flows and the areas surrounding the flows covered by open *Eucalyptus* dominated savanna.

The “basalt flows zone” is protected within Kinrara National Park, located on the Einasleigh Uplands with a size of 7734 ha. Vegetation in the park is dominated by semi-evergreen vine thicket growing on the cones, craters and rocky basalt flows with low soil development (Queensland Government, 2023b). The vine thicket comprises ~47 species of plants including the threatened species of *Ipomoea saintronanensis* (Queensland Government Department of National Parks, 2013). The low closed forest includes species such as *Gyrocarpus americanus* (helicopter tree), *Brachychiton australis* (bottle tree*), Pleiogynium timorense* (Burdekin plum) and *Eucalyptus tereticornis* (bluegum). Alongside the open mid layer of vine thicket, softwood scrubs are established on the rocky basalt substrate (Queensland Government, 2023b). The vine thicket on the basalt is predominantly composed of C_3 species (Charles-Dominique et al., 2015) and is established on the southern and western shore of Kinrara Lagoon.

Figure 18: Vegetation around the Kinrara Lagoon.

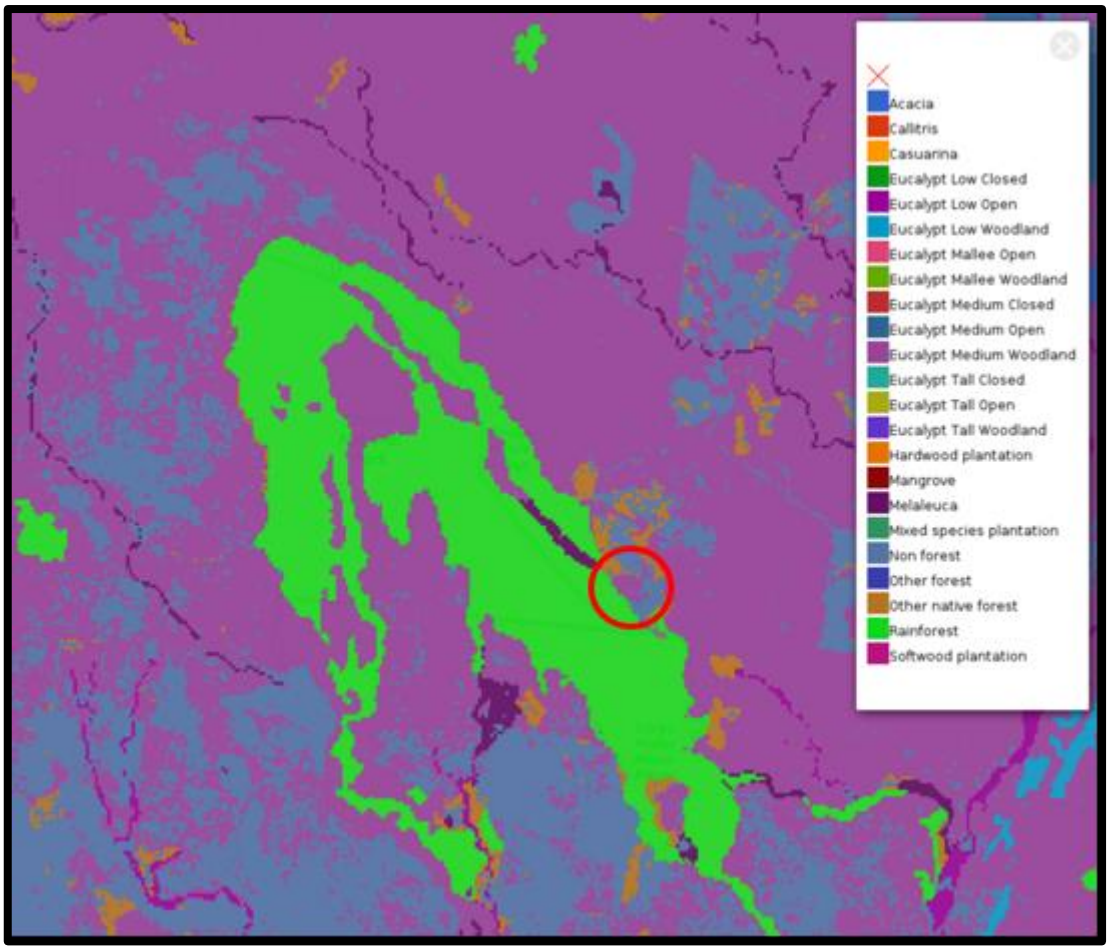

Figure 19: Forest of Australia 2018b. Surrounding Kinrara region. Lagoon indicated by red circle (Atlas of Living Australia, 2018).

The area surrounding the Holocene basalt flow, on deeply weathered basalt and granite substrates is classified as open woodland / savanna with a *Eucalyptus* spp. canopy and a Poaceae understory (Queensland Government, 2023a). This can be seen in Figure 18, showing the vegetation on the areas close to the lagoon and across the cattle station. The Kinrara Lagoon itself is bordered to the north, east and south by open eucalypt wooded savanna present and dominant across the property showing limited livestock impact (Cohen et al., 2017). Woody (C_3) species present around the lagoon include *Eucalyptus crebra* (narrow-leaved ironbark), *Corymbia dallachiana* (Dallachy's gum), *C. erythrophloia* (red bloodwood), *E. leptophleba (Molloy red box)* with the ground layer dense and generally dominated by C_4 grasses including *Heteropogon contortus* (black speargrass), *Themeda triandra* (kangaroo grass) and *H. triticeus* (giant speargrass) (Queensland Government., 2023a). Mixed C_3 and C_4 savanna is established on the eastern and northern margin of the lagoon and dominates the catchments draining into the lagoon (Figure 18 and 19).

Figure 20: Vine thicket growing on the wider Kinrara region basalt. Note how this vegetation community excludes grasses (C3) (Charles-Dominique et al., 2015).

Figure 21: Vine thicket growing on the basalt damming the lagoon.

5.1.3. Modern fire in the Kinrara region:

Fire has been monitored across northern Australia, including the Kinrara region, since 2000 with a number of data products available online (North Australia & Rangelands Fire Information., 2024). Figure 22 shows that the area immediately surrounding the lagoon has been burnt in the last 23 years, while the parts of the catchment draining into the lagoon have burnt 1-3 times with a notional fire return interval of 7 to 20 years, and all fires being prior to 2010. This is similar to the return interval over much of the pastoral land surrounding Kinrara Station. In significant contrast, the Undara Volcanic National Park to the east has been burnt every 1-3 years over the same period, where Ranger staff reinstituted a fire regime based on Indigenous fire management techniques in the 1990s. Based on this contrast the fire

history in the catchment draining into Kinrara lagoon on Kinrara Station is likely to have undergone major change over the last century. In part, the reduction in fire on Kinrara Station has been the result of reduced biomass resulting from cattle grazing and in more recent times active fire suppression in order to earn income from the Australian governments carbon credits scheme. (North Australia & Rangelands Fire Information., 2024)

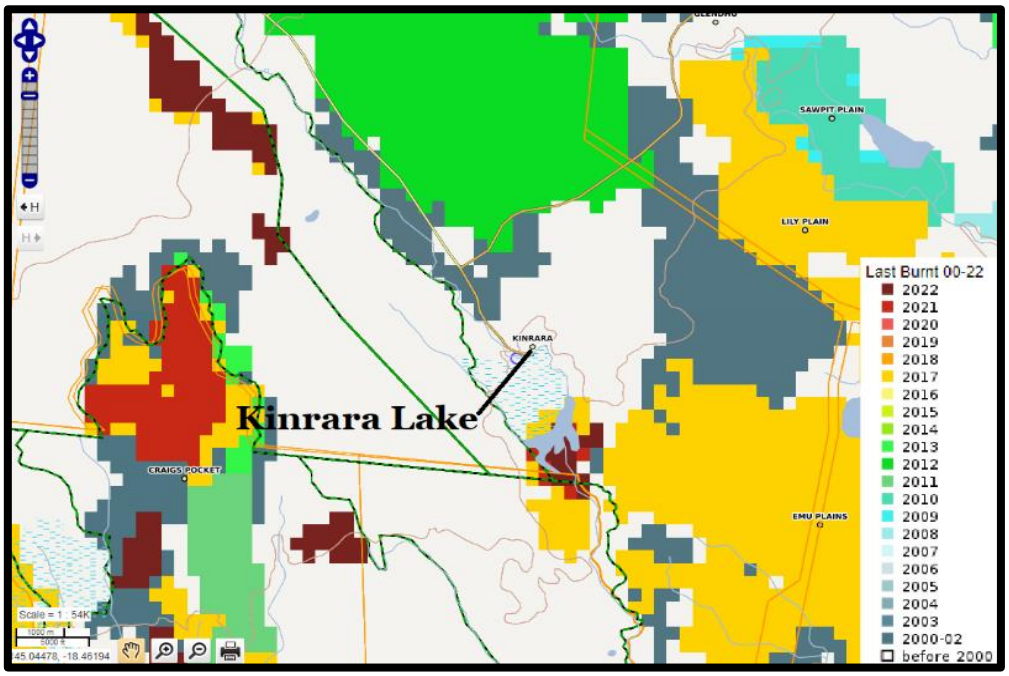

Figure 22: Kinrara map indicating years last burnt between 2000 to 2023 (North Australia & Rangelands Fire Information., 2024).

5.1.4. Indigenous and local historical knowledge:

The Gagu Badhun people are the Aboriginal custodians Traditional Owners of the Kinrara area and they have oral histories relating to the region. Kinrara Lagoon is potentially linked to the local Gagu Badhun people via oral histories associated with the creation of landscape features and associated water bodies. Two stories from the Gagu Badhun people describe the land being on fire, and of a witch doctor bringing a large volume of dust to the Kinrara area, suffocating the population across the land

(Cohen et al., 2017). These oral histories may relate to the eruption of the volcanoes within the region and will be discussed further when examining fire data from this study, though the local stories never explicitly mention a volcanic eruption. If these stories do relate to the eruption(s) from the Kinrara volcanic centre, it highlights how these stories have been handed down through generations for multiple millennia.

5.2. Coring and sampling preparation:

The deepest point in Kinrara Lagoon (18°30'4.428"S, 145° 2'27.744"E; 1.8 m depth) was cored during two expeditions. In September 2010, a 4m core was extracted using a manual piston coring system to the depth beyond which further penetration was not possible. In October 2018, a 7m core, penetrating the full sedimentary record was obtained using a hydraulic piston raft-mounted coring rig (Figure 23).

Figure 23: Raft-mounted hydraulic coring rig used in 2018.

Both cores measured 5 cm in diameter, were collected in 1 m drives and stored in plastic liners. The 7 m core was immediately frozen and halved in the laboratory (while frozen) using a diamond-tipped rocksaw. One half was archived and used for non-destructive geochemical analysis (ITRAX), and the sedimentological characteristics, including Munsell colour ,were noted from this half of the core. The other half of the core was subsampled in 2 cm increments, which were weighed, dried and reweighed to obtain water content. The 2 cm sub-samples were used to determine bulk density; these samples were then further divided into homogenous sub-samples for charcoal counting, analysis by hydrogen pyrolysis, and stable carbon-isotope analysis. Not all 2 cm sub-samples were initially used. Preliminary analysis was conducted on roughly every fifth sample. The resolution was increased to every 2 cm over points of interest within the core identified by the reconnaissance sampling or where mass accumulation rates were low and therefore the reconnaissance sampling proved to be at low temporal resolution. All intervals from the core were adjusted to represent the original 1 m interval recorded in the field before analysis, as core lengths measured in the laboratory could be lower than measured in the field due to shrinkage/compaction during coring, transport and storage.

5.3. Stratigraphy:

Stratigraphic descriptions were conducted at JCU and features recorded include, physical features such as structure, Munsell colour, mottles and visible components (bark, charcoal, shell fragments). Initial unit boundaries were also determined based on visual changes in stratigraphy and photos of all 1 m core sections were recorded. The unit boundaries were later further confirmed by data

derived from ITRAX, magnetic susceptibility, TOC and other techniques used throughout this thesis.

5.4. Bulk density and mass accumulation rates:

Bulk density was determined using a hole saw which had a radius of 2.5 cm drilled 2 cm deep into the split cores while frozen. The sediment volume was then calculated using the hole saw internal radius and the hole saw depth. Samples were weighed to provide wet sediment weight, freeze-dried and re-weighed to provide dry sediment weight. Dry bulk density in g/cm^3 was then calculated using the dry sediment weight divided by the volume sampled. This dry bulk density was then divided by the sedimentation rate derived from the age model to enable calculation of mass accumulation rate of charcoal in the sediments the lake in units of $mg/cm^2/y$ and the mass accumulation rate of SPAC in the sediments (MAR_{SPAC}) in $\mu g/cm^2/yr$).

5.5. Stable Polycyclic Aromatic Carbon (SPAC) abundance:

In preparation for stable polycyclic aromatic carbon (SPAC), total organic carbon (TOC) and stable carbon isotopes ($\delta^{13}C_{TOC}$ and $\delta^{13}C_{SPAC}$) analysis, samples were weighed and acidified with 2M HCl for 3 hours to remove all carbonate, followed by a re-weighing to determine carbonate abundance. The SPAC component was then isolated by the hydrogen pyrolysis technique (HyPy) (Figure 24). This is now a well-established technique to quantify pyrogenic carbon from sediment samples and used a pre-treatment for radiocarbon dating as discussed in previous chapters (Bird & Ascough, 2012; Bird et al., 2015; Saiz et al., 2015; Wurster et al., 2015; Wurster et al., 2021a).

Figure 24: Hydrogen pyrolysis rig.

In brief, ~250-350mg aliquots were mixed with a Mo catalyst (5-10% of sample weight) using an aqueous methanol solution of ammonium dioxydithiomolybdate [$(NH_4)_2MoO_2S_2$], sonicated and dried at 60 °C overnight. This sample/catalyst mixture was then placed into small inserts and weighed before and after the HyPy treatment to determine the sample loss.

These inserts were pressurized in the HyPy reactor to 150 bar of hydrogen with a purge gas flow of 5 L min^{-1} and heated at 300 °C min^{-1} to 250 °C and then at 8 °C min^{-1} to 550 °C, held for 5 min. Labile carbon is removed during the hydrogen pyrolysis reaction, and the remaining carbon is composed of a stable form of pyrogenic carbon with greater than seven condensed aromatic rings, or SPAC (Bird & Ascough, 2012; Bird et al., 2015; Saiz et al., 2015; Wurster et al., 2015; Wurster et al.,

2021a). TOC was then used, alongside %C of the remaining after HyPy to calculate the abundance of SPAC in each sample, converted as described above into MAR_{SPAC} in µg/cm^2/yr. SPAC abundance was corrected for any possible *in situ* production of SPAC during hydrogen pyrolysis technique using the technique presented in Wurster et al. (2012).

5.6. Stable carbon isotopes and total organic carbon:

The stable carbon isotope composition of the SPAC and TOC and the nitrogen content of TOC as measured by elemental analyser - isotope ratio mass spectrometery (EA-IRMS) using a ThermoScientific Flash EA with Smart EA option coupled via Confo IV to a Delta V^{Plus} continuous flow mass spectrometer at James Cook University's Advanced Analytical Centre. Carbon abundances were quantified by TCD (Thermal Conductivity Detector) response. Carbon isotope compositions are reported as per mil (‰) deviations from the VPDB (Vienna Pee Dee Belemnite) reference standard scale for $\delta^{13}C$ values. We used USGS-40 and two internal laboratory reference materials (Taipan and Chitin) within each analytical sequence for 3-point calibrations (normalization) of isotope delta-scale anchored to the VPDB scale. Our internal standards were calibrated using USGS40 and USGS41 international reference materials. Analytical uncertainty is better than ±0.1 ‰.

5.7. Chronology (methods):

Seventeen SPAC, bulk sediment and bark samples were dated to provide a chronology for the core. Unit 5 contained sparse trace amounts of datable material (macro plant remains, charcoal) with only a single date generated from the bottom of the core - between depths 699 – 680 cm - obtained from a single piece of bark (Appendix 2). In bark recovery, a visual check of Unit 5 was undertaken, followed by

sieving in four large 20 cm sections (561 – 581 cm, 581 – 601 cm, 660 – 680 cm and 680 – 699 cm). This lowermost saprolite/volcanogenic sediment unit yielded no datable material within the top and middle sections of the unit. The single bark sample was found at the bottom of the core, between 680-699 cm and sent to the Waikato radiocarbon laboratory with no other pre-treatment conducted at JCU. This bark dates to 35,300 cal yr BP, providing a time frame for Unit 5, with a linear relationship assumed from bark depth to the Unit 4 boundary. Sixteen bulk sediment radiocarbon samples – across the remainder of the core - were also sent to Waikato following hydrogen peroxide (30%) and HCl treatment at JCU.

The majority of the samples were pre-treated using hydrogen pyrolysis at JCU to isolate the SPAC component of the sediment and hence date only pyrogenic material. This technique has been shown to be effective in previous studies (James., etal 2024). All samples were acid-base-acid pre-treated prior to combustion and graphitization to produce a target for AMS dating. Combustion and graphitization were conducted at either the ANTARES AMS facility at the Australian Nuclear Science Technology Organisation (ANSTO; prefix OZ) in Sydney or the Waikato Radiocarbon lab in New Zealand (prefix WK). Radiocarbon ages were calibrated with the SHCal20 calibration data set (Bayliss et al., 2020) within the Bayesian age-depth modelling programme rbacon (Blaauw & Christen, 2011) which provides output as calibrated years before 1950 (cal yr BP).

5.8. Charcoal counting:

Macro charcoal counting was conducted at JCU for two size fractions >250 microns and 250-125 microns. This was achieved by taking a 1 cm^3 of each sample which were then soaked in household bleach for 24 hours to render the charcoal visible (Rehn et al., 2022). Bleached samples were then sieved at > 250 µm and 250-125 µm, with sample less than 125 µm being discarded (Rehn et al., 2022) (Figure 25 and 26). These samples were then placed into 15 ml vials and suspended in water. The bleached samples were then counted under a Dino-Lite Digital Microscope AM4113ZT. The DinoCapture 2.0 software was used to increase the contrast and the saturation of green shades which washed out all other colours besides black (Figure 25), allowing for easier counting. Digital photos were also taken and archived for each sample. The raw counts were then correlated by the sedimentation rate and converted to the charcoal particle flux into the lagoon (charcoal particles/cm^2/yr) .

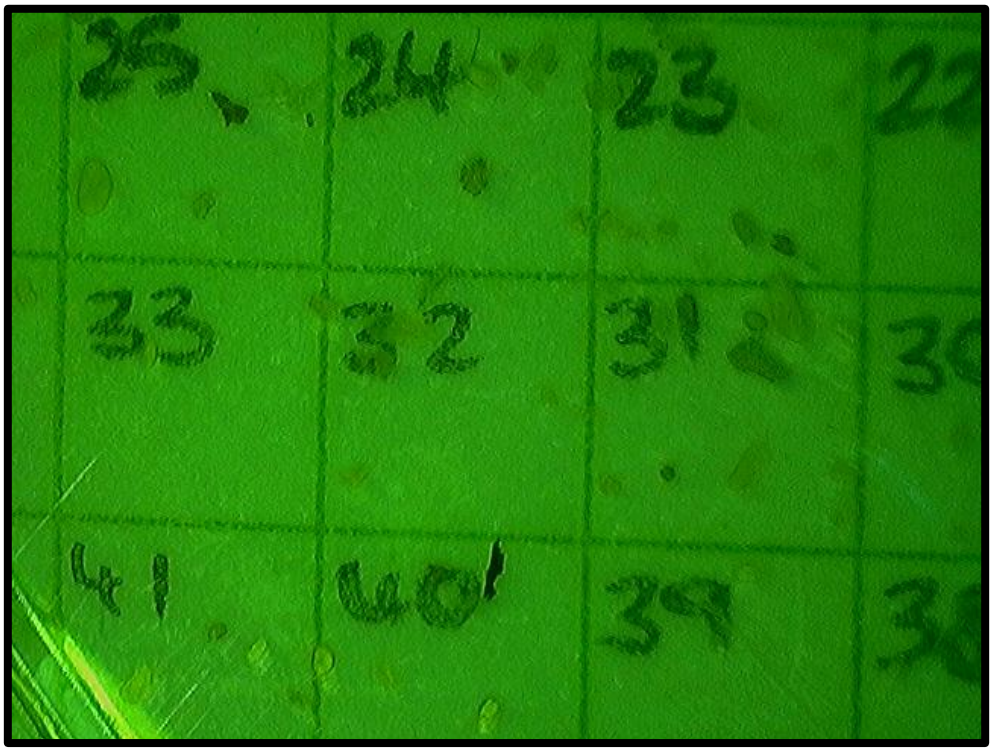

Figure 25: DinoCapture 2.0 image of charcoal surrounded by bleach sample with photo alteration done to the contrast and saturation to make the water green and the charcoal fragments black. Scale is indicated by 1 cm cubes.

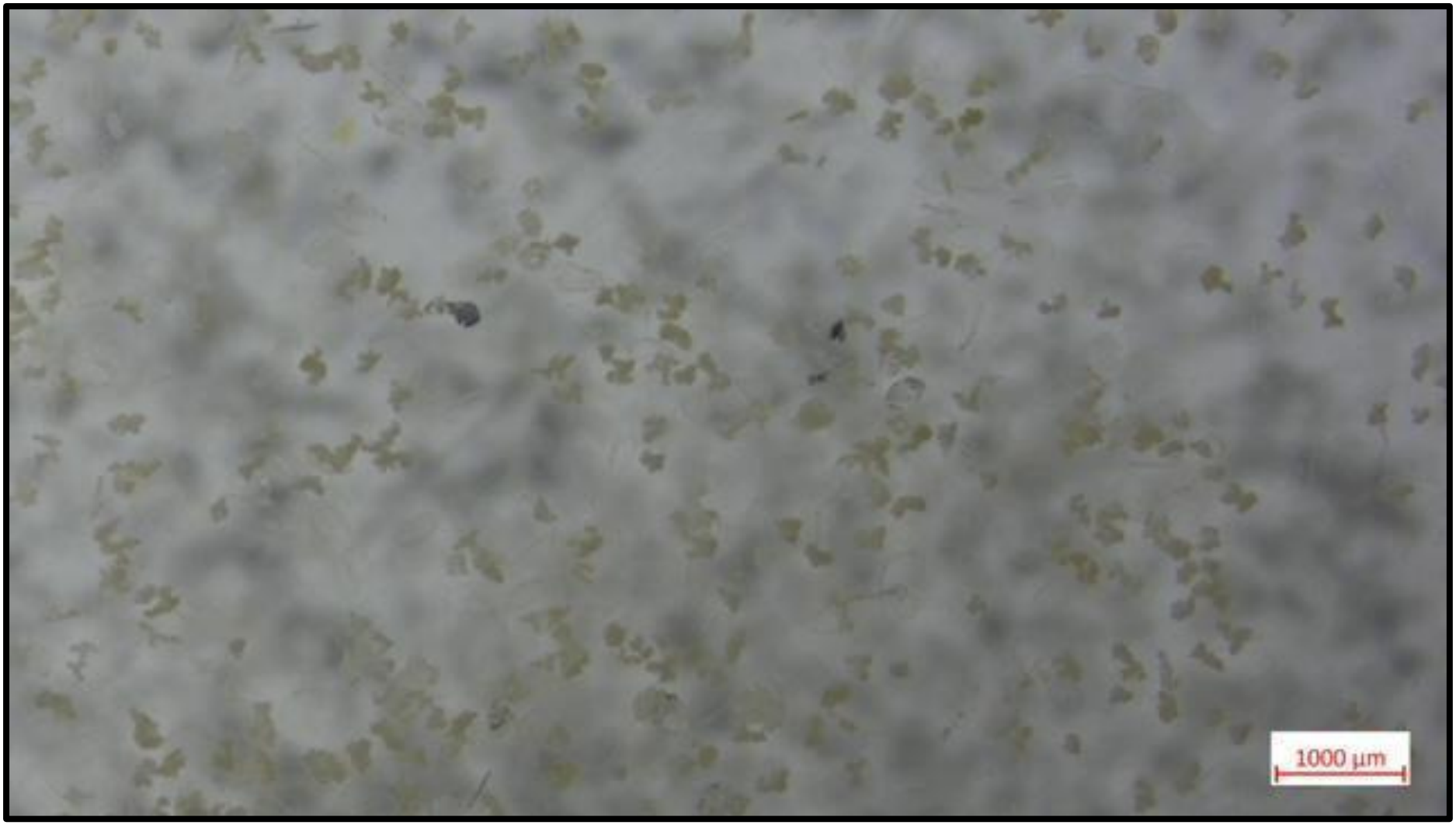

Figure 26: 250-125 microns 0-1 cm, showing the lack of charcoal in the upper layers.

5.9. Magnetic susceptibility and ITRAX:

Magnetic susceptibility was measured using a Bartington MS2 Dual Frequency Magnetic Susceptibility Meter at JCU, and at 5 mm intervals along the whole core prior to splitting. The archive half of the core was sent for ITRAX elemental scanning at the Institute of Environmental Research, Australian Nuclear Science and Technology Organization (ANSTO), Sydney. ITRAX X-ray fluorescence scanning is a non-destructive procedure able to produce X-ray Fluorescence (XRF), X-radiographic and optical images (Davies et al., 2015; Li et al., 2022). The XRF uses X-rays to excite samples which causes core materials to emit secondary X-rays, each characteristic according to elemental composition. (Longman et al., 2019)

Sediment analysis was conducted with a step size of 1000 µm, 30 kV, 55 mA and 10 s count times. The ITRAX data is reported in counts per seconds (cps), then normalised to account for variations throughout the core, according to differing amounts of organic matter, grain size, bulk density and water content (James et al., 2024). Data was then smoothed out using a 10-point running mean to reduce noise. A total of 38 elements were recorded including, Mg, Al, Si, P, S, Cl, Ar, K, Ca, Ti, V, Cr, Mn, Fe, Ni, Cu, Zn, Ge, Br, Rb, Sr, Y, Zr, Sb, Cs, Ba, La, Ce, Nd, Eu, Tb, Dy, Ho, Er, Tm, Hf, Pb, Bi, their corresponding interpretative use shown in Table 3. Not all elements ended up being included in this study, and the results section provides further details.

Table 3: Environmental interpretations of elements within a lagoon context.

Element	Environmental Interpretation	Reference
Al, Ti and Rb	Lithogenic Fluxes (detrital input)	(Boës et al., 2011; Davies et al., 2015; Li et al., 2022)
K	Increase in detrital input	(Kylander et al., 2011; Davies et al., 2015; Lewis et al., 2020)
Ti	Increased runoff	(Metcalfe et al., 2010; Burrows et al., 2014)
Fe and Si	Lithogenic (in *situ* lake processes)	(Haberzettl et al., 2005)
Fe and Mn	Changing redox conditions	(Davison, 1993)
Fe/Mn	Reducing conditions	(Haberzettl et al., 2005)
S/Ti	Presence of pyrite	(Moreno et al., 2007; James et al., 2024)
Si/Ti	Increase in biogenic silica	(Moreno et al., 2007)
Mn/Ti	Oxygenation of the water column	(Moreno et al., 2007)
Ca	Endogenically (in *situ* lake processes) or allogenically (limestone)	(Mueller et al., 2009)

Ca/∑Ti,Fe,Al	Increased endogenic carbonate precipitation (drier conditions)	(Mueller et al., 2009; James et al., 2024)
Inc/coh	Increased organic content	(Haberzettl et al., 2005)

Chapter 6. Results

6.1. Stratigraphic description:

The following core descriptions are based on examination of the analytical half core, as well as referring to the archival half. A brief summary is provided. Detailed stratigraphic results are presented in Table 4. Four sedimentary units and one partially volcanogenic unit were recovered from Kinrara Lagoon (Figure 27).

Figure 27: The Kinrara sediment profile, with the five visually distinct units identified by red dashed boundaries. Scale at right is 1 metre.

Unit 5 – 700-560 cm – This basal unit is at least partly volcanogenic in origin. It consists of deeper coarse sands (including uneven sand clusters), merging into finer upper clays. The lower sediments incorporate weathered granitic fragments containing K-feldspar, with basaltic rock materials more prominent approaching Unit 4 toward the top of the unit. The base of the core represents granite soil or saprolite but is dark and relatively organic rich, so is likely to have been at least periodically swampy. Small fragments of basaltic material begin to occur around 603 cm, with no visible basalt fragments below this depth (Figures 28, 29 and 30). Volcanic glass becomes visible between 601 – 581 cm, and in the 581 – 561 cm section, large quantities of basaltic fragments occur. This is consistent with the upper parts of the unit exhibiting higher magnetic susceptibility readings when compared to the sediments beneath (see section 6.5.1 below).

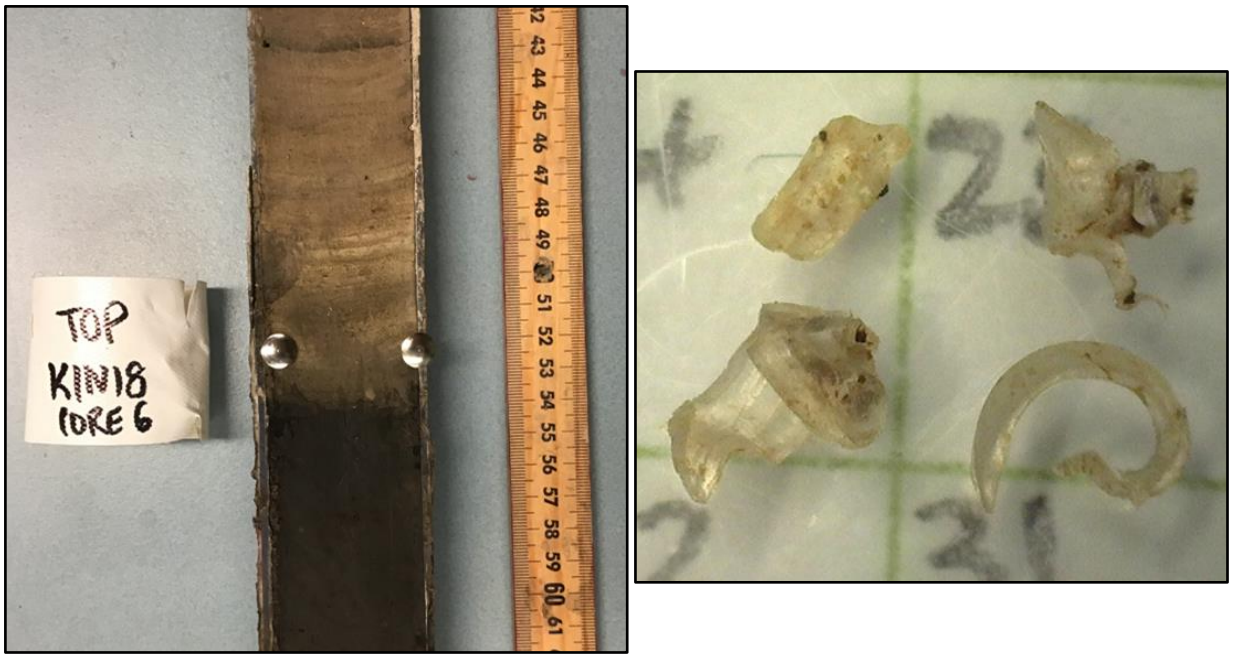

Figure 28: Left: Close-up image of the core showing a strongly defined change from the volcanogenic section (Unit 5) to the carbonate layer (Unit 4). Right: Close-up image of volcanic glass located between 601-581 cm. Scale in cm.

Figure 29: Close-up images of the volcanogenic unit. (A.) showing basalt and volcanic glass between 561 – 581 cm, (B.) showing volcanic glass between 581 – 601 cm, (C. and D.) showing close-ups of the K-feldspars and the transition to non-basaltic volcanic material located at the bottom of the core between 680 – 699 cm. Sclae A, C and D in mm. Pannel B scale in cm.

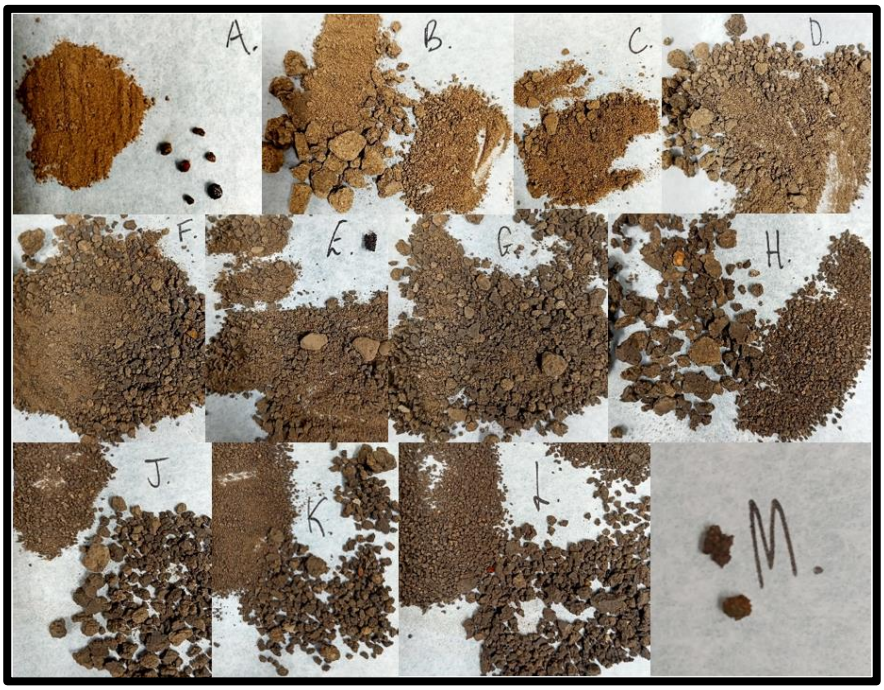

Figure 30: Close-up image of larger material from Unit 5 spanning the sections not sieved between 657 – 603 cm. (A.) 657 cm, (B.) 655 cm, (C.) 651 cm, (D.) 645 cm, (F.) 639 cm, (E.) 636 cm, (G.) 634cm, (H.) 632 cm, (J.) 624 cm, (K.) 614 cm, (L.) 607 cm, (M.) 603 cm. Larger fragments have been manually separated. Field of view in all cases except M is roughly 5 cm, fragments in M are 2 mm diameter.

Unit 4 – 560-380 cm – The beginning of this unit is defined by an abrupt change to carbonate marl (evident as clear, thin laminar carbonate layers), with inconsistent but well-defined black banding scattered throughout (Figure 27 and 28). A 3 cm layer of gastropods, distinctly separating Units 4 from 3 is included (Figure 31).

Figure 31: Close-up image of the core showing 384 to 387 cm section containing a gastropod layer (3 cms) which separates Unit 3 and Unit 4.

Unit 3 – 380-208 cm – the greenish-black silty mud continues, but with decreasing organic matter. Broken gastropod shell fragments are present as the main visible feature (Figure 28 and 32).

Unit 2 – 208-147 cm –This unit is characterized by greenish-black silty mud. Intact and broken gastropods are present throughout.

Unit 1 – 147-0 cm – The uppermost unit is rich in organics (evident in the dark-grey/brown colour displayed in Figure 27). Very fine sands and clays are embedded

throughout. Gastropods are also present, but only sporadically in comparison to the units below.

Table 4: The Kinrara sediment profile, detailed unit and stratigraphic results.

Unit interval (cm)	Layers (cm)	Munsell Colour	Gastropods	Organics	Stratigraphic Description
5. 700-556	700-654	Olive brown (2.5Y 4/4)	Absent	Absent	Clayey (37%) silt (57%) with minimal very fine sand (6%) at 668cm, no obvious bedding though fining upwards with coarse sands at the bottom, to silts and clays into the overlying unit. 10% black (10YR 2/1) <2mm throughout and yellow hue on the surface of the core (potentially secondary oxidation of sulphur)
	654-556	Very dark grey/dark reddish brown (5YR 3/1,2&3)	Absent	Absent	Clay rich (42%) silt (51%) with minor very fine sand (7%) at 562cm, blocky texture with no obvious bedding, colour grading to more pale with depth. Red (2.5YR 4/6) angular mottles <2mm. Gradational boundary with underlying bed. At 631cm, no very fine sand is present, clay becomes richer (52%) and silt slightly decreases (48%).
4. 556-384	556-546	Pale yellow (2.5Y 7/4)	Absent	1% black fragments (<1mm)	Very fine silty sand with carbonate linear ~1 mm laminations, fining upwards in beds 15-20 cm, colour grading to more pale with depth. Terminating at 556 cm with charcoal layer ~2 mm thick.
	546-417	Greyish brown (10YR 5/2)	2% shells and fragments (<3mm)	50% black fragments (<1mm)	Very fine sand (70%) with wavy ~1mm silty (27%) carbonate-rich marl laminations with minor clay (3%) at 435 cm, fining upwards in beds 10-15 cm.20 black 1-3mm thick irregular

					laminations throughout. Red (2.5YR 4/6) angular mottles; 30% <1mm, and 1% 3-4 mm. Terminating at 546 cm with charcoal layer ~2 mm thick. This ratio remains consistent to 465 cm; very fine sand (77%), silt (21%) and clay (2%), and 531 cm; very fine sand (76%), silt (21%) and clay (3%)
	417-387	Pale brown (10YR 6/3)	1% shell fragments (<1mm)	30% black fragments (<1mm), 100% charcoal layer ~2 mm at 391 cm	Silty (26%) very fine sand (71%) with minor clay (3%) at 387cm, carbonate marl silt, <1mm linear organic-rich beds
	387*-384	Greenish black (GLEY 2.5/5GY)	99.9% shells and shell fragments	-	Minimal sediment though organic rich very fine sands and silts, gradational boundary with underlying layer
3. 384-205	384-370	Greenish black (GLEY 2.5/5GY)	10% shell fragments (<1mm) from 471-478 cm	2% black fragments (<1mm)	Silty mud with blocky texture with no obvious bedding or features, bed is linear with sharp contact between the underlying shell layer.
	370-350	Greenish black (GLEY 2.5/5GY)	1% shell fragments (<1mm) from 351-358 cm	2% black fragments (<1mm)	Silt (55%) with similar clay (25%) and very fine sand (20%) at 365cm, blocky texture with no obvious bedding, 30% grey <3mm rounded (2.5Y 5/1) mottles. Bed is linear with sharp contact between the underlying bed.
	350-267	Greenish black (GLEY 2.5/10Y)	Absent	Absent	Silt (50%) with equal clay (25%) and very fine sand (25%) at 276cm, blocky clay with no obvious bedding or features.

					At 345cm very fine sand content increases (41%) with minor decreases in silt (45%) and clay (14%) at 345cm with no other distinguishable changes.
	367-245	Black (GLEY 2.5/N)	Absent	100% black with no discernible fragments	Organic-rich very fine sandy (33%) silt (54%) with minor clay (13%) at 264 cm, plastic texture, potentially charcoal throughout. Grading into the underlying unit.
	245-205	Greenish black (GLEY 2.5/10Y)	Absent	Absent	Clayey (36%) silt (55%) with minor very fine sand (9%) at 241 cm, blocky texture and no obvious bedding or features. Grading into the underlying unit.
2. 205-138	205-138	Black (10YR 2/1)	40% shells and fragments (<1.2cm, 3% <3 mm)	Absent	Organic-rich very fine sandy (32%) silt (47%) with minor clay (11%) at 147cm, blocky texture with no obvious bedding or features.
1. 138-0	138-114	Greyish brown (2.5Y 5/2)	15% shell fragments (<3mm) from 116-121 cm	15% black fragments (<1mm) from 129-138 cm	Very fine sandy (31%) silt (55%) with very fine sand (13%) at 126cm, very fine ~1mm bedding, colour grading from light (at the top to darker at the base – Munsell Colour was measured in the middle of the section).
	114-79	Black (10YR 2/1)	40% shells and fragments (<8mm)	7% black fragments (potentially charcoal)	Clay mud with some porosity due to the high density of shells. Large shells (~2 cm) preserved between 92-96cm and 110-114cm. 15% angular blocky grey (2.5Y 5/1) mottles. Sharp angular contact with underlying unit.
	79-72	Dark greyish brown	25% shells and	25% charcoal	Organic rich very fine sand (41%) and silt (48%) with minor clay (11%) at 75 cm, very fine

		(2.5Y 4/2)	fragments (3-5mm)	fragments (<1mm)	bedding (<1mm) and gritty texture due to increasing abundance of shells into the underlying bed. Sharp linear contact with the underlying shell-rich unit.
	72-51	Very dark grey (2.5Y 3/1)	7% shells and fragments (3-5mm)	9% black fragments (<1mm) 1% charcoal fragments (1-33mm)	Organic-rich sticky mud with fibrous herbaceous detritus, no obvious bedding.
	51-38	Dark olive grey (5Y 3/2)	1% shell fragments (<3mm)	1% black fragments (potentially charcoal)	Organic-rich silty (34%), very fine sand (60%) with minor clay (11%) at 40 cm, no obvious bedding, terminating with sharp ~1mm charcoal band.
	38-0	Very dark grey (10YR 3/1)	5% shell fragments (<3mm)	1% black fragments (potentially charcoal)	Wet marshy section at the top of the core, dark mud, organic-rich with minor woody and herb detritus, no obvious bedding, grading into underlying unit.

6.2. Chronology:

Results from the seventeen SPAC, bulk sediment and bark samples are presented in Table 5. Unit 5 contained sparse trace amounts of datable material (macro plant remains, charcoal) with only a single date generated from the bottom of the core (see previous section 5.6. Chronology (methods), for more details). This bark dates to 35,300 cal yr BP, providing a lower time frame for Unit 5, with a linear relationship assumed from bark depth to the Unit 4 boundary (Figure 32).

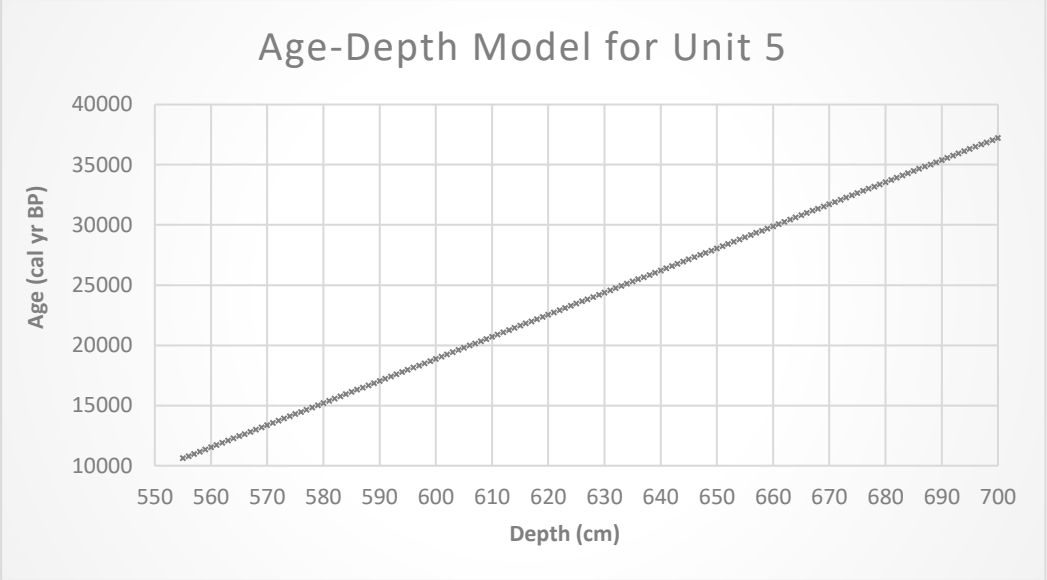

Figure 32: Linear relationship assumed from bark date to the Unit 4 boundary (first radiocarbon date).

Calibrated ages were used to model the age-depth relationship from the base of Unit 4 (at 10,651 cal yr BP) to the modern surface. Four radiocarbon dates returned significantly older results out of sequence and were labelled as outliers by the Bayesian model. These were excluded by the model (as listed in Table 5). Repeat analyses were undertaken where outlier ages were reported, resulting in dates that aligned closely with the overall chronological sequence. These were accepted by the Bayesian model (Figure 33). The old outlier samples may have incorporated radiocarbon-dead geogenic carbon associated with the Kinrara eruption(s), introduced into the charcoal poor carbonate marl unit. This possibility will be explored within the discussion section of this thesis.

Table 5: All 17 radiocarbon dates for the Kinrara core.

Lab	Lab Code	Sample Name	14C yr BP	±	cal yr BP	Component	Sedimentary Unit	Accepted/Excluded
Waikato	Wk-51097	0-1m 48-50 cm	191	25	267	Wood	1	Accepted
ANSTO	OZX796	K1 49-51 cm	860	30	729	SPAC	1	Accepted
ANSTO	OZX797	K2 40-41 cm	1905	30	1775	SPAC	2	Accepted
ANSTO	OZX798	K2 79-80 cm	2345	35	2590	SPAC	2	Accepted
Waikato	Wk-51538	2-3m 22.5-23.5 cm	3379	20	3527	SPAC	3	Accepted
Waikato	Wk-51937	2-3m 23.5-25 cm	3440	20	3637	Bulk	3	Accepted
ANSTO	OZX799	K3 49-51 cm	6380	25	6775	SPAC	3	Accepted
Waikato	Wk-51539	3-4m 24.5-25.5 cm	8796	23	-	SPAC	3	Excluded
Waikato	Wk-51938	3-4m 25.5-27 cm	7283	22	8063	Bulk	3	Accepted
ANSTO	OZY599	3-4m 80-82 cm	8020	45	8762	SPAC	4	Accepted
ANSTO	OZX801	K4 80-82 cm	8655	40	-	SPAC	4	Excluded
Waikato	Wk-51094	4-5m 69-71 cm	8621	30	9581	SPAC	4	Accepted
ANSTO	OZY596	4-5m 73-75 cm	16,140	490	-	SPAC	4	Excluded
Waikato	Wk-51541	5-6m 24.5-25.5 cm	8830	38	10,105	SPAC	4	Accepted
ANSTO	OZY598	5-6m 51-53 cm	13620	370	-	SPAC	4	Excluded
Waikato	Wk-51540	5-6m 53.5-54.5 cm	9423	30	10,617	SPAC	4	Accepted
Waikato	Wk-54174	KIN 18 Bark 644-622 cm	30900	263	35,300	Bark/Wood	5	Accepted

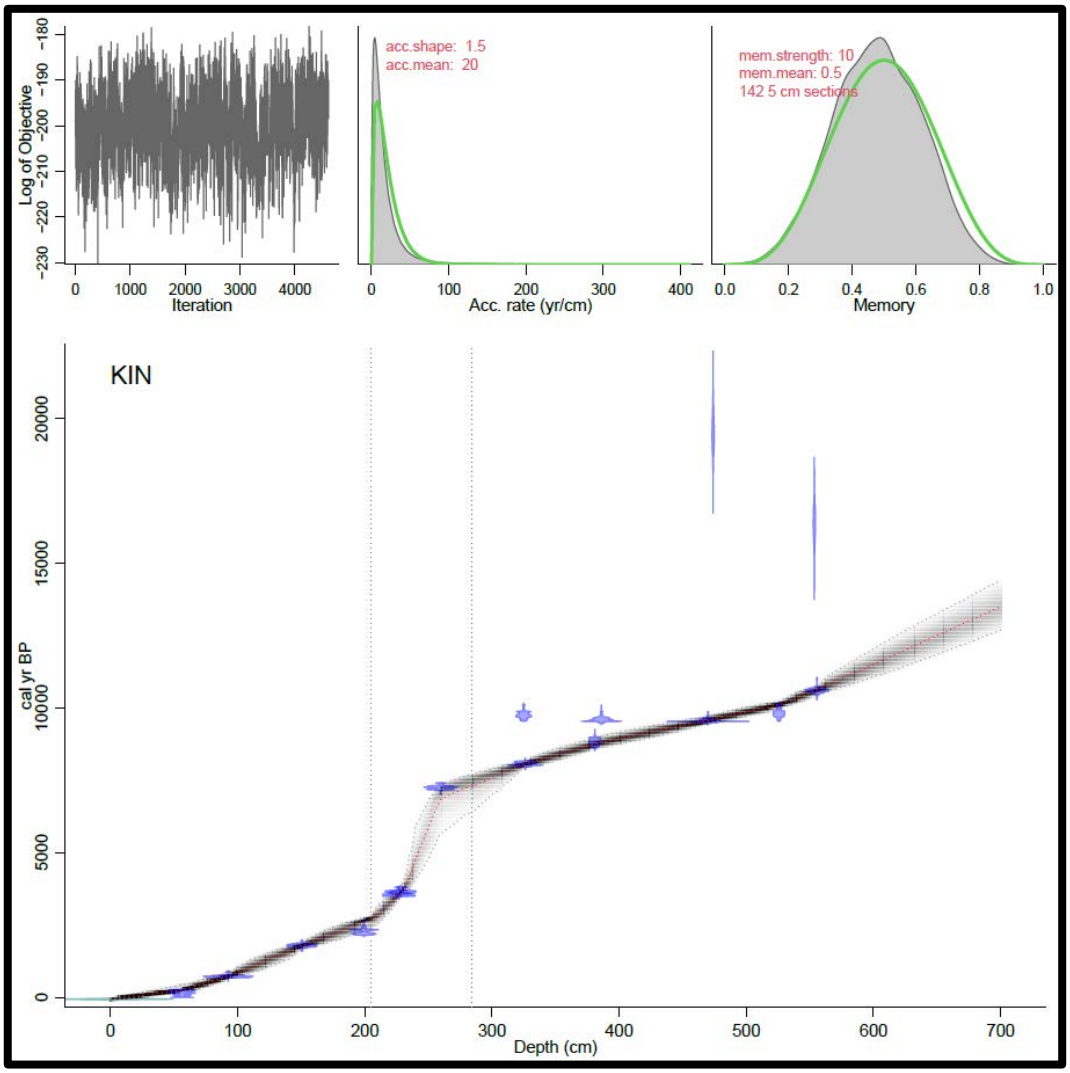

Figure 33: Age-depth model produced by the interpolation of dates and accumulations rates using Bayesian statistics. Upper and lower confidence limits are represented by the grey dotted lines and the red line represents the medial value. Dashed lines at ~200 cm and ~280cm represent large changes in accumulation rates taken into consideration by the Bayesian modelling. Note that below 570 cm, the age depth relationship from figure 32 above is used.

6.3. Mass accumulation rates:

The mass accumulation rate for each depositional unit was calculated based on the age-depth model in Figure 33 and a linear model for Unit 5, using the dry bulk density data in Figure 34 and 36. The Kinrara core exhibits variable total mass accumulation rates along its length, with the average for each unit provided in Table

6. The middle section of the core – Units 2 and 3 – demonstrates much slower accumulation than Units 1 and 4. Unit 5 exhibits an extremely slow mass accumulation rate compared to all other units. These trends will be further explored in the next section.

Table 6: The average mass accumulation rate in mg/cm²/y of all 5 units in the core.

Section	Average total mass accumulation rate (mg/cm²/y)
Unit 1, 0 – 147 cm	35.14
Unit 2, 147 – 208 cm	18.24
Unit 3, 208 – 380 cm	14.52
Unit 4, 380 – 560 cm	42.72
Unit 5, 560 – 700 cm	3.98

6.4. Stable carbon isotopes of total organic carbon and carbon:nitrogen ratios:

The whole core was analysed for nitrogen abundance, with the majority of samples with nitrogen below the detection limit. Therefore, a full C:N time series could not be constructed. Across all samples, two intervals of higher N abundance, enabling calculation of a C:N ratio are apparent, with values of 5 to 20 and corresponding to low $\delta^{13}C_{TOC}$ values (-37 ‰ to -28 ‰). These date to between 10,500 – 7000 cal yr BP and 2500 cal yr BP to modern and will be discussed later in the discussion chapter (Figure 41).

6.5. Physical and geochemical attributes of the Kinrara Lagoon sediment core:

The age-depth model and the bulk density determinations enable the calculation of mass accumulation rates. The results below are presented by unit number beginning with the oldest sediments (Unit 5) and progressing upward to the core top layer (Unit 1). Because Unit 5 covers an extended time span and is significantly different in many characteristics to the overlying units, Figures 34 and 35 show the results for Unit 5, and the lower part of Unit 4 for comparative purposes. Figures 36 and 37 show the results for Units 1-4, with Unit 5 for comparative purposes.

6.5.1. Unit 5 – 700-560 cm (37,227 – 11,500 cal yr BP):

Unit 5 spans an extended period of ~25,000 years over 140 cm from late MIS 3 to approximately the Pleistocene-Holocene boundary. It is clearly differentiated from younger units via bulk density, magnetic susceptibility and ITRAX geochemistry (Figure 34). Dry bulk density in the unit is comparatively high, averaging ~0.8 g/cm^{-3}, trending to slightly lower values of ~0.6 g/cm^{-3} towards the Unit 4 boundary. Magnetic susceptibility is very high (readings up to 350); erratic from the base of the core to 670 cm, abruptly decreasing and stabilising to relatively high (~50-100) values at the top of the unit when compared to Unit 4 onwards (values of ~0-10). ITRAX geochemistry indicates Unit 5 is dominated by mineral detritus, with high and relatively invariant concentrations of Si and, but relatively low Ca and Si/Ti. Overall, Si/Ti decreases steadily toward Unit 4. Ti and K are also high (Ti increases while K decreases up the unit), both consistent with an increasing basalt-derived minerogenic component mixed into the granite saprolite/soil.

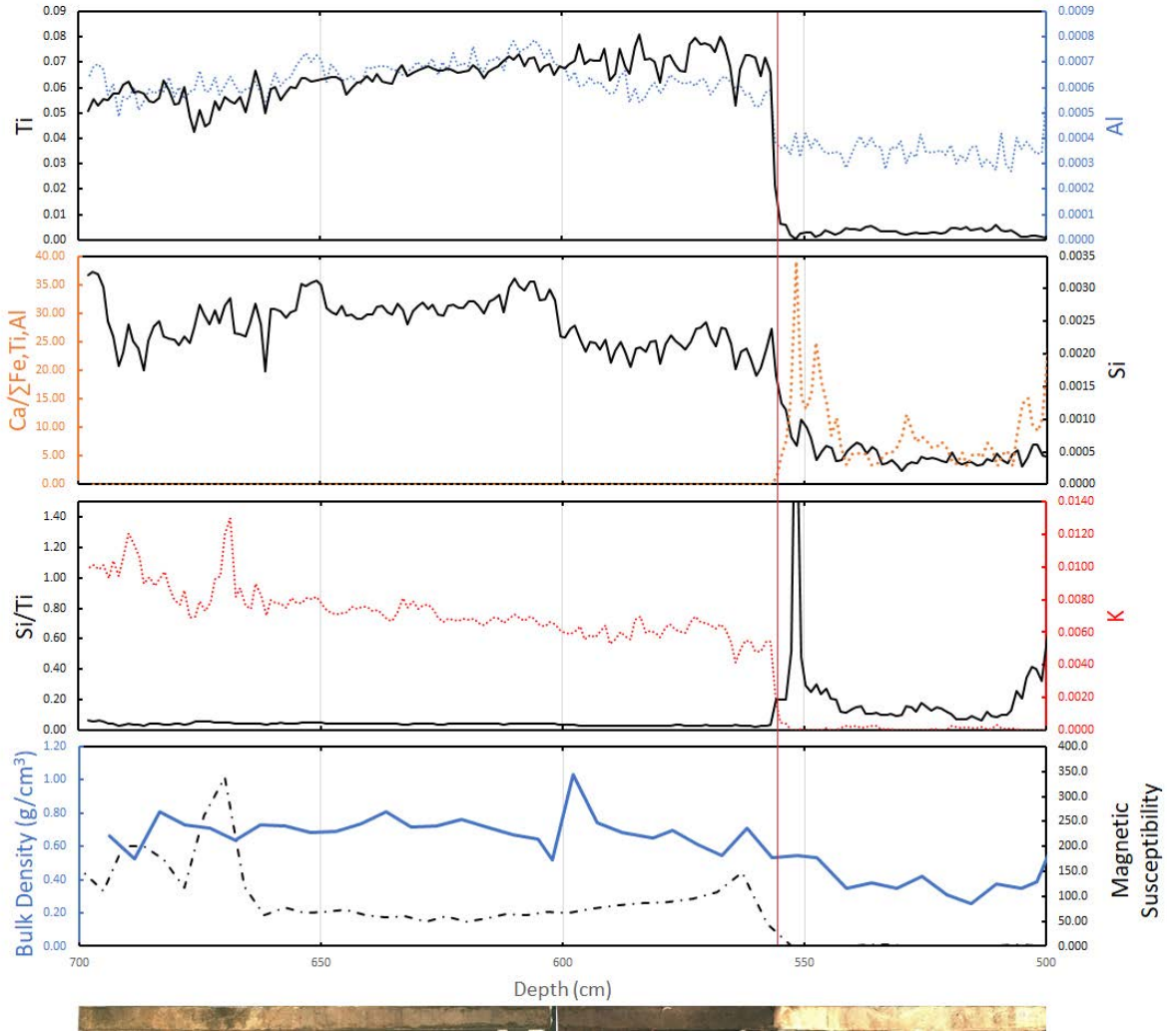

Figure 34: Unit 5 and 4 on a depth scale containing ITRAX data, dry bulk density and magnetic susceptibility. Red vertical line indicates boundary between Unit 5 and 4.

TOC is initially low at ~0.1 % then increases steadily to >1 % toward the upper part of the unit. This change is broadly mirrored by an increase in $\delta^{13}C_{TOC}$ values from -27 ‰ at the base to -13 ‰ toward the top, which then abruptly drops entering Unit 4, to -33 ‰ (Figure 35). C:N ranges from 15 to 20 from the base upwards, (though note that the majority of samples in this section contained no measurable nitrogen). SPAC accumulation rates are initially low (<10 µg/cm^{-2}/yr^{-1}) and increase to values >50 µg/cm^{-2}/yr^{-1} in the upper third of the unit. As with TOC this change is broadly mirrored by an increase in $\delta^{13}C_{SPAC}$ values from -23 ‰ at the base to values

of >-13 ‰ in the upper third of the unit. Charcoal flux is relatively low (between 0 – 0.2 particles/cm²/yr) throughout the entirety of the unit.

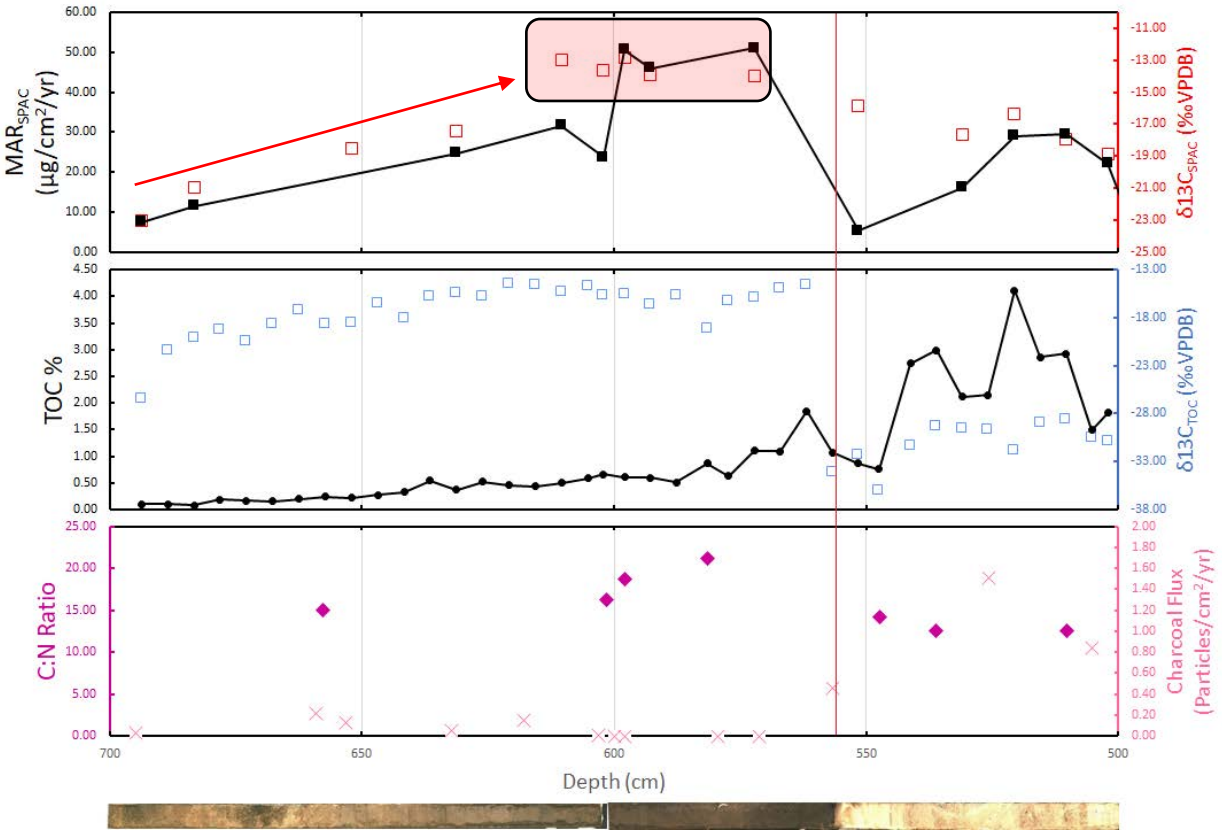

Figure 35: Unit 5 and 4 on a depth scale containing MAR$_{SPAC}$, δ^{13}C$_{SPAC}$, TOC%, δ^{13}C$_{TOC}$, C:N ratio and Charcoal Flux. Vertical red line indicates boundary between Unit 5 and 4. Red square indicating most likely period of time of the LGM. Red arrow pointing out the transition from woody to grassy stable carbon isotopes.

6.5.2. Unit 4 – 560–380 cm (11,500 – 8750 cal yr BP):

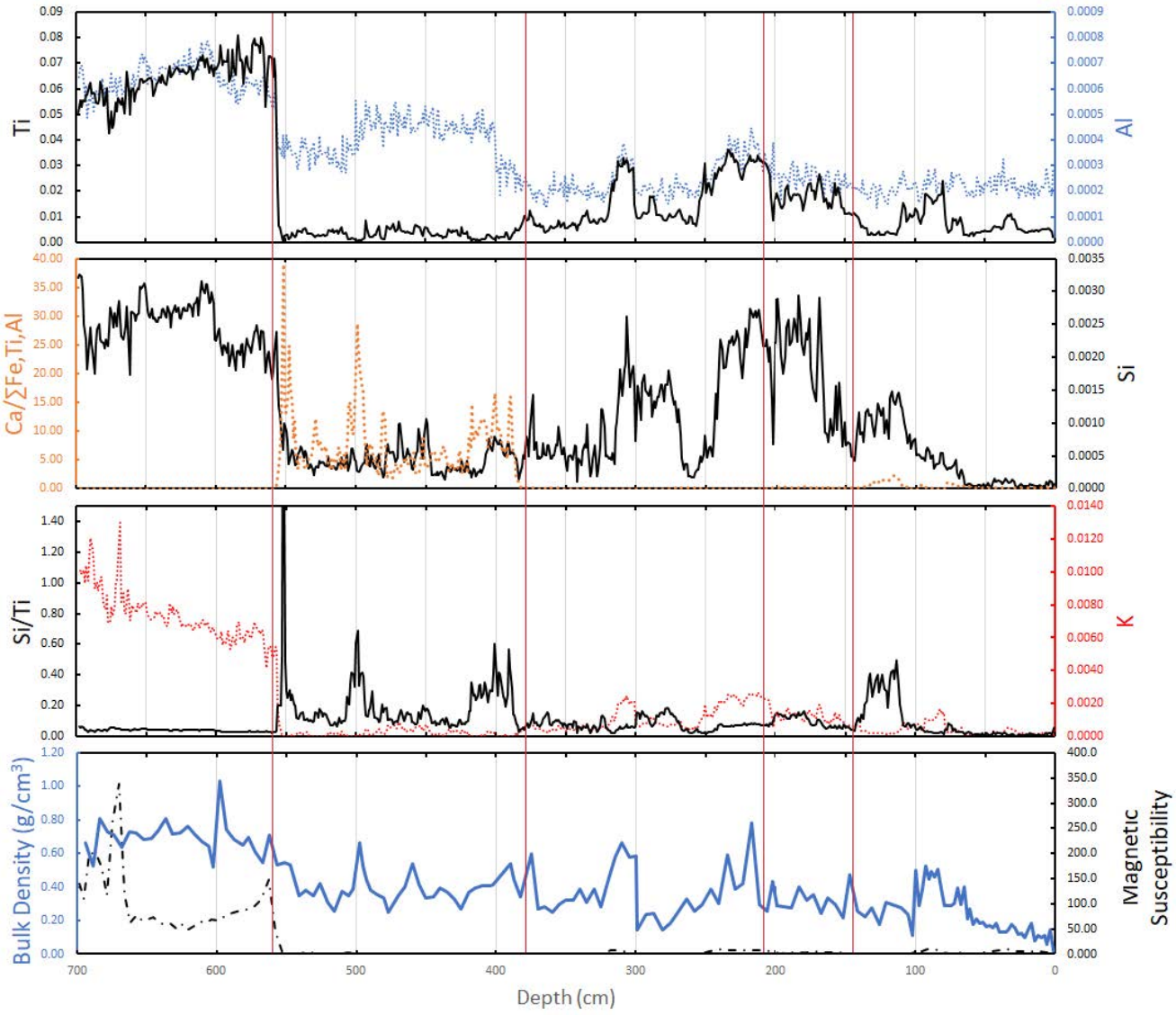

Figure 36: Unit 1-5 characteristics as a function of depth showing ITRAX data, dry bulk density and magnetic susceptibility data. Red lines indicate unit boundaries.

Unit 4 spans 2750 years over 180 cm within the early Holocene and is clearly separated by an abrupt change in most characteristics from Unit 5 below (Figure 36). Dry bulk density decreases to ~0.35 g/cm^{-3}, while magnetic susceptibility decreases sharply to very low values approaching zero. These remain low throughout the unit and the rest of the core. ITRAX geochemistry indicates Unit 4 is characterized by a sharp increase in Ca, which varies erratically through the unit with major peaks in

abundance at 560 and 500 cm. Mineral-derived elements, Ti, Si, Al and K all decrease at the Unit 5-4 boundary and fluctuate but remain low through Unit 4. Peaks in Si/Ti at around 550, 500 and 400 cm indicate pulses of quartz influx, while higher Al between 500 and 400 cm suggest an increase in clay minerals delivered to the site. TOC increases somewhat being generally above 2 % and C:N values range from 15 to 20 (Figure 37). C:N data is grouped within Unit 4 – this is the first section with consistently measurable nitrogen contents – an interval that corresponds with the low $\delta^{13}C_{TOC}$ values. $\delta^{13}C_{TOC}$ values are uniformly low at <-27 ‰ reaching as low as -37 ‰ between 560 and 380 cm. SPAC accumulation rates range between 5 and 30 $\mu g/cm^{-2}/yr^{-1}$, with no overall trend through the unit. In contrast, $\delta^{13}C_{SPAC}$ values decrease erratically from -16 ‰ at the base to values of -21 ‰ at the top of the unit. Charcoal flux continues to be very low between 0 – 1 particles/cm^2/yr throughout the entirety of the unit.

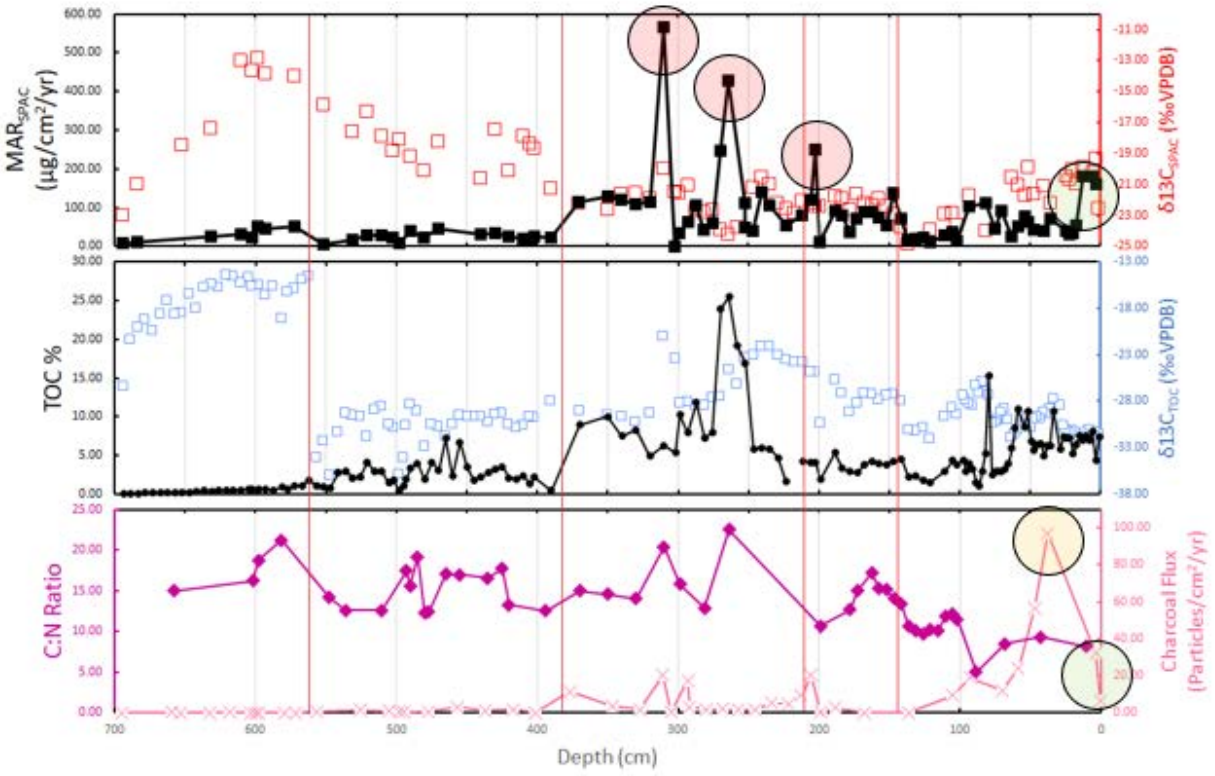

Figure 37: Units 1-5 on a depth scale containing MAR_{SPAC}, $\delta^{13}C_{SPAC}$, TOC%, $\delta^{13}C_{TOC}$, C:N ratio and Charcoal Flux. Red line indicates separation of Unit 5 to 1. Red Circles indicating three large fire events, green circles showing the sharp decrease in charcoal flux and change in stable carbon isotopes in present day and the yellow circle highlighting the rapid increase in charcoal flux.

6.5.3. Unit 3 – 380-208 cm (8750 – 3600 cal yr BP):

Unit 3 spans 5,150 years over 180 cm extending through the middle Holocene. Dry bulk density ranges widely from 0.15 to 0.8 g/cm^{-3}, and magnetic susceptibility remains close to zero (Figure 36). The large changes in bulk density are mirrored in the ITRAX geochemistry. Calcium becomes a very minor component throughout, but Si and Ti increase relative to Unit 4, with two broad intervals of high abundance between 320-270 cm and 230-210 cm, (indicative of higher clastic input at this time). Aluminium, indicative of a clay component, is lower in Unit 3 compared to Unit 4 but exhibits the same peaks in abundance as Ti and Si.

The major difference between Unit 4 and Unit 3 is a significant increase in TOC to values generally >5%, with a particularly organic-rich unit of up to 25% TOC between 270 and 230 cm (Figure 37). C:N values range from 15 to 20, similar to Unit 5, but the number of data points in Unit 3 are limited due to the majority of samples lacking detectable nitrogen. $\delta^{13}C_{TOC}$ values initially remain similar to Unit 4 but increase above 320 cm to values as high as -21 ‰. SPAC accumulation rates increase in Unit 3 compared to Unit 4 (averaging ~100 µg/cm^{-2}/yr^{-1}). Major peaks in accumulation rate up to 570 µg/cm^{-2}/yr^{-1} centre on 310 and 280 cm. $\delta^{13}C_{SPAC}$ values do not track the spikes in SPAC accumulation, remaining generally below -21 ‰ and as low as -24.5 ‰, with some broad oscillations evident between these values, and the lowest values coinciding with the peak in SPAC accumulation rate at 280 cm. Charcoal flux shows a slight relative increase between 0 – 2 particles/cm^2/yr, with two large spikes up to 20 particles/cm^2/yr, to coincide with the 310cm SPAC peak.

6.5.4. Unit 2 – 208-147 cm (3600 – 1700 cal yr BP):

Unit 2 spans 1900 years over 53 cm, covering the later Holocene. Most parameters lack variability over this interval (Figure 36). Dry bulk density is relatively consistent around ~0.3 g/cm^{-3}, and magnetic susceptibility remains close to zero. Calcium and K remain low, Si and Ti decrease through the interval while Al remains stable.

TOC averages ~5% with little variation. C:N values range from 10 to 20 with numerous samples containing measurable nitrogen. $\delta^{13}C_{TOC}$ values are also relatively stable around ~-28 ‰, characterising this second cluster of C:N data within the core (Figure 37). SPAC accumulation rates are relatively steady around ~100 µg/cm^{-2}/yr^{-1} (excluding a spike to 250 µg/cm^{-2}/yr^{-1} at the start of this unit). $\delta^{13}C_{SPAC}$ values are

also relatively invariant, at around -22 ‰. Charcoal flux is relatively low (between 0 – 0.2 particles/cm^2/yr) throughout the unit. One charcoal spike to 20 particles/cm^2/yr at the start of the unit coincides with the SPAC spike.

6.5.5. Unit 1 – 147-0 cm (1700 - 0 cal yr BP):

Unit 1 spans 1700 years over 147 cm, from the late Holocene to present. Variability in most parameters increases relative to Unit 2 (Figure 36). Dry bulk density exhibits a broad peak at around ~0.3 g/cm^{-3}, centred on 90 cm, thereafter, declining to <0.1 g/cm^{-3} toward the surface. Magnetic susceptibility remains close to zero, and Ca and K remain low. While Al remains constant through the unit, Si is elevated between 147 and 110 cm, and Ti is elevated from 110 to 80 cm. Both Si and Ti then decrease from 80 to 0 cm. The inverse relationship between Si and Ti means that Si/Ti exhibits a strong peak between 130 and 110 cm, similar in form and magnitude to peaks observed in Unit 4, suggestive of an increase in quartz relative to clay.

TOC is initially low at <2 % but increases progressively toward values of >5 % above 70 cm depth, with brief excursions to values above 10 % (centred on 80, 60 and 30 cm) (Figure 37). C:N values range from ~5 to 15 with a high number of samples containing nitrogen up to 100 cm depth above which N content significantly lowers . Values for $\delta^{13}C_{TOC}$ are initially low at <-30 ‰, then oscillate between -30 and -25 ‰ in several cycles toward 0 cm. SPAC accumulation rates generally increase through the unit from <50 µg/cm^{-2}/yr^{-1}, at the base to 150 µg/cm^{-2}/yr^{-1}, at 0 cm. $\delta^{13}C_{SPAC}$ values also increase erratically from -25 ‰ at the base of the unit to ~-20 ‰ in the upper 20 cm. Charcoal flux is initially at 0 particles/cm^2/yr and then rapidly

increases to 100 particles/cm^2/yr over the next ~90 centimetres. Values abruptly decrease to near zero in the uppermost 10cm.

Chapter 7. Discussion

The multiproxy Kinrara record provides a rare long and continuous archive of environmental change in the seasonally dry tropical savanna region of north Queensland. The record complements the relatively large number of records available from the wetter Atherton Tablelands region 140 km to the north. The sediments and the proxy record they contain exhibit several clear, often abrupt, changes that have been described in previous chapters and enable the delineation of 5 discrete units from the late Pleistocene to the modern. In this chapter, each of these time intervals is interpreted in terms of the evolution of environmental conditions at the site over the last ~37,000 cal yr BP. Delineation of these environmental conditions facilitates the interpretation of the evolution of fire regimes in the area and the drivers of changes in fire regimes.

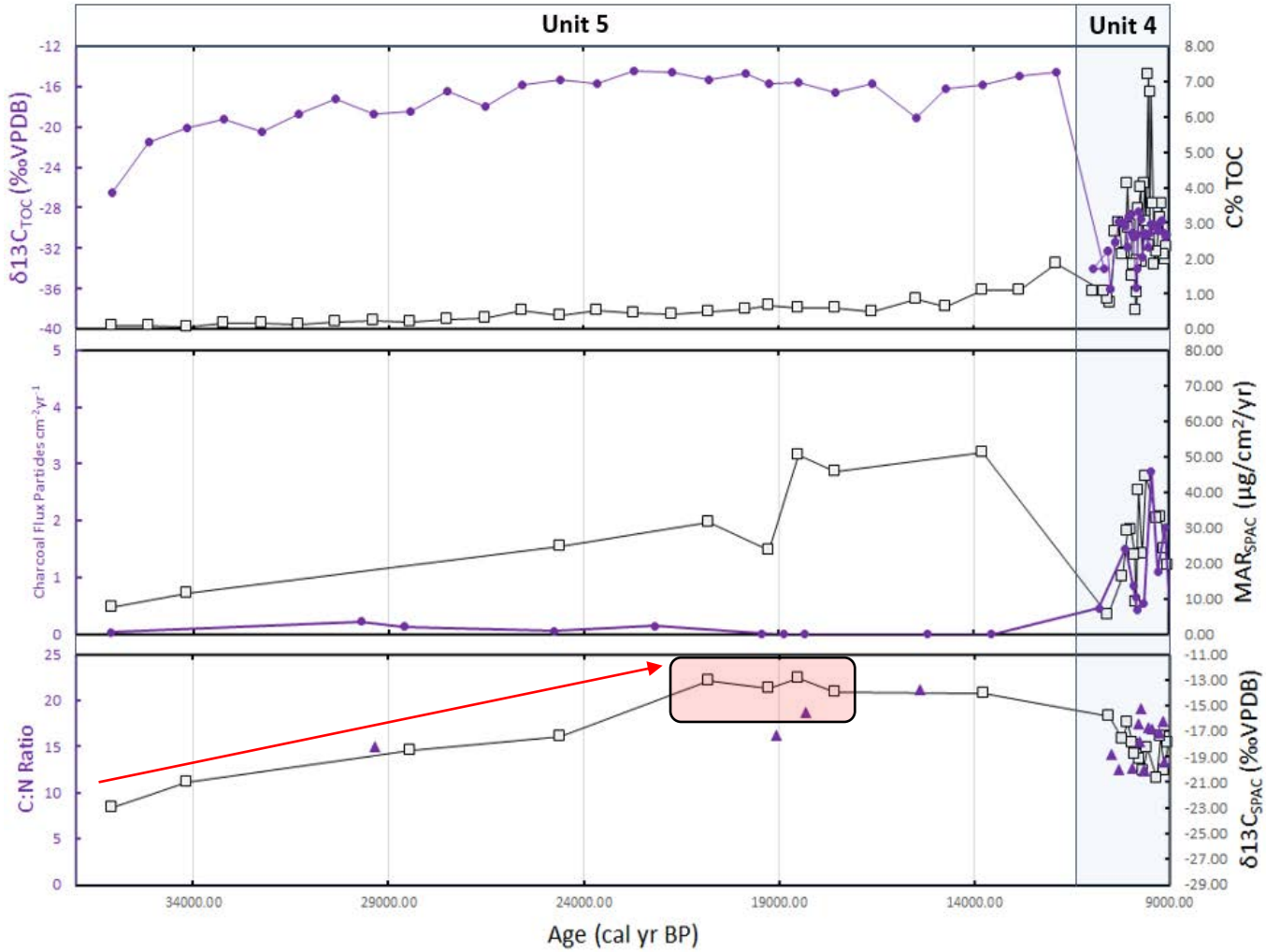

Figure 38: Mass accumulation rate of stable polycyclic carbon (MAR_{SPAC} (µg/cm²/yr¹), charcoal flux particles (cm^2y^{-1}) , C:N ratios and stable carbon isotopes ($\delta^{13}C_{SPAC}$) on the SPAC component of the samples through the Pleistocene and Holocene section of the Kinrara core. The red square indicates the most likely period of time of the LGM. The red arrow points out the gradual transition from woody to grassy stable carbon.

7.1. Late Pleistocene – dry and grassy: (Unit 5 – 700-560cm; 37,227 – 11,500 cal yr BP):

The oldest interval of the core, Unit 5, was deposited from ~37,000 cal yr BP, representative of late Pleistocene and final stages of Marine Isotope Stage (MIS) 3. Unit 5 also includes the Last Glacial Maximum (LGM). Dates are only available for the bottom and top of the unit, hence the detailed chronology of events within this period are uncertain. The unit predates the damming of the waterway by the Kinrara basalt flow, but the significant changes that occur through the interval indicate that it is at least in part accretionary. The unit is dominated throughout by high abundances of lithogenic elements indicating that the unit was not deposited in a lagoon environment (Figure 34 and 36 in results section).

The lowermost part of the unit appears saprolitic and mostly comprises weathered granitic material (Figure 34 in results section), with high magnetic susceptibility. While bedrock in the region is dominantly basalt at the surface, inliers of granite are known to occur (Queensland Government Department of Natural Resources and Mines, 1994), and the presence of weathered granite fragments in the interval suggests such an inlier occurs at shallow depth in the Kinrara catchment. Beginning at 603 cm there is an increase in fragments sourced from the nearby Kinrara volcano, likely as airfall or water-borne ash particles. A decrease in Si/Ti (Figure 34 in results section) is consistent with an increase in Ti-rich basaltic component in the sediments over the interval. The presence of these fragments further suggests that the Kinrara Volcano was active in some form well before the available earliest dates for Lava flows from the volcano 7000±2000 cal yr BP (Cohen et al., 2017).

The incorporation of basaltic fragments in the sequence provides further evidence that the sediment continued to accumulate, at least episodically, through the late Pleistocene and therefore contains an interpretable record of change. However, there being only two dates from the bottom and top of the unit, it is difficult to accurately determine the timing of the observed changes. Given the location of the site near the course of the creek that was dammed to form the lagoon, it seems plausible that sediment accumulation during this interval was driven by overbank deposition of sediment during flood events, or that the local environment was perennially swampy as a result of the continuous discharge from the nearby Kinrara spring. Similarly swampy, riparian areas occur upstream of the lagoon in the vicinity of the spring today.

TOC is initially very low (<0.1%) and remains low for the initial 50cm of the interval. It is possible that this section is a buried soil/saprolite. The earliest radiocarbon date of 37 000 cal yr BP is from this interval, and therefore provides an age for this soil/saprolite. $\delta^{13}C_{TOC}$ values generally in the range of -18 to -20 ‰ indicate a mixed C_3 and C_4 source, consistent with open savanna vegetation being present at the time (Figure 38). Fire was present in the landscape at low levels, indicated by low MAR_{SPAC} (10-20 µg/cm^2/yr), with relatively low $\delta^{13}C_{SPAC}$ (-21 to -23 ‰), indicating a significant fraction of C_3 biomass in the total biomass burnt.

Above 650 cm TOC increases, consistently and dramatically over the remainder of the interval, to values of slightly above >1 % in the upper 25 cm of the unit (Figure 38). This interval is suggested to be sedimentary in nature, with basalt fragments in samples from 603 cm clearly marking the sediments above this point as sedimentary. It is not possible to constrain the age at which sedimentation was

initiated, however, it is likely that an extended period of buildup was required to accumulate the 1 metre of sediment. It is thus also likely that this interval includes at least the LGM and possibly much of MIS 2, as well as the post-glacial period until the Holocene. $\delta^{13}C_{TOC}$ values increase to very high values of ~-13 to -14 ‰ indicating a transition to an almost treeless grassland/sedgeland at the site, at a time that may equate to the LGM. Grassland values are mirrored by the $\delta^{13}C_{SPAC}$ (-23 to -13 ‰). Cadd et al., (2021) have identified 28,600 to 17,700 cal yr BP as the period of maximum cooling and low productivity on the Australian continent and Li et al., (2023) have indicated the Tablelands region just north was 3-4˚C cooler at 18,000 cal yr BP than at present (Li et al., 2023). The LGM is also associated with relative aridity in northern Australia which is seen here in the Kinrara record (Reeves et al., 2013).

A small decline in $\delta^{13}C_{TOC}$ values as low as -18 ‰ in the upper 50 cm suggests that the Unit 5 interval does contain fluctuating periods of higher tree presence, possibly associated with an amelioration of conditions in the immediate post-glacial period. There is a distinct decrease to lower, then constant Ca/(Σ (Fe, Ti, Al) at 600 cm to indicate a change in the local environment occurs at this point. Fire incidence as represented by MAR_{SPAC} (20 to 40 µg/cm^2/yr) remains relatively low, consistent with relatively sparse vegetation cover accompanying glacial aridity, with $\delta^{13}C_{SPAC}$ (-13 to -14 ‰) corroborating the conclusion that local vegetation was dominated by C_4 grasses/sedges.

Overall, the results suggest that the period prior to the Holocene, likely covering the LGM and earlier, was comparatively dry with tree cover reducing into an almost completely C_4-dominated local landscape, with some evidence for a return

to slightly increased tree cover in post-glacial times. Fire incidence was low and the $\delta^{13}C_{SPAC}$ values corroborate the conclusion that at the LGM the area was covered by C_4 dominated vegetation. It should be noted that an increase in burning during this period does not appear to accompany fluctuating woody cover. This conclusion is consistent with the limited evidence from this time available from elsewhere in the region. This includes an abrupt increase in sclerophyll taxa at the expense of rainforest taxa in the record and relatively low microcharcoal counts at the LGM from Lynch's Crater, sclerophyll woodland at Lake Euramoo and the ODP-820 (a coastal record around 90km offshore from the Atherton Tablelands), transitioning toward rainforest in the post-glacial times after ~20,000-17,000 cal yr BP (Haberle, 2005; Moss & Kershaw, 2007; Kershaw et al., 2007; Moss et al., 2017). As a final note in section 4.5, PaleoView was used to generate annual mean precipitation and temperature trends. The model showed that between 21,000 to 9000 years ago the Kinrara region experienced around 15% less rainfall and the area was cooler which agrees with the data interpretation presented here (See section 2.2. palaeo-view model for the last 21,000 years)

The conclusion that tree cover in the area in glacial times was low, implies a significant lowering of rainfall, or significantly more variable inter-annual rainfall, or both. Grasses tend to be favoured in clay soils under conditions of water stress because trees rely to a greater degree on deep soil moisture than grasses, which access moisture only from the upper soil layers (Scanlan, 2002). The study site is largely on basalt-derived clay soils, and hence water stress may have significantly impacted tree cover in the past.

The Mitchell grasslands of central north Queensland, for example, exist in areas with generally <550 mm mean annual rainfall. While not a direct analogue (because Mitchell grasslands exist on alkaline cracking clays), this might suggest a lowering of mean annual rainfall from ~758 mm presently (see Chapter 5), to something under ~600mm, equivalent to a ~20% (or more) decrease. The decrease inferred for the Kinrara area is smaller than the 40% decrease in LGM rainfall at Girraween Lagoon in the Northern Territory (Rowe et al., 2021; Wurster et al., 2021a; Rowe et al., 2022a) but that site is significantly impacted by lower glacial sea level. The Girraween site was 330 km from the coast at the LGM, and rainfall was lowered partly by the gradient in rainfall away from the coast. The impact of lowered sea level is less significant for the north Queensland region, where the coast only retreated by 60-70 km at the LGM (See Figure 4 in 2.1. Palaeoenvironmental studies).

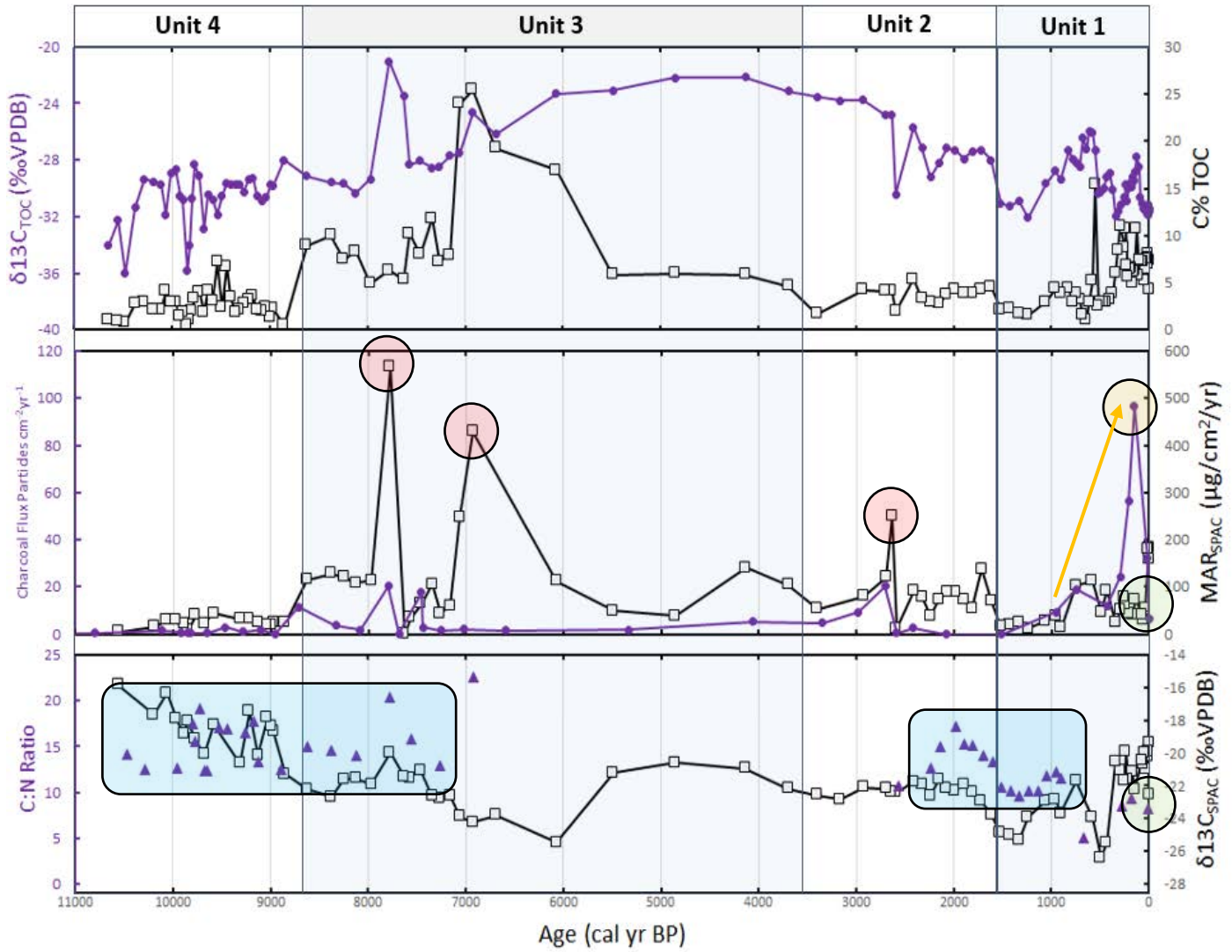

Figure 39: Mass accumulation rate of stable polycyclic carbon (MAR_{SPAC} (µg/cm²/yr)), charcoal flux particles (cm²yr¹), CN ratios and stable carbon isotopes ($\delta^{13}C_{SPAC}$) on the SPAC component of the samples through the Holocene section of the Kinrara core. Red circles = three large fire events, green circles = sharp decrease in charcoal flux and change in stable carbon isotopes in present day and the yellow circle and yellow arrow = a increase in charcoal flux. Blue squares show clumps of samples that contain measurable nitrogen.

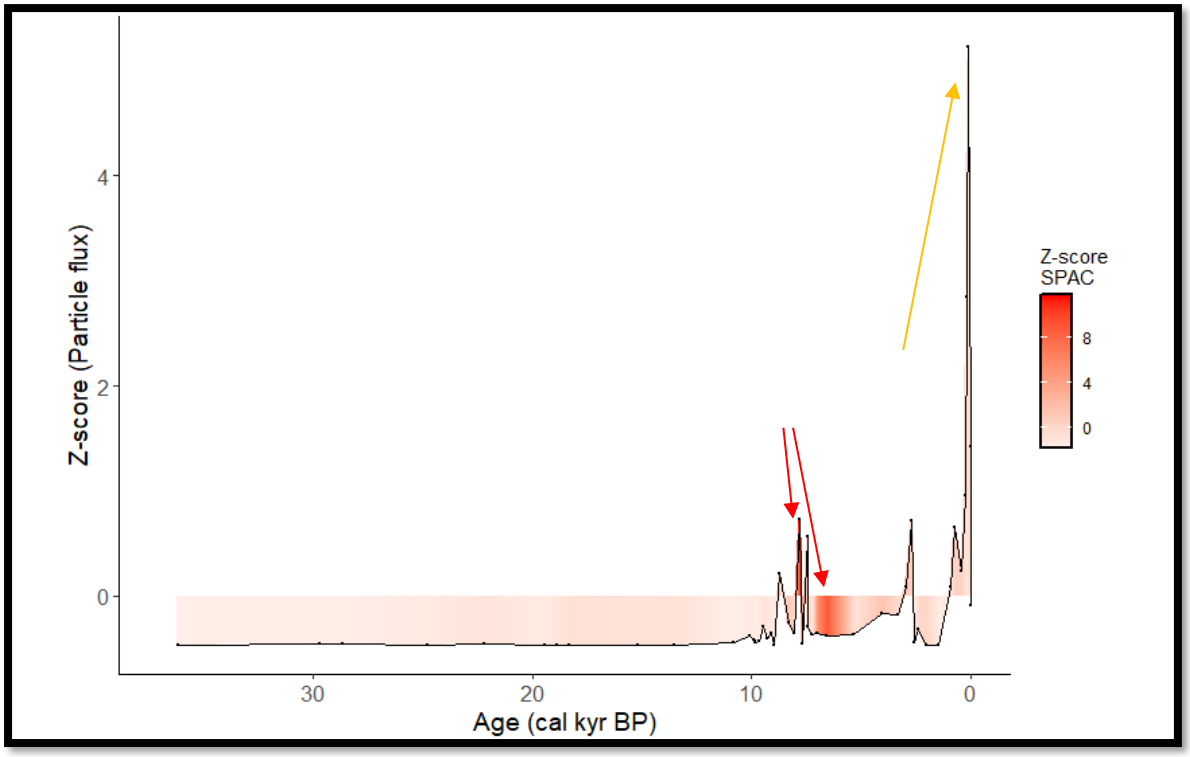

Figure 40: Z-score of charcoal particle flux and MAR_{SPAC}. Red arrows indicating inferred volcano eruptions and yellow arrow indicating point of increase in fire frequency (~500 cal yr BP).

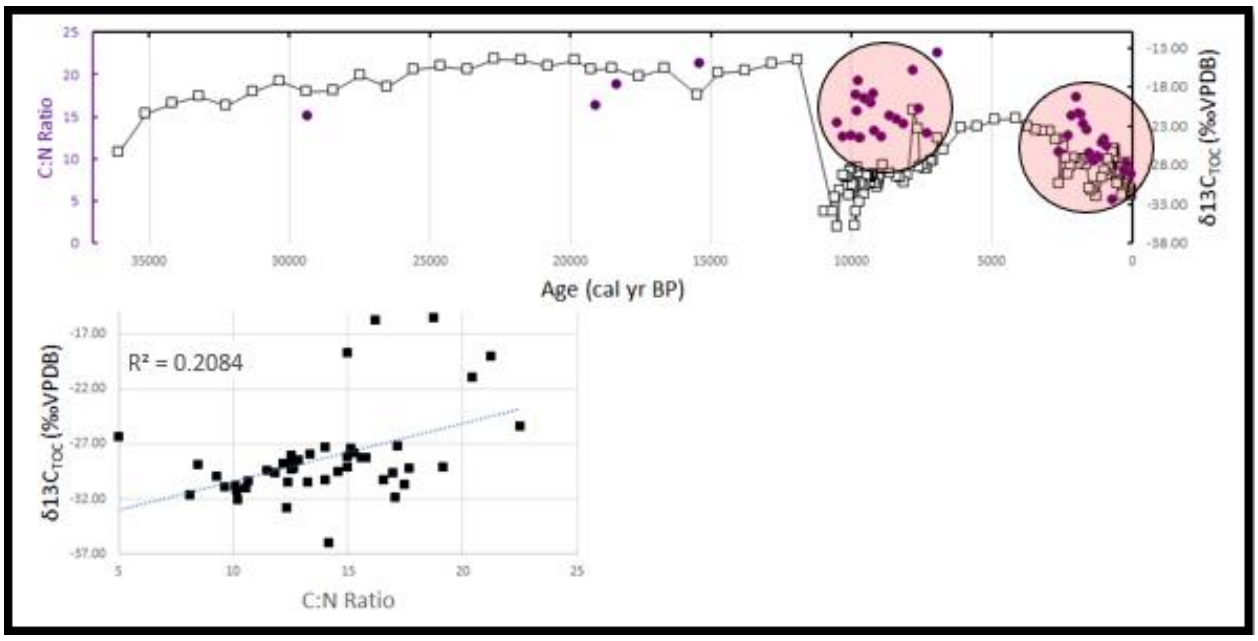

Figure 41: Stable carbon isotopes of the total organic component of the samples ($\delta^{13}C_{TOC}$), C:N Ratios on an age depth model. Relationship between $\delta^{13}C_{TOC}$ and carbon to nitrogen ratios (C:N Ratio). Red circle indicating clumping of C:N data.

7.2. Early Holocene - Rapid carbonate sedimentation: (Unit 4 – 560-380cm; 11,500 – 8750 cal yr BP):

The early Holocene interval of the core, represented by Unit 4, was deposited between 11,500 and 8750 cal yr BP, a time that incorporates the damming and initial development of the lagoon as well as rapid carbonate sedimentation, against a regional background of rising sea levels and the establishment of wetter and warmer Holocene environments following the LGM (Haberle., 2005; Luly et al., 2006; Wurster et al., 2021a; Rowe et al., 2022a; Li et al., 2023). Although the current dating of the basalts from the Kinrara volcano estimates some of the basalts flows to around 7000±2000 cal yr BP (Cohen et al., 2017), the specific basalt flow which caused the development of the lagoon by damming incoming water from the spring and overland flow along Glenlofty Creek has not yet been dated. Given that damming of the local river by basalt initiated rapid sedimentation at 11,500 cal yr BP it is reasonable to assume that the flow dates from that time. The abundant discharge of dissolved inorganic carbon with the Kinrara spring waters into the lagoon, resulting in carbonate precipitation on the waterbody floor, is also consistent with volcanic activity at this time.

Unit 4 is the section of the core that incorporates the early Holocene, which was the transition period to a much warmer and wetter period of time compared to the Last Glacial Maximum represented by Unit 5. James et al. (2024) presents a record of $\delta^{18}O$ from both authigenic carbonates and gastropods from the same core and found that Unit 4 records a progressive shift from drier to relatively wetter conditions between 11,000 and 8000 cal yr BP when compared to the Pleistocene. The inference of relatively wetter conditions is supported generally by other northern Australian tropical and/or savanna records which suggest that the early Holocene is

characterised by a transition from drier glacial conditions towards wetter conditions, yet still drier than the middle Holocene when the monsoon became fully active (Reeves et al., 2007; Reeves et al., 2013).

Overall, the available data indicates that at the start of the Holocene the Kinrara wetland underwent a rapid transition to a much larger, permanent lagoon, because of damming, and because of a regional trend to higher rainfall. The increase in lagoon size and water permanency, as well as the regional increase in precipitation, allowed for localised higher lagoon productivity, and associated changes in the vegetation around the lagoon (as discussed below). The precipitation of carbonates in Unit 4 does indicate that rainfall was insufficient to consistently overtop the dam during the wet season, thereby retaining DIC in the lagoon rather than flushing it out of the lagoon during wet season rains.

Unit 4 is dominated by carbonate; TOC is higher than in Unit 5 but as a result of the high carbonate concentrations remains relatively low at generally, <5%. TOC values show a slight trend upwards from 1% to 4%, indicating higher lagoon productivity and/or more organic transport into the lagoon from a more productive terrestrial environment compared to the late Pleistocene (Figure 39). Two broad cycles from minima of ~1% to maxima of >5% occur in the interval indicating changes in the relative balance between organic inputs and carbonate precipitation rates. Peaks in TOC of ~7% around 9500 cal yr BP – which is well above anything previously recorded – may indicate increases in organic input rather than clastic components, consistent with more water in the landscape at this time as has been inferred previously from the carbonate isotope record (James et al., 2024). This transition to a higher biomass environment is also very evident when looking at what

is being burnt ($\delta^{13}C_{SPAC}$) in the record, which shows a major transition from grasses to trees (see below).

The $\delta^{13}C_{TOC}$ values at the Unit 5/4 boundary layer dramatically drop from -14.6‰ in Unit 5 (essentially indicating only C_4 biomass) at 11,875 to -34‰ at 10,930 cal yr BP in Unit 4. Values in the unit then ranged broadly between -36‰ to -28‰ with an erratic overall upward trend for the next 2000 years to 9083 cal yr BP. The values of -30‰ to -38‰ are lower than would be anticipated from C_3 biomass in an open vegetation environment (Meyers., 1994; Meyers., 2003; Li et al., 2022). The C:N ratio of these samples, 1015, (see Figure 39 and 41) are lower than would be expected from higher plant dominated inputs (generally >20) but higher than the C/N ratios reported from algae (4-10) (Meyers., 1994; Meyers., 2003; Li et al., 2022), indicating a mix between the two. Thus, Unit 4 records significant inputs of algal-derived carbon, likely associated with carbonate precipitation during the interval. James et al (2024) report multiple scanning electron microscope instances of algal/cyanobacterial carbonate structures in this unit. This suggests some eutrophication of the water body, likely because there is no active outflow, so nutrients were retained in the lagoon.

There is a clear, but erratic decrease in $\delta^{13}C_{SPAC}$ values from -16 to -22 ‰ through Unit 4 that occurs at a steady rate (Figure 39). This indicates that during this period the surrounding environment changed from a dry grassy savanna environment to a more wooded savanna as a result of the increase in available moisture. This is consistent with other pollen records across the Atherton Tableland which document a transition to wetter conditions at the beginning of the Holocene

and the expansion of woody and/or rainforest taxa through the early Holocene (Haberle, 2005; Moss & Kershaw, 2007; Walker, 2007; Li et al., 2022).

Both MAR_{SPAC} and charcoal particle fluxes in Unit 4 are consistently relatively low through all of Unit 4 (Figure 39). This implies that fire frequency was low and the relative difference between MAR_{SPAC} and char fluxes also suggests fire intensity was low (Figure 39) through Unit 4. Fire regime appears to have been insensitive to the changing woodiness of the system as evidenced in the trend in $\delta^{13}C_{SPAC}$ values discussed above. This is counter-intuitive given the increase in total biomass available to burn that the $\delta^{13}C_{SPAC}$ values imply. It may indicate that a stable low intensity fire regime was maintained through Unit 4 by anthropogenic fire management irrespective of increasing rainfall over the interval and increasing tree cover.

Fire frequency and intensity measures are consistent and uniform across the whole unit with little fluctuation when compared to the rest of the core. This is supported by the carbonate stable isotope record, which suggests the early Holocene was a more stable but drier period when compared to the middle Holocene (James et al., 2024). One aspect of note is that Unit 4 transitioned from a grassier vegetation profile to a woodier savanna profile without the fire intensity changing. This indicates that the stable, warmer conditions of the early Holocene allowed for tree recruitment to take place and so tree cover increased in the landscape. Having an observed change in $\delta^{13}C$, but not other proxies, could also be a sign of indigenous management.

7.3. Middle Holocene – Peak monsoon : (Unit 3 – 380-208cm; 8750 – 3600 cal yr BP):

The core interval covering the middle Holocene, Unit 3, was deposited between 8750 – 3600 cal yr BP, and incorporates the period generally thought of as the warmest and wettest in the Holocene of northern Australia – the Holocene optimum (Williams et al., 2015). The boundary between Units 4 and 3 is clearly defined by a 3 cm gastropod layer (Figure 42). At the top of this boundary layer there is an abrupt decrease in carbonate content, concomitant increase in TOC% and a shift towards higher tree cover (Figure 39).

Figure 42: Close-up image of the core showing 384 to 387 cm section containing a gastropod layer (3 cm) which separates Unit 4 and Unit 3 between the years 8 825 - 8 795 cal yr BP. Scale is in centimetres.

James et al., (2024) noted a decrease of carbonate $\delta^{18}O$ values above the boundary in the small amount of carbonate that sporadically occurs in Unit 4 sediments, interpreted as a strengthening of monsoonal activity and increase in rainfall. The increase in rainfall at this time led, for the first time, to the consistent flushing of spring-derived DIC from the lagoon. Water levels in the lagoon breached

the Kinrara Basalt dam, allowing regular wet season flow into Glenlofty Creek, creating a low-DIC environment in which endogenic carbonate and gastropod growth could not occur. This shift happened rapidly, leading to the effectively instantaneous mass death of gastropods. Carbonate is absent above the first few centimetres of Unit 3, and an organic peaty sediment dominates the rest of Unit 3 indicating consistent and abundant wet season rainfall during the period of deposition of Unit 3 (James et al., 2024). This absence of endogenic carbonate and loss of molluscs suggests that an intensified monsoon dominated the region, with high precipitation throughout the middle Holocene (James et al., 2024).

As a result of the large decrease in carbonate content, and low clastic input to the site, possibly because of increased lagoon size, TOC% increases dramatically, initially to 5-15%, peaking at 25% at 7000 cal yr BP, before declining to 5% by 3000 cal yr BP. The increased C:N ratios (because of a decrease in N abundance to below measurable levels in the samples, Figure 39 and 41) indicates the source of this carbon changed from predominantly algal to dominantly higher plant-derived. The data are consistent with an increase in aquatic higher plant biomass in the lagoon, or increased input from exogenous sources. The $\delta^{13}C$ of TOC indicates this biomass is initially composed of C_3 macrophytes (~ -28 to -29 ‰). The source of this C_3 contribution is unlikely to be terrestrial C_3 trees, delivered by erosion from the catchment, as this would be accompanied by clastic input, not identified in the ITRAX data (Figure 36 in result section). A spike in $\delta^{13}C$ around 7600 cal yr BP to -21 ‰, and an overall trend to higher $\delta^{13}C$ values of around -22 ‰ toward the end of Unit 3 indicate the increased importance of a C_4 contribution. This is likely to have derived from C_4 sedge biomass in the lagoon or in its marginal seasonal damp lands.

The source of this C_4 contribution is unlikely to be terrestrial C_4 grass, because of the absence of increased terrigenous input as discussed in relation to erosion, as above.

Consistent with an inferred wetter climate, the $\delta^{13}C_{SPAC}$ values indicate an ongoing increase in the proportion of woody vegetation being incorporated into the mix of what is being burnt across the entirety of the middle Holocene, with values ranging initially from -22‰ to as low as -26‰ at 6000 cal yr BP followed by an increased to -21‰ after the major fire events in the record (discussed below) (Figure 39). This further supports the contention that the wider region was becoming more wooded and hence carried more biomass, especially between 7000 and 6000 cal yr BP where the low $\delta^{13}C_{SPAC}$ values show a dominant component of woody biomass being burnt, and/or more intense fires, that more completely consumed the fine grass C_4 -derived fuels burnt (Bird et al., 2015; Saiz et al., 2015). An alternative explanation for low $\delta^{13}C_{SPAC}$ values between -25‰ to -26‰ between 7500 to 6000 cal yr BP is that this period coincided with volcanic activity (which will be discussed below). This volcanic activity could have burned the C_3-dominated vine thicket, located on the basalt across the Kinrara region and surrounding the lagoon. This vine thicket charcoal could be providing charcoal with these low $\delta^{13}C_{SPAC}$ values carbon directly into the lagoon after burning across the basalt flows on the western margin of the lagoon. Following these eruption events between 6000 to 3600 (Unit 3) the $\delta^{13}C_{SPAC}$ remained steady and increased to around -20‰, indicating the more expected savanna tree/grass mix.

While char particle fluxes are somewhat higher and more variable in Unit 4 than earlier, MAR_{SPAC} increases dramatically from Unit 4 to 3 and exhibits two major spikes, almost an order of magnitude higher than the average for Unit 3 (see red

circles in Figure 39). These characteristics suggest two periods of intense fires occurred, the first at 7 778 cal yr BP (7.7 ka eruption event) which corresponded to a MAR_{SPAC} value of 566 µg/cm^2/yr followed by a period of limited fire across the landscape until the next large peak. This second peak occurs at 6 924 cal yr BP (6.9k eruption event) and corresponds to MAR_{SPAC} value of 428 µg/cm^2/yr. Given the high char particle fluxes associated with these events, the 7 778 and 6 924 burning events can be categorised as RIL (Rare, Intense, Large) according to the pyrome classification scheme of Archibaid et al., (2013) and applied to another Australian site – Girraween Lagoon - in Wurster et al., (2021) (Figure 40) (Archibaid et al., 2013; Wurster et al., 2021b).

These two massive fire events – notably the 7.7 ka timing - are best explained by volcanic activity that is known to have occurred locally at the same time. The volcanic flows from the Kinrara volcanic centre have a pooled $^{40}Ar/^{39}Ar$ age of 7000±2000 cal yr BP (Cohen et al., 2017). However, this pooled data is based on three samples (not including the flow that dams the lagoon, which has not been dated) of 9000±6000, 8000±4000 and 7000±2000 cal yr BP. While not conclusive, it is possible that there were multiple eruptions in this period of between ~4000 and ~1500 years in length (Cohen et al., 2017). The Kinrara record is consistent with the interpretation that there were two eruptions that resulted in significant intense fires in the Kinrara lagoon area at 7 778 and 6 924 cal yr BP. Since there is a hiatus of fire between the two peaks, it can also be inferred that these fires were initiated by two eruptions. The 7.7 ka eruption event deposited substantial amounts of charcoal into the lagoon, with a large area thereafter covered by unvegetated basalt, leading to low fire incidence. The 6.9k eruption event, burnt the partly regenerated vegetation around the lagoon, approximately a millennium later, again leading to a major influx

of char into the lagoon. As previously discussed, low $\delta^{13}C_{SPAC}$ values are also consistent with these fire events being caused by basalt lava flows initiating fires in vine thicket, or more completely burning the C_3 overstory of the savanna, as well as groundcover.

It should be noted that these large fire events are not evident in other records across tropical Australia – as reviewed in earlier chapters - and are unique to Kinrara. The Gugu Badhun, traditional owners of Kinrara region, retain an oral history of destruction explained through a witch doctor burning the land, a possible reference to this first fire peak able to completely burn the landscape (Cohen et al., 2017). The peak in MAR_{SPAC} at 7778 cal yr BP is coincident with the peak in TOC $\delta^{13}C$, suggesting the fire itself may have promoted an increase in C_4 sedge biomass in and/or around the lagoon in the immediate post-fire period. This could have occurred by increased sediment influx extending the shallower substrate which is preferred by the sedges.

The 6.9k eruption event is coincident with a sharp increase in TOC% up to 25% followed by a steady decline. This could indicate that this second fire event resulted in an influx of nutrients into the lagoon which stimulated productivity by macrophytes in the lagoon. However, a more complete interpretation of the second fire event is hampered by the relatively long (900 year) gap to the next sample after the peak. Fire is common in other savanna regions during this time. While fire incidence is variable from place to place, no other sites in the region suggest the occurrence of major short-lived peaks of the type seen within the Kinrara record, further suggesting that the peaks in the Kinrara record are likely directly due to the

Kinrara eruption(s) (Kershaw., 1971; Stevenson et al., 2001; Haberle, 2005; Walker, 2007; Burrows et al., 2014; Rehn, et al., 2021a).

The existence of these two major fire events, plausibly linked to volcanic activity, raises a conundrum as to why no fire event accompanied the eruption which resulted in the flow that dammed the waterway and spring at 11,500 cal yr BP. A plausible explanation is that, as the waterway was dammed at the end of Unit 5 – the end of the LGM – and due to the nature of the climate at this time there was only a limited amount of grassy biomass available to burn, unlike these burning events at a time where there is a greater mass of biomass due to the warmer and wetter climate of the Holocene. A second explanation could possibly be because the flow that blocked the waterway to make the lagoon occurred during the wet season (or indeed while it was raining) and hence fires were unable to carry any distance. A third alternate possibility is that the wind direction was such that fires carried to the southwest of that flow, away from the location, rather than to the south and southeast across the catchment of the newly formed lagoon.

Any role of people in managing fires during this period is difficult to assess, and indeed it is possible that the local population moved away from the area in response to the eruptions, implied by the drama of their oral histories. Fires of relatively higher intensity occur later in Unit 3 than occurred during the deposition of Unit 4. This may be suggestive of a relaxation of human fire management for some period of abandonment following the last eruptive phase of the volcano.

A similar interaction between humans and volcanic eruptions has been discussed from the wet tropics of West New Britain in PNG, inferred using phytolith

micro botanical remains, alongside archaeological evidence (Boyd et al., 2005). From this record, there is clear evidence of both human and vegetation response during four eruptions dated to 5900, 3600, 1700 and 1400 cal yr BP (Boyd et al., 2005). These PNG volcanic events resulted in massive forest decline (Boyd et al., 2005) which does suggest that a period of major disruption to vegetation would accompany a significant local volcanic event. These PNG volcanic episodes have shown that humans tended to change their surrounding landscape toward moderately uniform patterns and/ or a partitioning of the landscape was occurring after these events (Boyd et al., 2005). The paper does highlight how, in order for humans to re-occupy a landscape after a catastrophic event, the situation was not just about physical constraints but also the social processes of the occupants, and hence a understanding these social processes is critical to knowing how local communities would respond to catastrophic events (Boyd et al., 2005).

Any partitioning of the landscape within the Kinrara region after a volcanic event could be evidence of human activity. Unfortunately, though, without a significant body of archaeology evidence from the area surrounding Kinrara, all that can be inferred in relation to human response is from stories and oral histories placing the Gugu people within the region and it can be assumed that they would have moved away from the local landscape during eruptive phases. Perhaps this one story from the Gugu people suggesting a witch doctor destroyed the landscape gives slight insight into social processes and hence the passing down of this oral history is evidence in itself that the Gugu people were present during the eruptions and imply the need to be careful in approaching the area.

Apart from the short-lived major fires, there was uniformly low fire occurrence across the middle Holocene during peak monsoon conditions. Across northern Australia a general increase in fire occurred, post 4500 cal yr BP, possibly related to increasing rainfall variability and/or increased Indigenous fire management (Williams et al., 2010; Mooney et al., 2011; Williams et al., 2015). Kinrara follows this overall trend, with local exceptions evident as the two outliers in the SPAC (ug/cm^2/yr) data, fire peaks at 7 778 and 6 924 cal yr BP (MAR_{SPAC} higher than Unit 4, 115µg/cm^2/yr, and reasonably stable across all of Unit 3 (Figure 39). This general increase in later middle Holocene fire occurrence could be indicative of increasing seasonality promoting fire. That the more consistent monsoonal rains facilitated tree growth is indicated by the $\delta^{13}C_{TOC}$ values. This increased vegetative growth then cures and burns during at least episodic 'drier' dry seasons.

Overall, although the study area at this time was receiving more monsoonal rain when compared to the times equivalent to Units 4 and 5, it also experienced more intense burning toward the end of the time period represented by Unit 3. As char flux (the measure of fire frequency) shows little variation throughout Unit 3, this suggests that although fires are becoming more intense over this time, fire frequency remained similar to earlier times. This suggests the frequency of fires was similar, but when fires did occur, the fuel was woodier, resulting in larger more intense fires, replacing cool small grassier fires to some extent.

TOC values abruptly increase at the Unit 4/3 boundary layer (1% to 9% at 8 625 cal yr BP), plateau at around 10% until 7 157 cal yr BP, increase further to 24% at 7 060, and slowly decline to 6% at the Unit 3/2 boundary in the late Holocene (Figure 39). The increase in TOC% early in the middle Holocene reflects enhanced

monsoon activity and delivery of much more water into the Kinrara system. C:N data and $\delta^{13}C_{TOC}$ values of around -30‰ between 8750 to 7000 cal yr BP suggest that the lagoon still contained significant algal biomass. After 7000 cal yr BP to the Unit 3/2 boundary layers, $\delta^{13}C_{TOC}$ stabilises at around -24‰ and exhibits the same trend as the TOC. The $\delta^{13}C_{TOC}$ correlates with both volcanic events, especially the 7.7 ka eruption event. The 7.7 ka eruption sees a sharp increase in $\delta^{13}C_{TOC}$ from -29‰ to -21‰ which could be explained by a larger portion of vine thicket (C_3) being burnt near the lagoon edges on the basalt and incorporated into the relative to the low values of -30‰ derived from the algal input. After the 7.7 ka eruption event $\delta^{13}C_{TOC}$ values decrease again to -31‰, suggesting that there was a short brief period whereby the algal signal was proportionality diluted. Again, this can be explained by burning vine thicket on the basalt, this material then accumulating in the lagoon and not only incorporated into the $\delta^{13}C_{SPAC}$ but impacting $\delta^{13}C_{TOC}$.

In the middle Holocene, sites close to Kinrara on the neighbouring Atherton Tablelands, were transitioning from sclerophyll vegetation to rainforests, with the timing of maximum rainforest development estimated at 7000-6000 cal yr BP (Kershaw, 1971). Lake Euramoo for example, transitioned from eucalypt woodland into rainforest between 8600 to 5000 cal yr BP (Haberle, 2005; Li et al., 2022). Lagoon Barrine pollen records also indicate community replacement, from sclerophyll woodlands to rainforests around 7600 cal yr BP (Walker, 2007; Li et al., 2022). Rainforest also re-invaded Bromfield Swamp and Quincan Crater at around this time (Hiscock & Kershaw, 1992)

At Kinrara change over this period was from a Pleistocene open grassy landscape to middle Holocene more heavily wooded savanna, comparable with

events at Three-Quarter Mile Lake, located in central Cape York Peninsula (Luly et al., 2006). The trajectory of vegetation change is also similar to sites such as the Marura sinkhole and Girraween Lagoon, transformed from more open to more wooded savanna by the middle Holocene. Marura and Girraween are in the northeast and northwest of the Northern Territory (respectively), and demonstrate the broad geographical extent of monsoonal redevelopment in northern Australia (Wurster et al., 2021b; Rowe et al., 2022a).

Cape York Peninsula sites such as Big Willum Swamp and Sanamere Lagoon developed around 7900 cal yr BP/ 8 150 cal yr BP, due to an increase in effective monsoon precipitation (Luly et al., 2006; Moss et al., 2012; Stevenson et al., 2015a; Proske et al., 2017a; Rehn., et al., 2021b). Furthermore, Lake Barrine, 140 km north-east to Kinrara, experienced wetter, less seasonal conditions in the early Holocene and a significant increase in rainfall between 8600 to 5000 cal yr BP, which peaked around 7600 cal yr BP, with fully developed rainforest in the catchment by 7300 cal yr BP (Walker., 2007; Li et al., 2022). Additionally, many other key sites across the Tableland and Australia demonstrate the wide extent of the Holocene optimum, including Lake Euromoo which transitioned to a Mesophyll Rainforest (Haberle, 2005; Moss et al., 2012). These wetter conditions have been linked to the southward shift of the ITCZ around 8200 cal yr BP (Muller et al., 2008; James et al., 2024).

Overall, Unit 3 represents the middle Holocene section encompassing the time of peak monsoon development, leading to increased tree biomass, and overall, relatively low fire activity implying a relative decrease in rainfall seasonality. Furthermore, although, on average, fire activity was low throughout this interval – similar to other sites during the same period of time – two short-lived, large

instances of fire also occur, and these are not recorded from other sites. These two massive fire events can be explained by contemporaneous volcanic activity close to Kinrara.

7.4. Late Holocene to Modern – ENSO and Humans: (Unit 2 – 208-147cm, 3600 – 1700 cal yr BP and Unit 1 – 147-0cm, 1700 - 0 cal yr BP).

Units 2 and 1 span the late Holocene and encompass the intensification of ENSO, increased climate variability, clear indicators of Indigenous fire management and European arrival in Australia. These units have been separated based on the visual stratigraphic boundaries identified when describing the cores. Though some differences in proxies between the two units are evident, this chapter groups them to facilitate a general discussion of the late Holocene as a whole.

The Kinrara record shows carbonate being incorporated back into the sediment record at ~2800 cal yr BP. This implies increasing ENSO intensity, resulting in enhanced inter-annual variability and periodic lagoon level lowering that stopped flushing. This in turn enabled renewed episodic carbonate saturation in the lagoon, when compared to the onset of the monsoon period (Unit 3) (James et al., 2024). James et al., (2024) suggest that the record goes through a transition period at 2800 cal yr BP, into a more variable hydrologic regime with an overall trend to drier conditions towards the present. The transition period at 2800 cal yr BP equates to a peak in MAR_{SPAC} at 2700 cal yr BP with a short lag of 100 years, suggesting a possible mechanism for this fire spike might be enhanced seasonal drying (Figure 39). Further, this time accords directly with the return of sufficient N in the record to enable calculation of a C:N ratio. This second period of measurable N likely indicates an increased algal production. C:N values range between 10 to 20 and $\delta^{13}C_{TOC}$ vary between -33 to -25 (Figure 39 and 41). Thus, it is concluded that Units 2 and 1 record a significant increase in algal-derived carbon, associated with at least occasionally decreased lagoon flushing in the wet season and attendant nutrient increases (compared to Unit 3) from 2500 cal yr BP to the present day.

TOC remains consistent throughout Unit 2 and maintains similar $\delta^{13}C_{TOC}$ values to Unit 3 (of around 4%, slightly lower than the present day) potentially suggesting less organic transport into the lagoon from a less productive terrestrial environment when compared to the present (Figure 39). $\delta^{13}C_{TOC}$ values trend down from -24‰ to -28‰, then rises sharply. to -31‰ into Unit 1. It should be noted that at 2700 cal yr BP there is a sharp decline from -24‰ to -31‰ which corresponds to an increase in fire intensity and frequency over the same period (discussed above). In summary then, the record is consistent with increased ENSO variability after 2700 cal yr BP compared to the middle Holocene.

TOC values in Unit 1 increase from 4% to around 10% toward the present (Figure 39), indicating increased productivity in the lagoon or decreased clastic transport to the lagoon, or a combination of both. Notably, at 522 cal yr BP, a spike in TOC occurred (15%, only to shortly thereafter fall back to 3%), again suggesting variability that may relate to human fire management being undertaken on the broader landscape after 500 cal yr BP (see below). TOC fluctuates (ranging between 5 and 10%) from 370 cal yr BP, implying increased ENSO variability. $\delta^{13}C_{TOC}$ values in Unit 1 are similar to Unit 2. Through to the modern end of the record, values span between -26‰ to -31 ‰, with the lower values indicating periods of lower lagoon level (enhanced El Niño) resulting decreased wet season lagoon flushing with higher nutrient concentrations supporting in-lagoon productivity.

A peak in charcoal flux and MAR_{SPAC} occurs at 2700 cal yr BP, a time that James et al., (2024) equates with the intensification of ENSO after the middle Holocene. The timing of this peak closely correlates with other regional records

suggesting an increase in fire incidence at Lake Euramoo and Lizard Island (Haberle, 2005; Moss et al., 2012; Lambrides et al., 2020). MAR_{SPAC} and charcoal flux both demonstrate enhanced variability after 2700 cal yr BP, a pattern maintained for the remainder of the core. Sea level started to decline around 4000 to 3700 cal yr BP from a middle Holocene highstand on the adjacent coast, which also correlates with the Kinrara Unit 3 and 2 boundaries (Rowe et al., 2022a) and reached modern levels 1900 – 1700 cal yr BP the time of the Unit 2/1 boundary (Rowe et al., 2022a). Changes in oceanic-atmospheric interactions associated with both sea level decline events have been linked to weakening of the monsoon, intensification of ENSO and increased seasonality in rainfall (Haberle, 2005; Rowe et al., 2022a).

As a general trend across the broader region from the middle Holocene into the late Holocene, more variability is evident in multiple proxies (Haberle, 2005; Williams et al., 2010; Moss et al., 2012). This increased variability has been linked to ENSO intensification, resulting in greater inter-annual variability in rainfall. It is also considered that humans may have played an increasing role in modulating fire regimes and hence vegetation in the region during this time (Haberle, 2005; Williams et al., 2010; Moss et al., 2012; Rowe et al., 2022a). Before the period of inferred ENSO intensification, human occupation was sparse between 4000 – 3000 cal yr BP across the Atherton Tablelands, with an increase after 2500 cal yr BP, and a peak in occupation around 1500 cal yr BP (Haberle, 2005; Moss et al., 2012; Rowe et al., 2022a). Trends in the regional presence of people are not based on direct archaeological artifacts, but based on rainforest toxic nut cultivation (Haberle, 2005; Williams et al., 2010; Moss et al., 2012). Such evidence is here extrapolated to include the Kinrara area, with late Holocene increased and/ or permanent occupation local to the lagoon site.

Further away, a record from Girraween Lagoon (north Northern Territory) has indicated how ENSO intensification from approximately 3000 cal yr BP correlated to the beginning of increased influence of Indigenous fire management (Wurster et al., 2021a). Generally, across northern and central Australia, a rise in archaeological evidence of occupation over the past 2,000 years also has been suggested to correlate with increased climate variability (Williams et al., 2010; Williams et al., 2015).

In general, a broad body of evidence suggests the late Holocene was a period of relatively higher climatic variability, linked to ENSO intensification compared to the mid-Holocene (Haberle, 2005; Moss et al., 2012; Walker, 2007; Wurster et al., 2021a Li et al., 2023; Rowe et al., 2022a). Multiple sites appear to experience some form of landscape change, with various lags occurring at specific sites. Big Willium (western Cape York Peninsula) for example became a stable wetland around 2200 cal yr BP, burning increased across Lizard Island (Proske and Haberle, 2012) and Lake Euramoo experienced increased charcoal deposition from 2700 cal yr BP, alongside a transition from higher to lower mesophyll rainforest up to 70 cal yr BP (Haberle, 2005). These Lizard Island and Lake Euramoo increases in charcoal correlate closely with the fire peak occurring at Kinrara at 2700 cal yr BP (Figure 39). The Torres Straits islands similarly experienced decreased forest cover and increased charcoal flux beginning 3500 – 3000 cal yr BP, similar trends at sites in North East PNG date to between 4500 – 2000 cal yr BP, and in New Caledonia from 3200 cal yr BP (Haberle & Ledru, 2001; Stevenson et al., 2001; Stevenson, 2004; Jago & Boyd, 2005). Climate variability across the Gulf of Carpentaria is described as “more extreme” after 3000 cal yr BP, and Quincan Crater and Bromfield Swamp

catchments shift back into sclerophyll forest as a result of fluctuating wet-dry cycles (Stevenson et al., 2001; Stevenson, 2004; Haberle, 2005; Rowe, 2007; Stevenson et al., 2015a; Proske et al., 2017b; Rehn et al., 2021a; Rowe et al., 2022a).

Although there is no direct archaeological evidence from the Kinrara site, with other sites across Australia experiencing an increase in human populations due to multiple reasons – especially the Atherton Tablelands - Kinrara is likely to have been an attractive area to utilize. The Kinrara area was no longer subject to active volcanism and the year-round availability of spring-fed fresh water during a time of periodic ENSO related drought, and access to both savanna and vine forest resources, may have made it an attractive location for occupation. However, the information on fire incidence from this study does not suggest a substantial increase in human activity until around 500 cal yr BP, at which time it becomes clear that humans were activity managing the region through cool burning practices (discussed below). Moss et al., (2012) also suggest similar for Witherspoon Swamp, a site located ~5 – 10 km from any Atherton Tablelands rainforests, at the sclerophyll boundary zone. Moss et al. (2012) suggest Witherspoon Swamp was a 'good camping area', owing to the source of permanent water and extensive food resources, but that 'no archaeological data/ surveys conducted' (Moss et al., 2012). The authors agree on the breadth of discussion around Aboriginal communities within the nearby rainforest but a lack of artifacts directly indicating occupation. Witherspoon Swamp, and now Kinrara Lagoon, highlight the critical need for archaeological surveys to be conducted in proximity to wetlands to help determine the nature/ human-environment interactions in these savanna regions.

The MAR_{SPAC} record following ENSO intensification at 2800 cal yr BP, includes a spike at 2700 cal yr BP, with relatively lower values recorded between 2600 cal yr BP and 1700 cal yr BP (Figure 39). MAR_{SPAC} then declines to effectively zero between 1700 cal yr BP and 900 cal yr BP, indicating little fire was occurring in the landscape and/or fire were very low in intensity. This period, between 1700 to 900 cal yr BP, correlates with increases in zonal sea surface temperature in marine sediment cores (West Papua and south-east Australia, MD-98-2176 and MD03-2611, Lüning et al., 2020) recorded between 1500 to 1000 cal yr BP. These have been linked to decreased frequency and strength of the ENSO system, and ultimately leading to wetter conditions in eastern Australia (Lüning et al., 2020). A wetter climate may provide an explanation for a lack of fire in this period (Williams et al., 2010).

At Kinrara, it has also been suggested (based on the lowest carbonate $\delta^{18}O$ values) that between 1800 – 1500 cal yr BP a period of intensified precipitation occurred across the area, associated with a brief strengthening of monsoonal conditions (James et al., 2024). This in turn suggests the possibility that seasonality in rainfall was decreased, with decreased opportunity for the curing of fuel to support fire. The decrease in fire incidence to close to zero occurred at the boundary between Unit 2 and 1 and is the defining characteristic separating the upper two sedimentary units. This shift corresponds with a change in nature of the biomass burnt, noting that the very low SPAC abundance in the sediments means it is possible that the isotope results could be less reliable. It is possible, for example, that a small amount of relatively robust tree-derived charcoal from earlier burning became incorporated in the sediments. An alternative explanation for the low $\delta^{13}C_{SPAC}$ values is the source of dominantly C_3 vine thicket vegetation on the basalt that formed the southern and

western shore of the lagoon. This plant community may have burnt to some degree (as it burns now) or provided a proximal source of C3 charcoal from a past fire, mobilized into the lagoon.

From ~ 900 cal yr BP to 60 cal yr BP increased MAR_{SPAC} values of up to 100 µg/cm$^{2/}$yr suggest fire once again became a relatively common feature of the Kinrara environment, returning in a similar intensity to the 2600 – 1700 cal yr BP period. Indigenous fire management is evident in the limited change in fire intensity, the shift to more grasses being burnt, and an increase in fire frequency indicated by the increased char flux after 500 cal yr BP. This provides a strong indication that humans were actively managing the Kinrara region from at least that time. The large increase in $\delta^{13}C_{SPAC}$ from c.-26 to -19‰, reflective of increased grass burning, continued until ~60-70 cal yr BP. Char flux increased by an order of magnitude, which strongly suggests frequent fires corresponding to the active imposition of Indigenous fire management techniques.

At ~70-60 cal yr BP (equivalent to the late-1800s) MAR_{SPAC} rose rapidly to very high values of 190 µg/cm$^{2/}$yr , coincident with the timing of removal of Aboriginal peoples off country, and thus the removal of Indigenous fire management regime that had been in place from ~500 cal yr BP to ~70-60 cal yr BP.

This decoupling of fire frequency and fire intensity beginning 500 cal yr BP, with relatively moderate SPAC levels and an order of magnitude increase in fire frequency indicated by char flux, is similar to that discussed in the Girraween Lagoon record after ENSO initiation around 3000 cal yr BP (Wurster et al., 2021a, and as mentioned above). This was interpreted to be Indigenous management practices

intensifying across the landscape, potentially in response to ENSO, with reduced climatic predictability and incorporating drought during El Nino Phases. An increase in Indigenous populations may have also been a factor during this period (Wurster et al., 2021a). Given this char flux pattern and MAR_{SPAC} data in the Kinrara record, between 500 cal yr BP until the late 19th Century, can be characterized as part of a frequent cool small pyrome (FCS) (Figure 40) consistent with Indigenous cool burning practices (Archibaid et al., 2013; Wurster et al., 2021a).

Within the upper last few centimetres, encompassing the period of European management, a clear spike in MAR_{SPAC} to 200 µg/cm^2/yr – high SPAC levels - is recorded while char flux strongly decreases by an order of magnitude from ~ 100 to 10 particles/cm^2/yr. The increase in fire intensity in the past ~70-60 years since European arrival can be tied to the grass understory no longer being regularly burnt under Indigenous fire management techniques, leading to large fuel loads generating fewer but more intense and impactful dry season fires, ultimately burning more of the C3 biomass. This interpretation is supported by the most recent $\delta^{13}C_{SPAC}$ values being -22‰ when compared to values of -19‰ just ~140 years ago. A build-up in grassy fuel loads may have been somewhat offset followed by the establishment of cattle grazing on Kinrara Station over the last century.

European influence is also suggested in the charcoal flux and pollen record of Lake Euramoo from around 70 cal yr BP to the present, contemporaneous with exotic pollen species and a dramatic rise in charcoal associated with the timber industry during the early 19th century. At locations such as Lake Euramoo, the rainforest vegetation became dryer and more degraded, with increased invasive plant species assisting in hot fires (Haberle., 2005). Given the similarity to what was

occurring at Kinrara, this could suggest that the entire Tablelands extending into neighbouring regions experienced similar effects from European colonisation and loss of Aboriginal management practices across the landscape (Haberle, 2005; Mooney et al., 2011; Moss et al., 2012; Rowe et al., 2022a).

Chapter 8. Conclusions and Future Work

Fire is an integral component of tropical savannas ecosystems and the reconstruction of the past fire regimes of the Kinrara region from this study helps to better understand the links between fire, vegetation, climate and humans in the region over the last ~37,000 years. The late Pleistocene section of Unit 5 (from time 37,227 to 11,500 cal yr BP) is dominated throughout by lithogenic elements, including basaltic fragments, indicating that the unit was not deposited in a lagoon environment but at a time of local volcanic activity that predates known, dated volcanism associated with the Kinrara volcanic Centre (Cohen et al., 2017). This period encompasses a slow transition from a more wooded savanna to a grassland implying a period of significantly lower rainfall, likely during the last Glacial Maximum (though poorly constrained in age results). This relative aridity and maximum cooling associated with the LGM has been shown in other records and is present in the Kinrara record (Reeves et al., 2013; Li et al., 2023). This period had consistent relatively low levels of fire throughout. Starting at 37,000 cal yr BP more C_3 vegetation was being burnt which progressed to being C_4 dominated during what is likely to be the LGM.

The early Holocene from 11,500 to 8750 cal yr BP incorporated the damming, initial development of the lagoon by a basalt flow and rapid carbonate sedimentation likely emanating from the Kinrara spring, this occurred against a regional background of rising sea levels and the establishment of wetter and warmer Holocene environments following the LGM. The Kinrara perennial lagoon underwent a rapid transition to a much larger lake water body, partly because of the damming, but also because of a regional trend to higher rainfall. Fire intensity and frequency

remained relatively low during this period when compared to the entirety of the record. The $\delta^{13}C_{SPAC}$ values indicate a change from a dry grassy savanna to a more wooded savanna over this period. This transition from a dry grassy savanna to a wooded savanna is consistent with other regional records which document a transition to wetter conditions and an expansion of woody and/or rainforest during the early Holocene (Haberle, 2005; Moss & Kershaw, 2007; Walker, 2007; Li et al., 2022).

The middle Holocene 8750 – 3600 cal yr BP, was the warmest and wettest period in the record and equates broadly to the Holocene optimum. The monsoon was reliable and strong, leading to a regular seasonal flushing of the lagoon and therefore to an absence of carbonate precipitation. During this phase, two short periods of intense fire occurred, the first at 7778 cal yr BP and the second at 6924 cal yr BP. These two major peaks relate to local volcanism at the time and are not evident in other records across tropical Australia. When ignoring the two major peaks, the middle Holocene was uniformly medium and stable in terms of fire intensity and frequency (higher than Unit 4).

Units 2 and 1 span the late Holocene and encompass a period subject to the regional intensification of ENSO, increased environmental variability, and Indigenous fire management, until European arrival into north Queensland in the mid-19th Century. A peak in charcoal flux and MAR_{SPAC} occurs at 2700 cal yr BP which correlates with other regional records (Haberle & Ledru, 2001; Stevenson et al., 2001; Stevenson, 2004; Jago & Boyd, 2005; Haberle, 2005; Moss et al., 2012;

Lambrides et al., 2020). Evidence of Indigenous fire management is clear from 500 cal yr BP, until cessation of following European colonisation. The period associated with European arrival and settlement saw a switch back into less frequent, more intense fires.

Based on the results presented in this thesis, the study has contributed to our knowledge of savanna regions 0f how tropical savannas in northern Australia have reacted to past environmental change, including the response of fire regime, which provides a base for interpreting and implementing fire management practices into the future. Looking forward, an increase in resolution within the first metre of sediment - the past 900 years – would aid with the interpretation of what exactly is occurring within this period. Furthermore, La Niña and Na Niña cycles may become more apparent with an increase in resolution across the entirety of the late Holocene. Lastly, other proxies being measured on the site beyond the scope of this study and the scope of James et al., (2024) would aid in gaining a better overall picture. Proxies such as pollen would provide more insight into the vegetation across the landscape which would greatly aid in the fire interpretation.

Archaeological work within the Kinrara region / the wider surrounding region would really help tease out the signal of human impact on the region and aid with the interpretation of the MAR_{SPAC}, char flux and stable carbon isotope data. With the exception of the 500 year point of interest whereby the fire frequency increases dramatically, alongside clear indication from the MAR_{SPAC} data strongly suggesting cool burning fire practices are occurring and massive amount of grasses being burnt,

this seems very likely to a signal indigenous fire management making its mark on the landscape. Besides this very clear point from the data in this thesis, more archaeological evidence is needed to differentiate the impact of climatic variables (such as monsoon / ENSO), environmental aspects (volcanoes) and humans on the environment surrounding the lagoon. Archaeological work would aid in determining the degree of human involvement in the shifting landscape and the fire regimes. It also should be noted that there is clear evidence from this study, that active volcanism preceded known (dated) volcanism from the Kinrara volcanic centre, and this could be followed up by more dating, not least, of the flow that dammed the Lagoon.

Appendix

Appendix 1: Age cal yr BP, depth, dry bulk den and mass accumulation rate for the 5 units, swap between grey and white indicate unit swaps.

Age cal yr BP	Corrected Sediment Depth (cm)	Dry bulk den (g/cm3)	MAR = Sed Rate x Dry Bulk Den (mg/cm2/y)		Age cal yr BP	Corrected Sediment Depth (cm)	Dry bulk den (g/cm3)	MAR = Sed Rate x Dry Bulk Den (mg/cm2/y)
2.00	3.45	0.14	164.69		7778.00	310.00	0.67	35.76
3.00	5.75	0.06	132.59		7967.00	320.00	0.44	23.49
8.85	12.64	0.11	130.28		8121.00	330.00	0.39	25.36
35.40	17.24	0.18	31.48		8247.00	340.00	0.39	30.82
48.15	19.54	0.15	26.29		8374.00	350.00	0.32	25.28
62.11	21.84	0.10	16.26		8625.00	370.00	0.27	21.55
74.85	24.14	0.13	22.62		8854.00	390.00	0.54	47.09
143.90	35.63	0.13	21.87		8966.00	402.00	0.41	44.20
170.38	40.23	0.13	22.37		8992.00	405.00	0.41	47.35
211.76	47.13	0.17	28.78		9038.00	410.00	0.41	44.17
238.60	51.72	0.19	33.00		9129.00	420.00	0.37	40.51
252.11	54.02	0.19	31.54		9219.00	430.00	0.33	36.68
291.33	58.62	0.18	20.92		9309.00	440.00	0.40	43.92
344.75	63.22	0.21	17.94		9400.00	450.00	0.34	37.14
433.44	70.11	0.39	30.69		9489.00	460.00	0.54	60.85
492.19	74.71	0.29	22.53		9581.00	470.00	0.35	37.73
582.95	81.61	0.39	29.71		9677.00	480.00	0.34	35.19
746.74	93.10	0.52	36.81		9771.00	490.00	0.38	40.67
902.54	102.08	0.11	6.33		9819.00	495.00	0.53	54.80
958.89	105.21	0.23	12.96		9847.00	498.00	0.66	71.06
1057.58	110.42	0.28	14.65		9886.57	502.06	0.39	40.08
1240.08	120.83	0.31	17.71		9965.05	510.31	0.37	39.21
1332.75	126.04	0.18	9.99		10063.21	520.62	0.31	32.72
1425.40	131.25	0.28	15.68		10195.75	530.93	0.35	27.30
1520.38	136.46	0.22	12.27		10556.25	551.55	0.54	31.05

1616.66	141.67	0.25	13.73		13736.78	572.16	0.61	3.94
1715.53	146.88	0.48	25.04		17590.64	592.78	0.74	3.99
1810.42	152.08	0.22	11.86		18508.22	597.94	1.03	5.78
1896.57	157.29	0.30	18.06		19242.29	602.08	0.52	2.95
1985.00	162.50	0.33	19.60		20710.42	610.42	0.67	3.80
2071.28	167.71	0.24	14.70		24564.27	631.25	0.71	3.86
2152.68	172.92	0.36	22.88		28418.12	652.08	0.68	3.68
2238.13	178.13	0.32	19.60		34107.14	683.33	0.81	4.45
2324.28	183.33	0.40	24.05		36125.83	693.75	0.66	3.42
2412.19	188.54	0.28	16.36					
2589.18	198.96	0.29	17.00					
2634.84	202.33	0.43	31.93					
2693.53	205.81	0.26	15.32					
2925.56	211.63	0.30	7.48					
3161.11	217.44	0.78	19.28					
3398.83	223.26	0.42	10.28					
3694.54	229.07	0.39	7.67					
4132.62	234.88	0.59	7.88					
4852.90	240.70	0.31	2.46					
5487.45	246.51	0.39	3.54					
6071.00	252.33	0.30	2.97					
6686.00	258.14	0.25	2.40					
6924.00	263.95	0.33	8.05					
7060.00	269.77	0.25	10.69					
7157.00	275.58	0.19	11.10					
7265.00	281.40	0.14	7.68					
7342.00	287.21	0.24	18.21					
7460.00	293.02	0.24	11.73					
7571.02	298.84	0.14	7.47					

Appendix 2: Bark found at the bottom of the core between 680 – 699 cm. The only piece of datable material found within the lowest unit after sieving multiple 20 cm sections between 560 – 700cm.

Reference List

Andersen, A. N., Cook, G. D., & Williams, R. J. (2003). *Fire in tropical savannas: the Kapalga experiment*. Springer.

Andersen, A. N., Woinarski, J. C. Z., & Parr, C. L. (2012). Savanna burning for biodiversity: Fire management for faunal conservation in Australian tropical savannas. *Austral Ecology*, *37*(6), 658-667. https://doi.org/10.1111/j.1442-9993.2011.02334.x

Archibaid, S., Lehmann, C. E. R., Gomez-Dans, J. L., & Bradstock, R. A. (2013). Defining pyromes and global syndromes of fire regimes. *Proceedings of the National Academy of Sciences - PNAS*, *110*(16), 6442-6447. https://doi.org/10.1073/pnas.1211466110

Archibald, Sally & Beckett, Heath & Bond, William & Coetsee, Corli & Druce, Dave & Staver, A.. (2017). *Interactions between Fire and Ecosystem Processes*. 10.1017/9781139382793.015.

Atlas of Living Australia (2018). *forest of Astralia 2018b layer in the atlas of living australia*. Atlas of Living Australia. Retrieved from: https://auth.ala.org.au/cas

Australian Government. (2021). *Conservation Management Zones of Australia: North Australian Tropical Savanna*. Australian Government Department of Climate Change, Energy, the Environment and Water. Retrieved from: https://www.dcceew.gov.au/environment/biodiversity/publications/cmz-north-australian-tropical-savanna

Australian government. (2010). *Australian Climate Influences*. Retrieved from: http://www.bom.gov.au/watl/about-weather-and-climate/australian-climate-influences.shtml

Australian Government. (2024). *Digital Earth Australia*. Retrieved from: https://maps.dea.ga.gov.au/#share=s-mYmYKh57NcZV7nUN8vaV52ZNO5S

Barr, C. (2012). An island of opportunity: A concentration of late Quaternary sediment sites on North Stradbroke Island, Australia. *Quaternary International*, *279-280*, 40-40. https://doi.org/10.1016/j.quaint.2012.07.172

Barr, C., Tibby, J., Leng, M. J., Tyler, J. J., Henderson, A. C. G., Overpeck, J. T., Simpson, G. L., Cole, J. E., Phipps, S. J., Marshall, J. C., McGregor, G. B., Hua, Q., & McRobie, F. H. (2019). Holocene El Niño-Southern Oscillation variability reflected in subtropical Australian precipitation. *Scientific reports U6*

Bayliss, A., Blackwell, P. G., Boswijk, G., Bronk Ramsey, C., Heaton, T. J., Hogg, A. G., Hua, Q., Palmer, J. G., Pearson, C., Petchey, F., Reimer, P., Reimer, R., Southon, J., Turney, C. S. M., & Wacker, L. (2020). SHCal20 Southern Hemisphere Calibration, 0–55,000 Years cal BP. *Radiocarbon*, *62*(4), 759-778. https://doi.org/10.1017/RDC.2020.59

Beringer, J., Hutley, L. B., Abramson, D., Arndt, S. K., Briggs, P., Bristow, M., Canadell, J. G., Cernusak, L. A., Eamus, D., Edwards, A. C., Evans, B. J., Fest, B., Goergen, K., Grover, S. P., Hacker, J., Haverd, V., Kanniah, K., Livesley, S. J., Lynch, A., . . . Uotila, P. (2015). Fire in Australian savannas: from leaf to landscape. *Global Change Biology*, *21*(1), 62-81. https://doi.org/10.1111/gcb.12686

Berry, G. J., & Reeder, M. J. (2016). The Dynamics of Australian Monsoon Bursts. *Journal of the Atmospheric Sciences*, *73*(1), 55-69. https://doi.org/10.1175/JAS-D-15-0071.1

Bird, M. I., & Ascough, P. L. (2012). Isotopes in pyrogenic carbon: A review. *Organic Geochemistry*, *42*(12), 1529-1539. https://doi.org/https://doi.org/10.1016/j.orggeochem.2010.09.005

Bird, M. I., Haig, J., Hadeen, X., Rivera-Araya, M., Wurster, C. M., & Zwart, C. (2020). Stable isotope proxy records in tropical terrestrial environments. *Palaeogeography,*

Palaeoclimatology, Palaeoecology, 538, 109445-. https://doi.org/10.1016/j.palaeo.2019.109445

Bird, M. I., Moyo, C., Veenendaal, E. M., Lloyd, J., & Frost, P. (1999). Stability of elemental carbon in a savanna soil. *Global Biogeochemical Cycles*, *13*(4), 923-932. https://doi.org/10.1029/1999GB900067

Bird, M. I., Wynn, J. G., Saiz, G., Wurster, C. M., & McBeath, A. (2015). The Pyrogenic Carbon Cycle. *Annual Review of Earth and Planetary Sciences*, *43*(1), 273-298. https://doi.org/10.1146/annurev-earth-060614-105038

Birks, H. J. B., Lotter, A. F., Juggins, S., & Smol, J. P. (2012). *Tracking Environmental Change Using Lake Sediments: Vol. 5: Data Handling and Numerical Techniques* (Vol. 5). Springer.

Birks, H. J. B., Smol, J. P., & Last, W. M. (2001). *Tracking environmental change using lake sediments*. Kluwer Academic Publishers.

Blaauw, M., & Christen, J. A. (2011). Flexible paleoclimate age-depth models using an autoregressive gamma process. *Bayesian Analysis*, *6*(3), 457-474, 418. https://doi.org/10.1214/11-BA618

Black, M. P., Mooney, S. D., & Martin, H. A. (2006). A >43,000-year vegetation and fire history from Lake Baraba, New South Wales, Australia. *Quaternary Science Reviews*, *25*(21), 3003-3016. https://doi.org/10.1016/j.quascirev.2006.04.006

Boës, X., Rydberg, J., Martinez-Cortizas, A., Bindler, R., & Renberg, I. (2011). Evaluation of conservative lithogenic elements (Ti, Zr, Al, and Rb) to study anthropogenic element enrichments in lake sediments. *Journal of Paleolimnology*, *46*(1), 75-87. https://doi.org/10.1007/s10933-011-9515-z

Bond, W. J., Midgley, G. F., & Woodward, F. I. (2003). The importance of low atmospheric CO2 and fire in promoting the spread of grasslands and savannas. *Global Change Biology*, *9*(7), 973-982. https://doi.org/10.1046/j.1365-2486.2003.00577.x

Bowman, D. M. J. S., & Prior, L. D. (2004). Impact of Aboriginal Landscape Burning on Woody Vegetation in Eucalyptus tetrodonta Savanna in Arnhem Land, Northern Australia. *Journal of Biogeography*, *31*(5), 807-817. https://doi.org/10.1111/j.1365-2699.2004.01077.x

Boyd, W. E., Lentfer, C. J., & Parr, J. (2005). Interactions between human activity, volcanic eruptions and vegetation during the Holocene at Garua and Numundo, West New Britain, PNG. *Quaternary Research*, *64*(3), 384-398. https://doi.org/https://doi.org/10.1016/j.yqres.2005.08.017

Bureau of Meterology. (2001). *Map of Climate Zones of Australia*. Retrieved from: http://www.bom.gov.au/climate/how/newproducts/images/zones.shtml

Bureau of Meterology. (2016). *Climate classification maps*. Retrieved from: http://www.bom.gov.au/jsp/ncc/climate_averages/climate-classifications/index.jsp?maptype=tmp_zones#maps

Bureau of Meterology. (2019a). Annual rainfall Craigs Pocket Station. Retrieved from:http://www.bom.gov.au/jsp/ncc/cdio/weatherData/av?p_display_type=dataGraph&p_stn_num=032082&p_nccObsCode=139&p_month=13

Bureau of Meterology. (2019b). *Maps of recent, past and average conditions*. Retrieved from: http://www.bom.gov.au/climate/maps/

Bureau of Meterology. (2019c). *Monthly mean maximum temperature Mount Surprise Township*. Retrieved from: http://www.bom.gov.au/jsp/ncc/cdio/weatherData/av?p_nccObsCode=36&p_display_type=dataFile&p_startYear=&p_c=&p_stn_num=030036

Burrows, M. A., Fenner, J., & Haberle, S. G. (2014). Humification in northeast Australia: Dating millennial and centennial scale climate variability in the late Holocene. *The Holocene*, *24*(12), 1707-1718. https://doi.org/10.1177/0959683614551216

Butler, D. W., Fensham, R. J., Murphy, B. P., Haberle, S. G., Bury, S. J., Bowman, D. M. J. S., & Silman, M. (2014). Aborigine-managed forest, savanna and grassland: biome switching in montane eastern Australia. *Journal of Biogeography*, *41*(8), 1492-1505. https://doi.org/10.1111/jbi.12306

Cadd, H., Petherick, L., Tyler, J., Herbert, A. V., Cohen, T. J., Sniderman, K., Barrows, T. T., Fulop, R. H., Knight, J., Kershaw, A. P., Colhoun, E. A., & Harris, M. R. P. (2021). A continental perspective on the timing of environmental change during the last glacial stage in Australia. Quaternary Research, 102, 5–23. https://doi.org/10.1017/qua.2021.16

Calvo, E., Marshall, J. F., Pelejero, C., McCulloch, M. T., Gagan, M. K., & Lough, J. M. (2007). Interdecadal climate variability in the Coral Sea since 1708 A.D. *Palaeogeography, Palaeoclimatology, Palaeoecology*, *248*(1), 190-201. https://doi.org/10.1016/j.palaeo.2006.12.003

Carcaillet, C., Almquist, H., Asnong, H., Bradshaw, R. H. W., Carrión, J. S., Gaillard, M. J., Gajewski, K., Haas, J. N., Haberle, S. G., Hadorn, P., Müller, S. D., Richard, P. J. H., Richoz, I., Rösch, M., Sánchez Goñi, M. F., von Stedingk, H., Stevenson, A. C., Talon, B., Tardy, C., . . . Willis, K. J. (2002). Holocene biomass burning and global dynamics of the carbon cycle. *Chemosphere*, *49*(8), 845-863. https://doi.org/10.1016/S0045-6535(02)00385-5

Catullo, R. A., & Scott Keogh, J. (2014). Aridification drove repeated episodes of diversification between Australian biomes: Evidence from a multi-locus phylogeny of Australian toadlets (Uperoleia: Myobatrachidae). *Molecular Phylogenetics and Evolution*, *79*, 106-117. https://doi.org/10.1016/j.ympev.2014.06.012

Charles-Dominique, T., Staver, A. C., Midgley, G. F., & Bond, W. J. (2015). Functional differentiation of biomes in an African savanna/forest mosaic. *South African journal of botany*, *101*, 82-90. https://doi.org/10.1016/j.sajb.2015.05.005

Cohen, B. E., Mark, D. F., Fallon, S. J., & Stephenson, P. J. (2017). Holocene-Neogene volcanism in northeastern Australia: Chronology and eruption history. *Quaternary Geochronology*, *39*, 79-91. https://doi.org/10.1016/j.quageo.2017.01.003

Coulter, S. E., Turney, C. S. M., Kershaw, P., & Rule, S. (2009). The characterization and significance of a MIS 5a distal tephra on mainland Australia. *Quaternary Science Reviews*, *28*(19), 1825-1830. https://doi.org/10.1016/j.quascirev.2009.04.018

Crutzen, P. J., & Goldammer, J. G. (1993). *Fire in the environment: the ecological, atmospheric, and climatic importance of vegetation fires* (Vol. ES 13). Wiley.

David, B., McNiven, I., Mitchell, R., Orr, M., Haberle, S., Brady, L., & Crouch, J. (2004). Badu 15 and the Papuan-Austronesian Settlement of Torres Strait. *Archaeology in Oceania*, *39*(2), 65-78. https://doi.org/10.1002/j.1834-4453.2004.tb00564.x

Davies, S. J., Lamb, H. F., & Roberts, S. J. (2015). Micro-XRF Core Scanning in Palaeolimnology: Recent Developments. In I. W. Croudace & R. G. Rothwell (Eds.), *Micro-XRF Studies of Sediment Cores: Applications of a non-destructive tool for the environmental sciences* (pp. 189-226). Springer Netherlands. https://doi.org/10.1007/978-94-017-9849-5_7

Davison, W. (1993). Iron and manganese in lakes. *Earth-Science Reviews*, *34*(2), 119-163. https://doi.org/https://doi.org/10.1016/0012-8252(93)90029-7

Denniston, R. F., Wyrwoll, K.-H., Polyak, V. J., Brown, J. R., Asmerom, Y., Wanamaker, A. D., LaPointe, Z., Ellerbroek, R., Barthelmes, M., Cleary, D., Cugley, J., Woods, D., & Humphreys, W. F. (2013). A stalagmite record of Holocene Indonesian-Australian

summer monsoon variability from the Australian tropics. *Quaternary Science Reviews*, *78*, 155–168. https://doi.org/10.1016/j.quascirev.2013.08.004

Department of National Parks, R., Sport and Racing. (2013). Kinrara National Park Management Statement 2013. *Queensland Government*.

Department of Climate Change, Energy , the environment and Water. (2015). *Conservation Management Zones of Australia North Australian Tropical Savanna*. Australian Government The Department of the Environment and Energy. Retrieved from: https://www.environment.gov.au/biodiversity/publications/cmz-north-australian-tropical-savanna

Diaz, H. F., & Markgraf, V. (1992). *El Nino: historical and paleoclimatic aspects of the southern oscillation*. Cambridge University Press.

Dixon, B. C., Tyler, J. J., Lorrey, A. M., Goodwin, I. D., Gergis, J., & Drysdale, R. N. (2017). Low-resolution Australasian palaeoclimate records of the last 2000 years. *Climate of the Past*, *13*(10), 1403-1433. https://doi.org/10.5194/cp-13-1403-2017

Donders, T. H., Haberle, S. G., Hope, G., Wagner, F., & Visscher, H. (2007). Pollen evidence for the transition of the Eastern Australian climate system from the post-glacial to the present-day ENSO mode. *Quaternary Science Reviews*, *26*(11), 1621-1637. https://doi.org/10.1016/j.quascirev.2006.11.018

Edwards, A. C., Maier, S. W., Hutley, L. B., Williams, R. J., & Russell-Smith, J. (2013). Spectral analysis of fire severity in north Australian tropical savannas. *Remote Sensing of Environment*, *136*, 56-65. https://doi.org/10.1016/j.rse.2013.04.013

Field, E., McGowan, H. A., Moss, P. T., & Marx, S. K. (2017). A late Quaternary record of monsoon variability in the northwest Kimberley, Australia. *Quaternary International*, *449*, 119-135. https://doi.org/10.1016/j.quaint.2017.02.019

Finsinger, W., Kelly, R., Fevre, J., & Magyari, E. K. (2014). A guide to screening charcoal peaks in macrocharcoal-area records for fire-episode reconstructions. *The Holocene*, *24*(8), 1002-1008. https://doi.org/10.1177/0959683614534737

Fitzsimons, J., Russell-Smith, J., James, G., Vigilante, T., Lipsett-Moore, G., Morrison, J., & Looker, M. (2012). Insights into the biodiversity and social benchmarking components of the Northern Australian fire management and carbon abatement programmes. *Ecological Management & Restoration*, *13*(1), 51-57. https://doi.org/10.1111/j.1442-8903.2011.00624.x

Fordham, D. A., Saltré, F., Haythorne, S., Wigley, T. M. L., Otto-Bliesner, B. L., Chan, K. C., & Brook, B. W. (2017). PaleoView: a tool for generating continuous climate projections spanning the last 21 000 years at regional and global scales. *Ecography*, *40*(11), 1348-1358. https://doi.org/doi:10.1111/ecog.03031

Froyd, C. A., & Willis, K. J. (2008). Emerging issues in biodiversity & conservation management; the need for a palaeoecological perspective. *Quaternary Science Reviews*, *27*(17-18), 1723-1732. https://doi.org/10.1016/j.quascirev.2008.06.006

Gagan, M. K., Hendy, E. J., Haberle, S. G., & Hantoro, W. S. (2004). Post-glacial evolution of the Indo-Pacific Warm Pool and El Niño-Southern oscillation. *Quaternary International*, *118*, 127-143. https://doi.org/10.1016/S1040-6182(03)00134-4

Goodwin, I. D., Browning, S., Lorrey, A. M., Mayewski, P. A., Phipps, S. J., Bertler, N. A. N., Edwards, R. P., Cohen, T. J., van Ommen, T., Curran, M., Barr, C., & Stager, J. C. (2014). A reconstruction of extratropical Indo-Pacific sea-level pressure patterns during the Medieval Climate Anomaly. *Climate dynamics*, *43*(5-6), 1197-1219. https://doi.org/10.1007/s00382-013-1899-1

GoogleEarth. (2019). *Kinrara Swamp 18°30'4.43"S 145° 2'27.74"E*. Retrieved from: https://www.google.com/earth/

Griffiths, M. L., Kimbrough, A. K., Gagan, M. K., Drysdale, R. N., Cole, J. E., Johnson, K. R., Zhao, J.-X., Cook, B. I., Hellstrom, J. C., & Hantoro, W. S. (2016). Western Pacific hydroclimate linked to global climate variability over the past two millennia. *Nature communications*, *7*(1), 11719-11719. https://doi.org/10.1038/ncomms11719

Grove, R., & Chappell, J. (2000). *El Ni~no, history and crisis: studies from the Asia-Pacific region*. White Horse Press.

Haberle, S. G. (2005). A 23,000-yr Pollen Record from Lake Euramoo, Wet Tropics of NE Queensland, Australia. *Quaternary Research*, *64*(3), 343-356. https://doi.org/10.1016/j.yqres.2005.08.013

Haberle, S. G., Hope, G. S., & van der Kaars, S. (2001). Biomass burning in Indonesia and Papua New Guinea: natural and human induced fire events in the fossil record. *Palaeogeography, Palaeoclimatology, Palaeoecology*, *171*(3), 259-268. https://doi.org/10.1016/S0031-0182(01)00248-6

Haberle, S. G., & Ledru, M.-P. (2001). Correlations among Charcoal Records of Fires from the Past 16,000 Years in Indonesia, Papua New Guinea, and Central and South America. *Quaternary Research*, *55*(1), 97-104. https://doi.org/https://doi.org/10.1006/qres.2000.2188

Haberzettl, T., Fey, M., Lücke, A., Maidana, N., Mayr, C., Ohlendorf, C., Schäbitz, F., Schleser, G. H., Wille, M., & Zolitschka, B. (2005). Climatically induced lake level changes during the last two millennia as reflected in sediments of Laguna Potrok Aike, southern Patagonia (Santa Cruz, Argentina). *Journal of Paleolimnology*, *33*(3), 283-302. https://doi.org/10.1007/s10933-004-5331-z

Hanebuth, T., Stattegger, K., & Grootes, P. M. (2000). Rapid Flooding of the Sunda Shelf: A Late-Glacial Sea-Level Record. *Science*, *288*(5468), 1033-1035. https://doi.org/10.1126/science.288.5468.1033

Haug, G. H., Hughen, K. A., Sigman, D. M., Peterson, L. C., & Röhl, U. (2001). Southward migration of the intertropical convergence zone through the Holocene. *Science (New York, N.Y.)*, *293*(5533), 1304–1308. https://doi.org/10.1126/science.1059725

Hesse, P. P., Magee, J. W., & van der Kaars, S. (2004). Late Quaternary climates of the Australian arid zone: a review. *Quaternary International*, *118*, 87-102. https://doi.org/10.1016/S1040-6182(03)00132-0

Hiscock, P., & Kershaw, P. (1992). Palaeoenvironments and prehistory of Australia's tropical Top End. In. Longman Cheshire.

Hope, G., Chokkalingam, U., & Anwar, S. (2005). The stratigraphy and fire history of the Kutai Peatlands, Kalimantan, Indonesia. *Quaternary Research*, *64*(3), 407-417. https://doi.org/https://doi.org/10.1016/j.yqres.2005.08.009

Jago, L. C. F., & Boyd, W. E. (2005). How a wet tropical rainforest copes with repeated volcanic destruction. *Quaternary Research*, *64*(3), 399-406. https://doi.org/https://doi.org/10.1016/j.yqres.2005.08.012

James, J., Comley, R., Wurster, C. M., Levchenko, V., Gadd, P., & Bird, M. I. (2024). Holocene savanna hydroclimate record from Kinrara Lake, north-east Queensland, Australia. *Palaeogeography, Palaeoclimatology, Palaeoecology*, *637*, 111985. https://doi.org/10.1016/j.palaeo.2023.111985

Johnson, C. N. (2016). Fire, people and ecosystem change in Pleistocene Australia. *Australian Journal of Botany*, *64*(8), 643. https://doi.org/10.1071/BT16138

Kershaw, A. P. (1971). A Pollen Diagram from Quincan Crater, North-East Queensland, Australia. *The New Phytologist*, *70*(4), 669-681. https://doi.org/10.1111/j.1469-8137.1971.tb02567.x

Kershaw, A. P., Bretherton, S. C., & van der Kaars, S. (2007). A complete pollen record of the last 230 ka from Lynch's Crater, north-eastern Australia. *Palaeogeography,*

Palaeoclimatology, Palaeoecology, *251*(1), 23-45. https://doi.org/10.1016/j.palaeo.2007.02.015

Kylander, M. E., Ampel, L., Wohlfarth, B., & Veres, D. (2011). High-resolution X-ray fluorescence core scanning analysis of Les Echets (France) sedimentary sequence: new insights from chemical proxies. *Journal of Quaternary Science*, *26*(1), 109-117. https://doi.org/https://doi.org/10.1002/jqs.1438

Lambrides, A. B. J., McNiven, I. J., Aird, S. J., Lowe, K. A., Moss, P., Rowe, C., Harris, C., Maclaurin, C., Slater, S. A., Carroll, K., Cedar, M. H., Petchey, F., Reepmeyer, C., Harris, M., Charlie, J., McGreen, E., Baru, P., & Ulm, S. (2020). Changing use of Lizard Island over the past 4000 years and implications for understanding Indigenous offshore island use on the Great Barrier Reef. *Queensland archaeological research*, *23*, 43-109. https://doi.org/10.25120/qar.23.2020.3778

Lewis, R. J., Tibby, J., Arnold, L. J., Barr, C., Marshall, J., McGregor, G., Gadd, P., & Yokoyama, Y. (2020). Insights into subtropical Australian aridity from Welsby Lagoon, north Stradbroke Island, over the past 80,000 years. *Quaternary Science Reviews*, *234*, 106262. https://doi.org/https://doi.org/10.1016/j.quascirev.2020.106262

Li, T., Comley, R., Zhang, E., Zhou, Y., Zhou, X., Munksgaard, N. C., Zhu, Z., Haig, J., Zheng, F., & Bird, M. I. (2023). Paleo-temperature inferred from brGDGTs over the past 18 cal ka BP from Lake Barrine, tropical NE Australia. *Quaternary Science Reviews*, *310*, 108125. https://doi.org/https://doi.org/10.1016/j.quascirev.2023.108125

Li, T., Wurster, C. M., Haig, J., Zhou, Y., Zwart, C., Ren, J., Comley, R., Munksgaard, N. C., Gadd, P. S., & Bird, M. I. (2022). Environmental change inferred from multiple proxies from an 18 cal ka BP sediment record, Lake Barrine, NE Australia. *Quaternary Science Reviews*, *294*, 107751. https://doi.org/https://doi.org/10.1016/j.quascirev.2022.107751

Liu, Z., Otto-Bliesner, B. L., He, F., Brady, E. C., Tomas, R., Clark, P. U., Carlson, A. E., Lynch-Stieglitz, J., Curry, W., Brook, E., Erickson, D., Jacob, R., Kutzbach, J., & Cheng, J. (2009). Transient Simulation of Last Deglaciation with a New Mechanism for Bølling-Allerød Warming. *Science*, *325*(5938), 310-314. https://doi.org/10.1126/science.1171041

Longman, J., Veres, D., & Wennrich, V. (2019). Utilisation of XRF core scanning on peat and other highly organic sediments. *Quaternary International*, *514*, 85-96. https://doi.org/https://doi.org/10.1016/j.quaint.2018.10.015

Lopes dos Santos, R. A., De Deckker, P., Hopmans, E. C., Magee, J. W., Mets, A., Sinninghe Damsté, J. S., & Schouten, S. (2013). Abrupt vegetation change after the Late Quaternary megafaunal extinction in southeastern Australia. *Nature Geoscience*, *6*(8), 627-631. https://doi.org/10.1038/ngeo1856

Luly, J. G., Grindrod, J. F., & Penny, D. (2006). Holocene palaeoenvironments and change at Three-Quarter Mile Lake, Silver Plains Station, Cape York Peninsula, Australia. *Holocene (Sevenoaks)*, *16*(8), 1085-1094. https://doi.org/10.1177/0959683606069398

Lüning, S., Gałka, M., García-Rodríguez, F., & Vahrenholt, F. (2020). The Medieval Climate Anomaly in Oceania. *Environmental reviews*, *28*(1), 45-54. https://doi.org/10.1139/er-2019-0012

Ma, X., Huete, A., Cleverly, J., Eamus, D., Chevallier, F., Joiner, J., Poulter, B., Zhang, Y., Guanter, L., Meyer, W., Xie, Z., & Ponce-Campos, G. (2016). Drought rapidly diminishes the large net CO2 uptake in 2011 over semi-arid Australia. *Scientific Reports*, *6*(1), 37747. https://doi.org/10.1038/srep37747

Maraseni, T. N., Reardon-Smith, K., Griffiths, G., & Apan, A. (2016). Savanna burning methodology for fire management and emissions reduction: a critical review of

influencing factors. *Carbon Balance and Management*, *11*(1), 1-11. https://doi.org/10.1186/s13021-016-0067-4

Mariani, M., Fletcher, M. S., Holz, A., & Nyman, P. (2016). ENSO controls interannual fire activity in southeast Australia. *Geophysical Research Letters*, *43*(20), 10,891-810,900. https://doi.org/10.1002/2016GL070572

Marlon, J. R., Kelly, R., Daniau, A.-L., Vannière, B., Power, M. J., Bartlein, P., Higuera, P., Blarquez, O., Brewer, S., Brücher, T., Feurdean, A., Romera, G. G., Iglesias, V., Maezumi, S. Y., Magi, B., Courtney Mustaphi, C. J., & Zhihai, T. (2016). Reconstructions of biomass burning from sediment-charcoal records to improve data–model comparisons. *Biogeosciences*, *13*(11), 3225-3244. https://doi.org/10.5194/bg-13-3225-2016

Metcalfe, S. E., Jones, M. D., Davies, S. J., Noren, A., & MacKenzie, A. (2010). Climate variability over the last two millennia in the North American Monsoon region, recorded in laminated lake sediments from Laguna de Juanacatlán, Mexico. *The Holocene*, *20*(8), 1195-1206. https://doi.org/10.1177/0959683610371994

Meyer, C. P., Cook, G. D., Reisen, F., Smith, T. E. L., Tattaris, M., Russell-Smith, J., Maier, S. W., Yates, C. P., & Wooster, M. J. (2012). Direct measurements of the seasonality of emission factors from savanna fires in northern Australia: SAVANNA BURNING EMISSION FACTORS. *Journal of Geophysical Research: Atmospheres*, *117*(D20). https://doi.org/10.1029/2012JD017671

Meyers, P. A. (1994). Preservation of elemental and isotopic source identification of sedimentary organic matter. *Chemical Geology*, *114*(3), 289-302. https://doi.org/https://doi.org/10.1016/0009-2541(94)90059-0

Meyers, P. A. (2003). Applications of organic geochemistry to paleolimnological reconstructions: a summary of examples from the Laurentian Great Lakes. *Organic Geochemistry*, *34*(2), 261-289. https://doi.org/https://doi.org/10.1016/S0146-6380(02)00168-7

Mishra, A. K., Placzek, C., Wurster, C., & Whitehead, P. W. (2019). New radiocarbon age constraints for the 120 km-long Toomba flow, north Queensland, Australia. *Australian Journal of Earth Sciences*, *66*(1), 71-79. https://doi.org/10.1080/08120099.2019.1523227

Mooney, S. D., Harrison, S. P., Bartlein, P. J., Daniau, A. L., Stevenson, J., Brownlie, K. C., Buckman, S., Cupper, M., Luly, J., Black, M., Colhoun, E., D'Costa, D., Dodson, J., Haberle, S., Hope, G. S., Kershaw, P., Kenyon, C., McKenzie, M., & Williams, N. (2011). Late Quaternary fire regimes of Australasia. *Quaternary Science Reviews*, *30*(1-2), 28-46. https://doi.org/10.1016/j.quascirev.2010.10.010

Moore, C. E., Beringer, J., Evans, B., Hutley, L. B., McHugh, I., & Tapper, N. J. (2016). The contribution of trees and grasses to productivity of an Australian tropical savanna. *Biogeosciences*, *13*(8), 2387-2403. https://doi.org/10.5194/bg-13-2387-2016

Moreno, A., Giralt, S., Valero-Garcés, B., Sáez, A., Bao, R., Prego, R., Pueyo, J. J., González-Sampériz, P., & Taberner, C. (2007). A 14kyr record of the tropical Andes: The Lago Chungará sequence (18°S, northern Chilean Altiplano). *Quaternary International*, *161*(1), 4-21. https://doi.org/https://doi.org/10.1016/j.quaint.2006.10.020

Moss, P., Cosgrove, R., Haberle, S., & Ferrier, Å. (2012). Peopled Landscapes: Archaeological and Biogeographic Approaches to Landscapes. In (pp. 329-341).

Moss, P. T., Cosgrove, R., Ferrier, Å., & Haberle, S. G. (2012). Holocene environments of the sclerophyll woodlands of the Wet Tropics of northeastern Australia. In (Vol. 34, pp. 329). ANU E Press.

Moss, P. T., Dunbar, G. B., Thomas, Z., Turney, C., Kershaw, A. P., & Jacobsen, G. E. (2017). A 60 000-year record of environmental change for the Wet Tropics of north-eastern Australia based on the ODP 820 marine core. *Journal of Quaternary Science*, *32*(6), 704-716. https://doi.org/10.1002/jqs.2977

Moss, P. T., & Kershaw, A. P. (2007). A late Quaternary marine palynological record (oxygen isotope stages 1 to 7) for the humid tropics of northeastern Australia based on ODP Site 820. *Palaeogeography, Palaeoclimatology, Palaeoecology*, *251*(1), 4-22. https://doi.org/https://doi.org/10.1016/j.palaeo.2007.02.014

Moss, P. T., Tibby, J., Petherick, L., McGowan, H., & Barr, C. (2013). Late Quaternary vegetation history of North Stradbroke Island, Queensland, eastern Australia. *Quaternary Science Reviews*, *74*, 257-272. https://doi.org/10.1016/j.quascirev.2013.02.019

Mueller, A. D., Islebe, G. A., Hillesheim, M. B., Grzesik, D. A., Anselmetti, F. S., Ariztegui, D., Brenner, M., Curtis, J. H., Hodell, D. A., & Venz, K. A. (2009). Climate drying and associated forest decline in the lowlands of northern Guatemala during the late Holocene. *Quaternary Research*, *71*(2), 133-141. https://doi.org/https://doi.org/10.1016/j.yqres.2008.10.002

Muller, J., Kylander, M., Wüst, R., Weiss, D., Martinez-Cortizas, A., LeGrande, A., Jennerjahn, T., Behling, H., & Jacobson, G. (2008). Possible evidence for wet Heinrich phases in tropical NE Australia: the Lynch's Crater deposit. *Quaternary Science Reviews*, *27*, 468-475. https://doi.org/10.1016/j.quascirev.2007.11.006

Mustaphi, C., & Pisaric, M. (2014). A classification for macroscopic charcoal morphologies found in Holocene lacustrine sediments. *Progress in Physical Geography*, *38*. https://doi.org/10.1177/0309133314548886

NAFI. (2024). *NAFI North Australia & Rangelands Fire Information*. Retrieved from: https://www.firenorth.org.au/nafi3/

Neldner, V. J., Niehus, R. E., Wilson. B.A., McDonald., & W.J.F., F., A.J. Accad, A. (2023). The Vegetation of Queensland. Descriptions of Broad Vegetation Groups. *Version 6.0. Queensland Herbarium and Biodiversity Science, Department of Environment and Science*.

Notaro, M., Wyrwoll, K.-H., & Chen, G. (2011). Did aboriginal vegetation burning impact on the Australian summer monsoon? *Geophysical Research Letters*, *38*(11). https://doi.org/10.1029/2011GL047774

O'Connell, J. F., & Allen, J. (2004). Dating the colonization of Sahul (Pleistocene Australia–New Guinea): a review of recent research. *Journal of Archaeological Science*, *31*(6), 835-853. https://doi.org/10.1016/j.jas.2003.11.005

Ondei, S., Prior, L. D., Williamson, G. J., Vigilante, T., & Bowman, D. M. J. S. (2017). Water, land, fire, and forest: Multi-scale determinants of rainforests in the Australian monsoon tropics. *Ecology and Evolution*, *7*(5), 1592-1604. https://doi.org/10.1002/ece3.2734

Petherick, L. M., Moss, P. T., & McGowan, H. A. (2017). An extended Last Glacial Maximum in subtropical Australia. *Quaternary International*, *432*, 1-12. https://doi.org/10.1016/j.quaint.2015.11.015

Prebble, M., Sim, R., Finn, J., & Fink, D. (2005). A Holocene pollen and diatom record from Vanderlin Island, Gulf of Carpentaria, lowland tropical Australia. *Quaternary Research*, *64*(3), 357-371. https://doi.org/10.1016/j.yqres.2005.08.005

Proske, U., & Haberle, S. G. (2012). Island ecosystem and biodiversity dynamics in northeastern Australia during the Holocene; unraveling short-term impacts and long-term drivers. *Holocene (Sevenoaks)*, *22*(10), 1097–1111. https://doi.org/10.1177/0959683612441840

Proske, U., Stevenson, J., Seddon, A. W., & Taffs, K. (2017a). Holocene diatom records of wetland development near Weipa, Cape York, Australia. *Quaternary International*, *440*, 42-54.

Proske, U., Stevenson, J., Seddon, A. W. R., & Taffs, K. (2017b). Holocene diatom records of wetland development near Weipa, Cape York, Australia. *Quaternary International*, *440*, 42-54. https://doi.org/10.1016/j.quaint.2016.09.014

Queensland Government. (1994). *EINASLEIGH SHEET SE55-09, 1:250 000 GEOLOGICAL SERIES MAP SECOND EDITION 1994, 1:250 000 GEOLOGICAL SERIES EXPLANATORY NOTES 1994*. Retrieved from: https://geoscience.data.qld.gov.au/dataset/cr076508

Queensland Government. (2023a). *Regional ecosystem details for 9.8.1*. Queensland Government. Retrieved from: https://apps.des.qld.gov.au/regional-ecosystems/details/?re=9.8.1

Queensland Government. (2023b). *Regional ecosystem details for 9.8.7*. Queensland Government. Retrieved from: https://apps.des.qld.gov.au/regional-ecosystems/details/?re=9.8.7

Queensland Government. (2022). *Alphabetical register of Pastoral Holdings 1863-1880*. Queensland Government. Retrieved from: https://www.data.qld.gov.au/dataset/register-pastoral-holdings-1863-to-1880/resource/460e3f22-df6f-4a84-9b67-7fc4b412c9c1

Queensland Government Department of Environment, Science and Innovation., (2012). Retrieved from: https://www.qld.gov.au/environment/climate

Reeves, J. M., Bostock, H. C., Ayliffe, L. K., Barrows, T. T., De Deckker, P., Devriendt, L. S., Dunbar, G. B., Drysdale, R. N., Fitzsimmons, K. E., Gagan, M. K., Griffiths, M. L., Haberle, S. G., Jansen, J. D., Krause, C., Lewis, S., McGregor, H. V., Mooney, S. D., Moss, P., Nanson, G. C., . . . Institutionen för naturgeografi och, k. (2013). Palaeoenvironmental change in tropical Australasia over the last 30,000 years – a synthesis by the OZ-INTIMATE group. *Quaternary Science Reviews*, *74*, 97-114. https://doi.org/10.1016/j.quascirev.2012.11.027

Reeves, J. M., Chivas, A. R., Garcia, A., & De Deckker, P. (2007). Palaeoenvironmental change in the Gulf of Carpentaria (Australia) since the last interglacial based on Ostracoda. *Palaeogeography, Palaeoclimatology, Palaeoecology*, *246*(2), 163-187. https://doi.org/10.1016/j.palaeo.2006.09.012

Rehn, E., Rowe, C., Ulm, S., Gadd, P., Zawadzki, A., Jacobsen, G., Woodward, C., & Bird, M. (2021a). Multiproxy Holocene Fire Records From the Tropical Savannas of Northern Cape York Peninsula, Queensland, Australia. *Frontiers in ecology and evolution*, *9*. https://doi.org/10.3389/fevo.2021.771700

Rehn, E., Rowe, C., Ulm, S., Woodward, C., & Bird, M. (2021b). A late-Holocene multiproxy fire record from a tropical savanna, eastern Arnhem Land, Northern Territory, Australia. *Holocene (Sevenoaks)*, *31*(5), 870-883. https://doi.org/10.1177/0959683620988030

Rehn, E., Rowe, C., Ulm, S., Woodward, C., Zawadzki, A., Jacobsen, G., & Bird, M. I. (2022). Integrating charcoal morphology and stable carbon isotope analysis to identify non-grass elongate charcoal in tropical savannas. *Vegetation History and Archaeobotany*, *31*(1), 37-48. https://doi.org/10.1007/s00334-021-00836-z

Risbey, J. S., Pook, M. J., McIntosh, P. C., Wheeler, M. C., & Hendon, H. H. (2009). On the Remote Drivers of Rainfall Variability in Australia. *Monthly Weather Review*, *137*(10), 3233-3253. https://doi.org/10.1175/2009MWR2861.1

Ritchie, E. G., & Bolitho, E. E. (2008). Australia's Savanna Herbivores: Bioclimatic Distributions and an Assessment of the Potential Impact of Regional Climate Change.

Physiological and biochemical zoology : PBZ, *81*(6), 880-890. https://doi.org/10.1086/588171

Rowe, Cassandra, Rehn Emma, Brand, M., Hutley, L. B., Comley, R., Levchenko, V., Zwart, C., Wurster, C. M., & Bird, M. I. (2022a). Holocene climate–fire–vegetation feedbacks in tropical savannas: Insights from the Marura sinkhole, East Arnhem Land, northern Australia. *Journal of Vegetation Science*, *33*(6), e13158. https://doi.org/https://doi.org/10.1111/jvs.13158

Rowe, C. (2006). Landscapes in Western Torres Strait History. In (pp. 270-286). Aboriginal Studies Press.

Rowe, C. (2007). A palynological investigation of Holocene vegetation change in Torres Strait, seasonal tropics of northern Australia. *Palaeogeography, Palaeoclimatology, Palaeoecology*, *251*(1), 83-103. https://doi.org/10.1016/j.palaeo.2007.02.019

Rowe, C., Stevenson, J., Connor, S., & Adeleye, M. (2022b). Fire and the Transformation of Landscapes. *The Oxford Handbook of the Archaeology of Indigenous Australia and New Guinea*, 0. https://doi.org/10.1093/oxfordhb/9780190095611.013.12

Rowe, C., Wurster, C. M., Zwart, C., Brand, M., Hutley, L. B., Levchenko, V., & Bird, M. I. (2021). Vegetation over the last glacial maximum at Girraween Lagoon, monsoonal northern Australia. *Quaternary Research*, *102*, 39-52. https://doi.org/10.1017/qua.2020.50

Rule, S., Brook, B. W., Haberle, S. G., Chris, S. M. T., Kershaw, A. P., & Johnson, C. N. (2012). The Aftermath of Megafaunal Extinction: Ecosystem Transformation in Pleistocene Australia. *Science*, *335*(6075), 1483-1486. https://doi.org/10.1126/science.1214261

Russell-Smith, J., Murphy, B. P., Meyer, C. P., Cook, G. D., Maier, S., Edwards, A. C., Schatz, J., & Brocklehurst, P. (2009). Improving estimates of savanna burning emissions for greenhouse accounting in northern Australia: limitations, challenges, applications. *International Journal of Wildland Fire*, *18*(1), 1-18. https://doi.org/https://doi.org/10.1071/WF08009

Saiz, G., Goodrick, I., Wurster, C., Nelson, P. N., Wynn, J., & Bird, M. (2018). Preferential Production and Transport of Grass-Derived Pyrogenic Carbon in NE-Australian Savanna Ecosystems. *Frontiers in Earth Science*, *5*. https://doi.org/10.3389/feart.2017.00115

Saiz, G., Wynn, J. G., Wurster, C. M., Goodrick, I., Nelson, P. N., & Bird, M. I. (2015). Pyrogenic carbon from tropical savanna burning: production and stable isotope composition. *Biogeosciences*, *12*(6), 1849-1863. https://doi.org/10.5194/bg-12-1849-2015

Salinger, M. & Renwick, James & Mullan, Brett. (2001). Interdecadal Pacific Oscillation and South Pacific Climate. *International Journal of Climatology*. *21*. 1705 - 1721. 10.1002/joc.691.

Saltré, F., Rodríguez-Rey, M., Brook, B. W., Johnson, C. N., Turney, C. S. M., Alroy, J., Cooper, A., Beeton, N., Bird, M. I., Fordham, D. A., Gillespie, R., Herrando-Pérez, S., Jacobs, Z., Miller, G. H., Nogués-Bravo, D., Prideaux, G. J., Roberts, R. G., & Bradshaw, C. J. A. (2016). Climate change not to blame for late Quaternary megafauna extinctions in Australia. *Nature communications*, *7*(1), 10511. https://doi.org/10.1038/ncomms10511

Scanlan, J. (2002). Some tree-grass dynamics in Queensland's grazing lands. *Rangeland Journal - RANGELAND J*, *24*. https://doi.org/10.1071/RJ02003

Scheiter, S., Higgins, S. I., Beringer, J., & Hutley, L. B. (2015). Climate change and swamplong-term fire management impacts on Australian savannas. *New Phytologist*, *205*(3), 1211-1226. https://doi.org/10.1111/nph.13130

Schneider, T., Bischoff, T., & Haug, G. H. (2014). Migrations and dynamics of the intertropical convergence zone. *Nature*, *513*(7516), 45-53. https://doi.org/10.1038/nature13636

Scott, A. C., Chaloner, W. G., Belcher, C. M., & Roos, C. I. (2016). The interaction of fire and mankind: Introduction. *Philosophical transactions of the Royal Society of London. Series B, Biological sciences*, *371*(1696), 20150162. https://doi.org/10.1098/rstb.2015.0162

Steinke, S., Mohtadi, M., Prange, M., Varma, V., Pittauerova, D., & Fischer, H. W. (2014). Mid- to Late-Holocene Australian–Indonesian summer monsoon variability. *Quaternary Science Reviews*, *93*, 142-154. https://doi.org/10.1016/j.quascirev.2014.04.006

Stephenson, P. J., Burch-Johnston, A. T., Stanton, D., & Whitehead, P. W. (1998). Three long lava flows in north Queensland. *Journal of Geophysical Research: Solid Earth*, *103*(B11), 27359-27370. https://doi.org/10.1029/98JB01670

Stevenson, J. (2004). A late-Holocene record of human impact from the southwest coast of New Caledonia. *The Holocene*, *14*(6), 888-898. https://doi.org/10.1191/0959-683604hl755rp

Stevenson, J., Brockwell, S., Rowe, C., Proske, U., & Shiner, J. (2015a). The palaeo-environmental history of Big Willum Swamp, Weipa: An environmental context for the archaeological record. *Australian Archaeology*, *80*(1), 17-31. https://doi.org/10.1080/03122417.2015.11682041

Stevenson, J., Brockwell, S., Rowe, C., Proske, U., & Shiner, J. (2015b). The palaeoenvironmental history of Big Willum Swamp, Weipa: an environmental context for the archaeological record.

Stevenson, J., Dodson, J. R., & Prosser, I. P. (2001). A late Quaternary record of environmental change and human impact from New Caledonia. *Palaeogeography, Palaeoclimatology, Palaeoecology*, *168*(1), 97-123. https://doi.org/10.1016/S0031-0182(00)00251-0

Stevenson, J., & Hope, G. (2005). A comparison of late Quaternary forest changes in New Caledonia and northeastern Australia. *Quaternary Research*, *64*(3), 372-383. https://doi.org/https://doi.org/10.1016/j.yqres.2005.08.011

Thomas, P. A., & McAlpine, R. (2010). *Fire in the forest*. Cambridge University Press. https://doi.org/10.1017/CBO9780511780189

Trauernicht, C., Murphy, B.P., Prior, L.D. (2016). Human-Imposed, Fine-Grained Patch Burning Explains the Population Stability of a Fire-Sensitive Conifer in a Frequently Burnt Northern Australia Savanna. *Ecosystems 19*, 896–909.

Tothill, J. C., Mott, J. J., & Australian Academy of, S. (1985). *Ecology and management of the world's savannas*. Australian Academy of Science in conjunction with C.A.B.

Voelker, S. L., Brooks, J. R., Meinzer, F. C., Anderson, R., Bader, M. K. F., Battipaglia, G., Becklin, K. M., Beerling, D., Bert, D., Betancourt, J. L., Dawson, T. E., Domec, J. C., Guyette, R. P., Körner, C., Leavitt, S. W., Linder, S., Marshall, J. D., Mildner, M., Ogée, J., . . . Sveriges, l. (2016). A dynamic leaf gas-exchange strategy is conserved in woody plants under changing ambient CO2: evidence from carbon isotope discrimination in paleo and CO2 enrichment studies. *Global Change Biology*, *22*(2), 889-902. https://doi.org/10.1111/gcb.13102

Walker, D. (2007). Holocene sediments of Lake Barrine, north-east Australia, and their implications for the history of lake and catchment environments. *Palaeogeography, Palaeoclimatology, Palaeoecology*, *251*(1), 57-82.

Walker, M. J. C., Berkelhammer, M., Bjorck, S., Cwynar, L. C., Fisher, D. A., Long, A. J., Lowe, J. J., Newnham, R. M., Rasmussen, S. O., & Weiss, H. (2012). Formal subdivision of the Holocene series/epoch; a discussion paper by a working group of INTIMATE (Integration of ice-core, marine and terrestrial records) and the Subcommission on Quaternary Stratigraphy (International Commission on Stratigraphy). Journal of Quaternary Science, 27(7), 649-659. https://doi.org/10.1002/jqs.2565

White, W. M. (2013). *Geochemistry*. John Wiley & Sons Inc.

Whitehead, P. W. (2010). The regional context of the McBride Basalt Province and the formation of the Undara Lava flows, tubes, rises and depressions.

Whitlock, C., & Larsen, C. (2001). Charcoal as a Fire Proxy. In (Vol. 3, pp. 75-97). https://doi.org/10.1007/0-306-47668-1_5

Williams, A. N., Ulm, S., Goodwin, I. D., & Smith, M. (2010). Hunter-gatherer response to late Holocene climatic variability in northern and central Australia. *Journal of Quaternary Science*, *25*(6), 831-838. https://doi.org/https://doi.org/10.1002/jqs.1416

Williams, A. N., Ulm, S., Turney, C. S., Rohde, D., & White, G. (2015). Holocene Demographic Changes and the Emergence of Complex Societies in Prehistoric Australia. *PLoS One*, *10*(6), e0128661. https://doi.org/10.1371/journal.pone.0128661

Willis, K. J., Araújo, M. B., Bennett, K. D., Figueroa-Rangel, B., Froyd, C. A., & Myers, N. (2007). Correction for Willis et al., How can a knowledge of the past help to conserve the future? Biodiversity conservation and the relevance of long-term ecological studies. *Philosophical transactions of the Royal Society of London. Series B. Biological sciences*, *362*(1488), 2367-2367. https://doi.org/10.1098/rstb.2007.2000

Wirrmann, D. *et al.* (2011) 'Mid- to late Holocene environmental and climatic changes in New Caledonia, southwest tropical Pacific, inferred from the littoral plain Gouaro-Déva', *Quaternary Research*, 76(2), pp. 229–242. doi:10.1016/j.yqres.2011.04.007.

Wurster, C. M., Lloyd, J., Goodrick, I., Saiz, G., & Bird, M. I. (2012). Quantifying the abundance and stable isotope composition of pyrogenic carbon using hydrogen pyrolysis. *Rapid Commun Mass Spectrom*, *26*(23), 2690-2696. https://doi.org/10.1002/rcm.6397

Wurster, C. M., McBeath, A. V., & Bird, M. I. (2015). The carbon isotope composition of semi-labile and stable pyrogenic carbon in a thermosequence of C3 and C4 derived char. *Organic Geochemistry*, *81*, 20-26. https://doi.org/10.1016/j.orggeochem.2015.01.008

Wurster, C. M., Rowe, C., Zwart, C., Sachse, D., Levchenko, V., & Bird, M. I. (2021a). Indigenous impacts on north Australian savanna fire regimes over the Holocene. *Scientific Reports*, *11*(1), 23157. https://doi.org/10.1038/s41598-021-02618-z

Wurster, C. M., Rowe, C., Zwart, C., Sachse, D., Levchenko, V., & Bird, M. I. (2021b). Indigenous impacts on north Australian savanna fire regimes over the Holocene. *Scientific Reports*, *11*(1), 23157-23157. https://doi.org/10.1038/s41598-021-02618-z

Wyrwoll, K.-H., & Miller, G. H. (2001). Initiation of the Australian summer monsoon 14,000 years ago. *Quaternary International*, *83*, 119-128. https://doi.org/10.1016/S1040-6182(01)00034-9

Yates, C. P., Edwards, A. C., & Russell-Smith, J. (2008). Big fires and their ecological impacts in Australian savannas: size and frequency matters. *International Journal of Wildland Fire*, *17*(6), 768. https://doi.org/10.1071/WF07150